Epigenetic and genetic mechanisms through which Myostatin regulates muscle wasting

Lua, Gavian Bing Jia

2016

Epigenetic and genetic mechanisms through which Myostatin regulates muscle wasting

Lua Bing Jia Gavian

School of Biological Sciences

2016

Epigenetic and genetic mechanisms through which Myostatin regulates muscle wasting

Lua Bing Jia Gavian

School of Biological Sciences

A thesis submitted to the Nanyang Technological University in partial fulfillment of the requirement for the degree of Doctor of Philosophy

2016

Table of Contents

Acknowledgements

I thank my supervisor, Professor Ravi Kambadur, for his constant guidance on during my post-graduate studies. You not only taught me science, you also taught me how to work as a scientist. I am glad to have joined you and your team and I truly appreciate the compassion you have given me as well as the freedom to generate ideas which allowed creative growth. It has made me realize that this is an important trait a scientist should have and that creativity is the key to success not only in the scientific career but also in our everyday lives. I also thank Professor Mridula and Craig for their contributions and suggestions of ideas, and reviewing my thesis extensively. It has been a smooth experience working with the both of you. Thank you for your guidance.

Next, I extend my gratitude to all lab members who have contributed to my thesis. Specifically, I thank Vinay, who has provided help in several experiments. Thank you for putting in the effort and long hours in completing experiments. Sabeera, Holly and Preeti, for help in muscle injury work and dissections. Chu Ming, for counting of satellite cells. Piyush, for advice on cloning. Prasanna, for help with adenovirus work.

Thank you mummy for the constant encouragement to "study hard" and also, during tough times, constantly reminding me that this is my future. Thank you Sis for finding a way out in times of need and also all the advices on marriage, and also giving a heads-up on starting a family. Thank you both of you for being there when I was down and understanding the time constraints I have and that little time is left for family time. Thank you Dad for letting me make my own career decisions. Thank you for making sure I eat and sleep well and that my room and clothes are cleaned. Not forgetting my fiancée who has been supportive of my post-graduate studies and being understanding of the nature of my work. Thank you for the work-related and non-work

related advices you have given me. I am glad to have you in my life and I look forward to starting a family with you.

Lastly, thank you Lord Jesus Christ. You are our Lord and Saviour. Thank you for dying on the cross for us so that we are redeemed of our sins forever, so that we are blessed, so that we never have to feel lost and insecure. Thank you for putting me at the right place, at the right time. Thank you for loving me Lord, I give all honor, praise and glory to you, our Lord and savior, Lord Jesus Christ!

List of figures

List of tables

List of abbreviations

3'	3 prime
5'	5 prime
β-ME	Beta-Mercaptoethanol
ActRIIb	Activin Receptor Type IIb
AKT	Protein kinase B
ATCC	American Type Culture Collection
ATP	Adenosine triphosphate
Bcl2	B-cell lymphoma 2
bFGF	Basic fibroblast growth factor
bHLH	Basic Helix-Loop-Helix
BMD	Becker muscular dystrophy
BMP	Bone morphogenetic protein
BSA	Bovine Serum Albumin
CE	Cre
CEE	Chicken Embryo Extract
CDK	Cyclin-dependent kinases
ChIP	Chromatin immunoprecipitation
CMPC	Cardiomyocyte progenitor cells
CXCR-4	C-X-C chemokine receptor type 4
DNA	Deoxyribonucleic acid
DM	Dermatomyositis
DMD	Duchenne muscular dystrophy
DMEM	Dulbecco's Modified Eagle Medium
DMSO	Dimethyl Sulfoxide
dNTP	Deoxynucleotide triphosphate
dUTP	Deoxyuridine triphosphate
EDTA	Ethylenediaminetetraacetate
ECM	Extracellular matrix
EtBr	Ethidium Bromide
EtOH	Ethanol
FACS	Fluorescence-activated cell sorting
FBS	Fetal Bovine Serum

FGF	Fibroblast growth factor
FSHD	Facioscapulohumeral muscular dystrophy
GDF8	Growth and differentiation factor 8
GFP	Green fluorescent protein
H & E	Haematoxylin and Eosin
HDAC1	Histone Deacetylase 1
HDAC4	Histone Deacetylase 4
HEB	HeLa E-box binding protein
Hesr	Hairy and enhancer of split-related
HGF	Hepatocyte growth factor
HRP	Horseradish peroxidase
HS	Horse Serum
IBM	Inclusion body myositis
ICC	Immunocytochemistry
IGF-1	Insulin-like growth factor 1
IHC	Immunohistochemistry
LARII	Luciferase assay reagent II
LF2000	Lipofectamine 2000
LGMD2A	Limb girdle muscular dystrophies type 2A
LGMD2B	Limb girdle muscular dystrophies type 2B
LIF	Leukemia inhibitory factor
miRNA	microRNA
MM	Miyoshi myopathy
MRF	Myogenic regulatory factor
Mstn	Myostatin
mTOR	Mammalian target of rapamycin
MuRF-1	Muscle RING-finger protein-1
Myf5	Myogenic factor 5
MyHC	Myosin Heavy Chain
MYH	Myosin Heavy Chain
MyoD	Myoblasts determination protein 1

NP40	Nonidet P-40
NGS	Normal Goat Serum
NSS	Normal Sheep Serum
NM	Nemaline myopathy
Pax3	Paired box 3
Pax7	Paired box 7
PBS	Phosphate-buffered saline
PCNA	Proliferating cell nuclear antigen
pre-miRNA	precursor miRNA
PDGF	Platelet-derived growth factor
PI	Protease Inhibitor
Pri-miRNA	Primary miRNA
PMSF	Phenylmethanesulfonylfluoride
P/S	Penicillin and Streptomycin
Rb	Retinoblastoma protein
RISC	RNA-induced silencing complex
RNase	Ribonuclease
RNA	Ribonucleic acid
RT	Room temperature
qPCR	Quantitative PCR
SDF-1	Stromal cell-derived factor 1
SDS	Sodium dodecyl sulfate
SDS-PAGE Polyacrylamide Gel	Sodium Dodecyl Sulfate
	Electrophoresis
SF	Scatter factor
Sirt1	NAD-dependent protein deacetylase sirtuin-1
SRF	Serum Response Factor
TA	Tibialis anterior
TBST	Tris-buffered Saline with Tween-20
TCF3	Transcription factor 3
TCF4	Transcription factor 4

TCF12	Transcription factor 12
TGF-β	Transforming growth factor beta
TNF-α	Tumor necrosis factor alpha
TUNEL	Terminal deoxynucleotidyl transferase dUTP nick end labeling
UTR	Untranslated region
PM	Primary degenerative myopathic disorder

Abstract

Myostatin (Mstn) is a secreted growth factor that negatively regulates proliferation and differentiation of myoblasts. While the downstream signaling pathways and targets genes of Myostatin have been well studied, the involvement of microRNAs (miRNAs) in Myostatin regulation of myogenesis remains to be fully characterized. Here in this thesis, we have performed miRNA microarray on RNA isolated from myoblast and myotube models of Myostatin gain- and loss-of-function. Subsequent bioinformatics analysis identified miR-34a as a downstream target of Myostatin. Molecular analysis confirmed that Myostatin transcriptionally upregulates miR-34a expression via NF-κB. Similar to the known effect of Myostatin, overexpression of miR-34a resulted in impaired myoblast proliferation and inhibited myogenic differentiation. Furthermore, AntagomiR-mediated knockdown of miR-34a not only enhanced myogenesis but also rescued Myostatin-mediated inhibition of myoblast proliferation and differentiation. Mechanistically, we find that miR-34a targets the MyoD transcription co-factor TCF12, thereby impairing MyoD function, reducing myogenin expression and preventing myogenic differentiation.

Satellite cells are quiescent muscle stem cells that have critical functions in post natal muscle growth and repair. Quantitative PCR confirmed that miR-34a expression was elevated in quiescent satellite cells. However, upon activation of satellite cells *in vitro* the levels of miR-34a decreased. Similarly, in response to Notexin-induced injury and satellite cell activation, endogenous miR-34a levels were reduced until day 3 post-injury, which we propose is permissive for efficient satellite cell activation and muscle repair. Consistent with this, overexpression of miR-34a in Notexin-injured skeletal muscle led to reduced activation of satellite cells as indicated by low numbers of MyoD positive cells and eventual atrophy of regenerated skeletal muscle fibres. Further analysis confirmed that ectopic expression of miR-34a downregulates Notch1 and impedes Notch1 signaling, which we hypothesize is the molecular mechanism behind the impaired

satellite cell activation. Given that Myostatin negatively regulates satellite cell activation we propose that Myostatin functions through miR-34a to regulate satellite cell activation and proliferation and resulting muscle healing.

Collectively the results presented here identify a novel Myostatin target and outlines a new mechanism through which Myostatin regulates myogenesis.

1. Introduction

In this thesis, my objectives were to study the regulation of miRNAs by Mstn and the role of these miRNAs during myogenesis. As I have performed extensive studies in skeletal muscle, this literature review would focus on skeletal muscle, its formation and signaling pathways involved.

1.1 Skeletal muscle

There exists 3 major types of muscles in humans; Cardiac, smooth and skeletal muscle. Skeletal muscle weighs approximately half the weight of a healthy individual and forms the major bulk of the body mass. Skeletal muscles are striated muscle tissues present throughout the body and it consists of a heterogeneous population of cells required for our daily locomotion activities. Movement occurs when skeletal muscles contract voluntarily in response to the somatic nervous system. As these muscles are attached to the bones via bundles of collagen called tendons, contraction pulls the bones thus allowing motions to take place. Besides locomotion, the skeletal muscle also functions to store glycogen, amino acid catabolism and uptake of excess circulatory glucose.

Skeletal muscles are made up of tubular structures known as muscle fibers (muscle cell). The basic unit of a muscle fiber is the sarcomere. Sarcomeres consist of thin and thick myofilaments and therefore contribute to the striated appearance (light and dark bands) of cardiac and skeletal muscle due to the overlapping of both myofilaments (Figure 1.1). Thin myofilaments are mainly composed of actin and thick myofilaments are mainly composed of myosin [1, 2].

The dark bands of sarcomeres correspond to the A band and is the length of a bundle of myosin filaments. The light bands correspond to the I band and are mainly actin filaments. In the middle of each I band is the Z-line and actin filaments anchors into the Z-line of each

sarcomere. In the center of the A-band is a region known as the H-zone and it is where myosin does not overlap with actin filaments. The M line, present in the A band, functions to anchor myosin filaments via protein fibers. Sarcomeres lie in the region between two Z-lines within myofibers which consists of repeating units of sarcomeres [1, 2].

Myofibers are made up of individual contractile proteins comprising of bundles of actin and myosin myofilaments and run the entire length of the muscle fiber (Figure 1.1). Each myofibril is surrounded by a network of transverse (T) tubules and channels known as the sarcoplasmic reticulum which stores calcium required for the contraction of muscles.

Bundles of myofibrils come together to form a single muscle fiber. Each muscle fiber is surrounded by the sarcolemma and capillaries. The sarcolemma, also known as myolemma, is the cell membrane of striated muscle fiber cells. Beneath the sarcolemma is the sarcoplasm which consists of gelatinous fluid, glycogen, fats and mitochondria for cellular energy production. Bundles of muscle fibers form a single fascicle and the endomysium surrounds each muscle fiber (Figure 1.2). The endomysium is a protective sheath of loose fibrous connective tissue. It is enriched with capillaries to supply blood for each of the muscle fibers within the muscle and it is continuous with the perimysium which is a protective sheath of dense fibrous connective tissue surrounding each fascicle. The perimysium is continuous with the epimysium which surrounds the entire skeletal muscle [1, 2].

A

Sarcolemma

Mitochondrion

Myofibril

Dark A band   Light I band   Nucleus

B

Thin (actin) filament

Thick (myosin) filament

Z disc   H zone   Z disc

I band   A band   I band   M line

Sarcomere

C

M line

Z disc   Z disc

Thin (actin) filament

Elastic (titin) filaments

Thick (myosin) filament
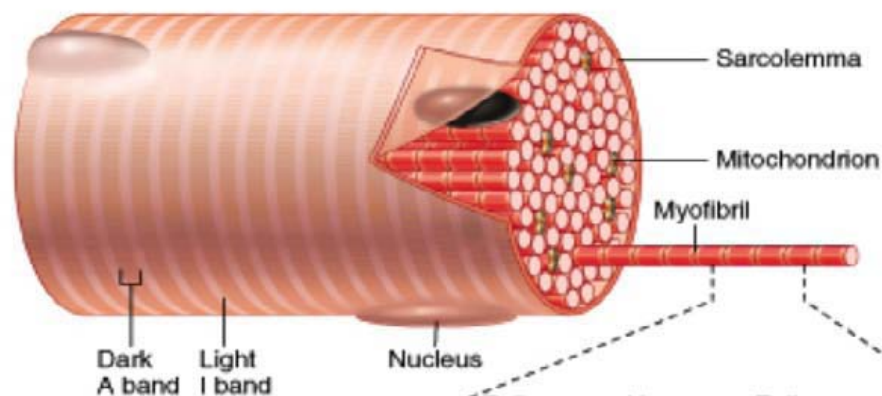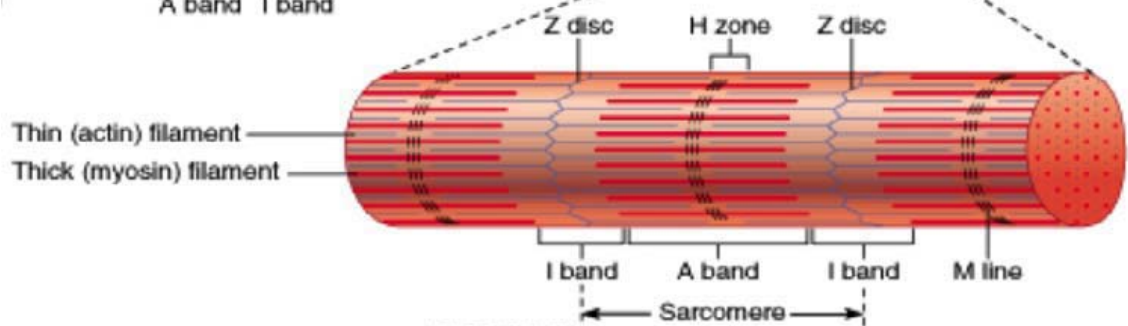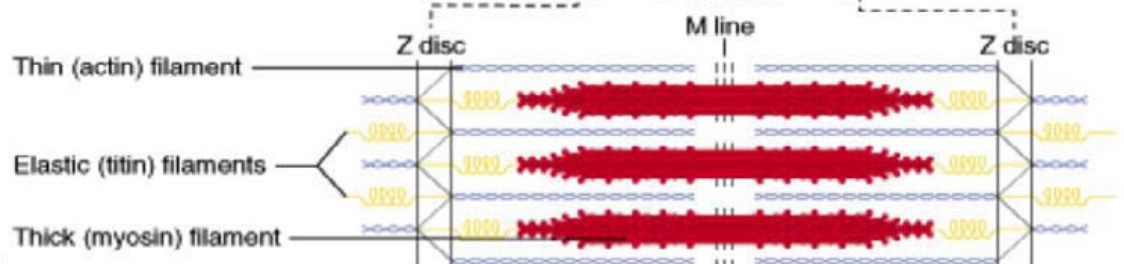
Figure 1.1: ***Microstructure of a skeletal muscle fiber.*** *(A) The skeletal muscle fiber is made up of bundles of myofibrils. (B) Each myofibril is made up of repeated units of sarcomeres which are composed of thin (actin) and thick (myosin) filaments and is encapsulated by the sarcolemma. (C) Each sarcomere spans across 1 Z-disc to the next Z-disc and consists of an A-band and 2 I-bands.*

3
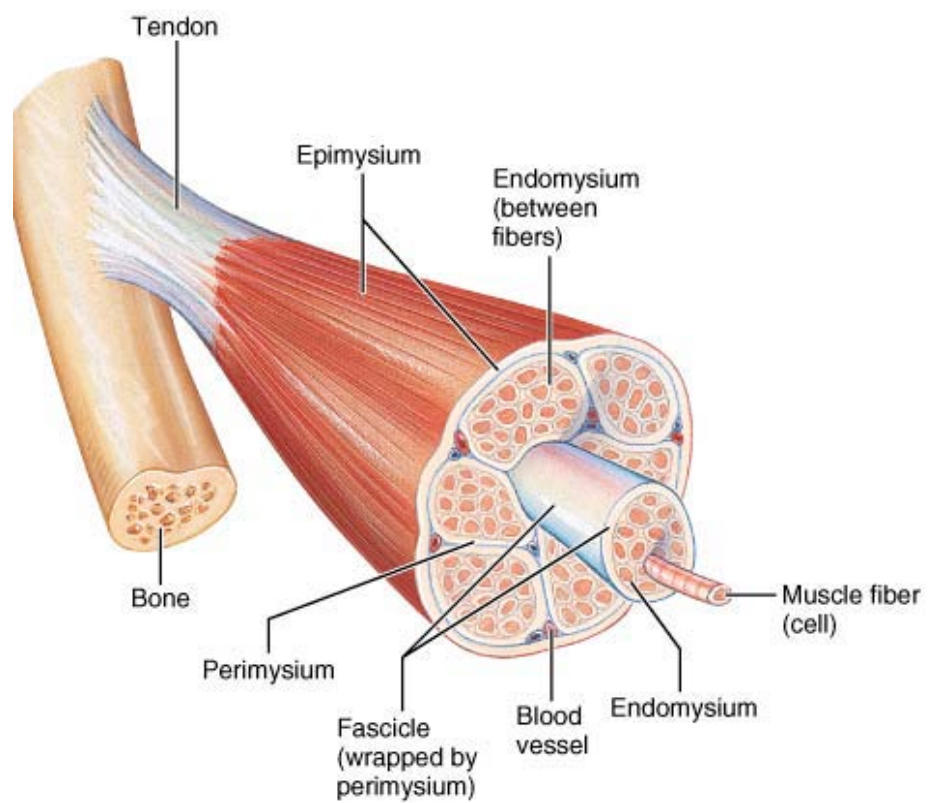
Figure 1.2: *Detailed structure of a skeletal muscle connected to the bone via tendons.* *The basic unit of the skeletal muscle is the muscle fiber. Each muscle fiber is surrounded by the endomysium which consists of capillaries and nerves. Muscle fibers come together*

to form bundles of fibers known as fascicles which are covered by the perimysium. Bundles of fascicles in turn form the skeletal muscle which is covered by the epimysium. The skeletal muscle is attached to the bone by tendons.

1.2 Muscle fiber types

There are 2 types of muscle fibers and they can be categorized into slow twitch (Type I) and fast twitch (Type II) muscle fibers. Skeletal muscle fibers have varying metabolic capabilities and thus different overall functions. Slow twitch muscles utilize oxygen more efficiently to generate ATP and are able to perform muscle contractions for extended periods before reaching fatigue. This is achieved by the high number of mitochondria in slow twitch fibers. In addition, these fibers also have many capillaries and their myoglobin content is higher as compared to the fast glycolytic fibers (Type II) which explains their reddish color. Their rate of contraction is slower than fast twitch muscles.

Fast twitch muscles provide ATP by anaerobic metabolism and are able to provide more forceful, quick bursts of contractions as compared to Type I fibers. However, they reach fatigue quickly [1, 2]. Fast twitch fibers, often referred to a white muscle, have larger muscle fiber diameter and motor unit size as compared to slow twitch fibers. Fast twitch fibers can be further divided into Type IIa, IIb and IIx subgroups. Type IIb fibers are the classic fast twitch fibers, whereas type IIa fibers are intermediate fast twitch fibers, are able to generate ATP via both aerobic and anaerobic metabolism. Type IIx fibers have properties similar to type IIa and b in terms of contraction and half-relaxation time. However, its resistance to fatigue [3] and maximum velocity of shortening is intermediate of type IIa and IIb [4]. Slow twitch (Type 1) fibers and intermediate fast twitch (Type IIa) fibers are more oxidative, when compared to the fast twitch (Type IIb) fibers which are more glycolytic. In addition, these fibers differ by their composition of myosin heavy chain isoforms (MyHC); Slow twitch fibers (MyHC-1) are encoded by MYH7, Type IIa fibers (MyHC-2A) are encoded by MYH2, Type IIx fibers (MyHC-2X) are encoded by MYH1 and Type IIb fibers are encoded by MYH4 [5]. All 4 fiber types are present in several mammalian species, mice and rats. However, in the muscles of

humans only types I, IIa and IIb exists. The composition of muscles often consists of a mixture of fiber types e.g. Type I and IIa, IIa and IIx or IIx and IIb MyHCs [6]. The mixture of fiber types can and often changes especially in response to exercise [7] or electrical stimulations [8]. In addition, muscle fiber switching also occurs in response to muscle atrophy such as denervation [9] and the fiber switch profile depends on the muscular atrophy disease. For example, in diseases/conditions such as denervation, spinal cord injury and during periods of prolonged unloading, such as during limb immobilization, prolonged bed rest and space flight (microgravity), a conversion from slow twitch to fast twitch occurs. On the other hand, conditions such as fasting and cachectic-like muscle wasting, which is associated with underlying chronic illnesses (such as diabetes, sepsis, cancer, aids and ageing), a conversion from fast to slow twitch fibers occurs (reviewed in [10]).

1.3 Myogenesis

1.3.1 Embryonic myogenesis

Mammalian skeletal myogenesis is a multi-step and complex process that begins during the first week of embryonic development. During embryogenesis, the three germ layers (ectoderm, mesoderm and endoderm) are determined in early gestation. The mesoderm is divided into paraxial, intermediate and lateral mesoderm. The paraxial mesoderm which is present on both sides of the notochord and neural tube develops into the somites which progressively form from cranial to caudal positions, in response to changes in gene expression and morphogen gradients [11].

Skeletal muscles originate from somites of the mesoderm. The polarities of somites are established with increasing retinoic acid and this allows distinction of dorso-ventral compartments [12]. The most ventral portion of the somites forms the mesenchymal sclerotome which consists of cartilage and bone precursors. The most dorsal of the

somites becomes the dermomyotome which develops into epaxial and hypaxial skeletal muscle [13].

All skeletal muscles, except head muscles, are derived from the dermomyotome. The dermomyotome is a sheet-like structure where the edges bend inward towards the sclerotome (Figure 1.3). Cells in the dermomyotome express Paired-box transcription factors 3 and 7 (Pax3 and Pax7) but have low expression of the basic helix-loop-helix transcription factor Myogenic factor 5 (Myf5) [14]. Pax3 expressing cells direct cells in the dermomyotome into myogenic lineage and these Pax3-myogenic precursors express Pax7, later on, producing muscle progenitors for embryonic and fetal myogenesis [15-17].

From the lips of the dermomyotome, muscle pioneer cells migrate beneath the dermomyotome epithelium and begin to differentiate. As the primary myotome develops, muscle progenitors are added to the myotome and these cells elongate into cylindrical fibers i.e. muscle fibers begin forming by fusion of fusion-competent myoblasts. The myotome is a primitive muscle structure containing Myogenic Differentiation 1 (MyoD), another member of the bHLH transcription factor family, and Myf5 positive committed muscle cells [18, 19].

During late embryonic and fetal stage, muscle progenitors arise from the dermomyotome. These cells translocate from the central dermomyotome and are responsible for the continued muscle growth during late embryonic myogenesis [15]. These fetal myoblasts develop and fuse to form secondary myofibers [20] by fusion at the ends of primary and secondary myofibers. Myofibers begin to express different myosin heavy chain isoforms which distinguishes fast and slow twitch muscles in adults [21].

As development proceeds, the central region of the dermomyotome fragments. This leads to the migration of muscle progenitors which integrates into the primary myotome [22]. These muscle progenitors

give rise to muscle stem cells (satellite cells) that will reside in post-natal skeletal muscle and are known progenitors involved in adult skeletal muscle myogenesis [22, 23]. These muscle stem cells are found in between the basal lamina and sarcolemma of skeletal muscles.
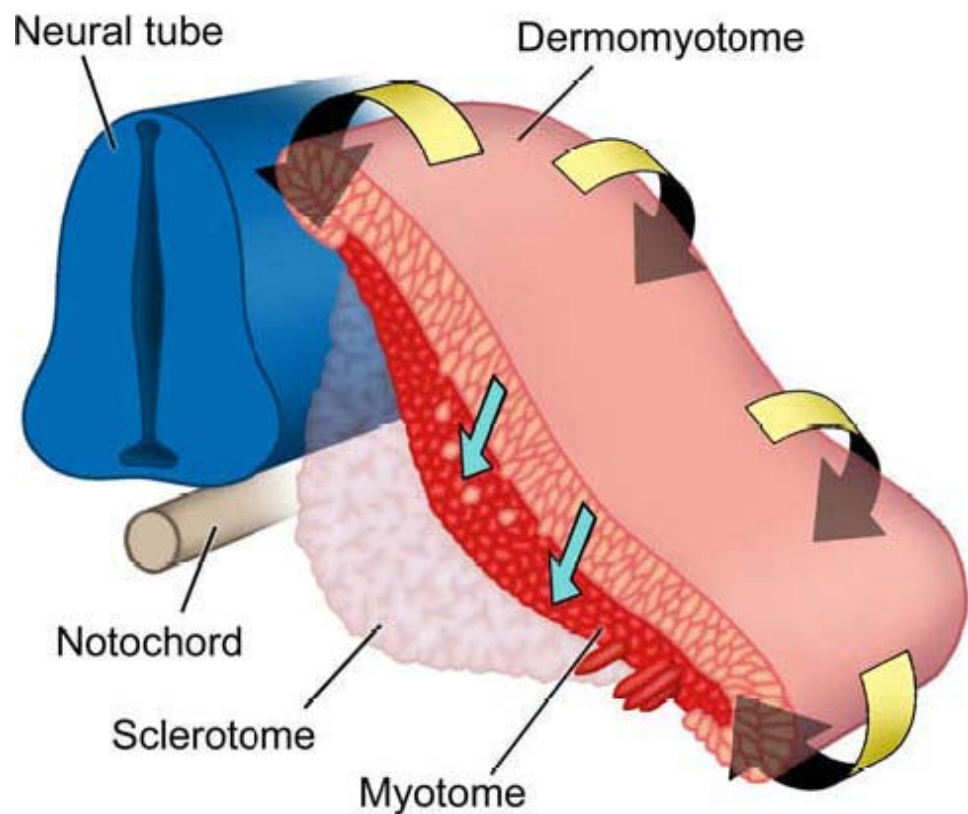
Figure 1.3: ***Migration of myogenic precursor cells from the dermomyotome to myotome.*** *During embryonic myogenesis, cells in the dermomyotome begin to express Pax3 and Pax7. These muscle pioneer cells begin to migrate from the lips of the dermomyotome to the myotome. More muscle progenitor cells are added to the myotome as the primary myotome develops and the formation of myofibers results when these muscle progenitor cells fuses.*

1.3.2 Myogenic proteins involved in embryonic myogenesis

Transcription factors Pax3 and Pax7 are important in embryonic myogenesis. It is known that Pax3 required during the beginning/early stages of embryonic skeletal myogenesis while Pax7 is vital and expressed in satellite cells during post-natal skeletal myogenesis [17].

Myf5 is the first myogenic regulatory factor (MRF) expressed during embryogenesis. It is upregulated in the paraxial mesoderm and functions in concert with other MRFs (Myogenin, MRF4 and MyoD) during the development of the myotome [24, 25]. The expression of Myf5 commits myogenic cells in to muscle lineage. In most muscle progenitors, Myf5 may function similarly to Pax transcription factors [26] where their signaling pathways converges. Ultimately, Pax3 and Pax7 function to activate MyoD which is a transcription factor crucial in regulating muscle differentiation. The rapid activation of MyoD allows the alignment of myoblasts and also the transcription of myogenin which is required for the activation of muscle specific genes and therefore the initiation of differentiation programme. Eventually myoblasts fuses to form myotubes and myofibers following the upregulation of myogenin.

During embryonic myogenesis, Pax3 and Pax7 are able to partially compensate for each other, and myogenesis in Pax3:Pax7 double knockout results in formation of early embryonic muscle of the myotome. This is more defective as compared to Pax3 loss-of-function mutant mice [17]. In addition, loss of Pax3 lineage results in the formation of embryonic lethality Pax7 positive cells. In contrast, removal of Pax7 positive cells leads to defects only in later stages of development; limbs with fewer myofibers and smaller muscles [27, 28].

Similarly, the functions of Myf5 and MyoD have been shown to be redundant during myogenesis. In Myf5 knockout mice, embryonic myogenesis was delayed but was resumed upon MyoD expression

[29]. Reciprocally, MyoD knockout mice compensates for the loss of MyoD by prolonging Myf5 expression [30]. In addition, MyoD:Myf5 double knockout mice lacked myogenin and skeletal muscle [31].

1.4 *In vitro* cell culture models

C2 and C2C12 are well established murine skeletal myoblast cell lines used for research purposes. Both of these cell lines were originally obtained from adult C3H leg muscle where injury was induced via crushing. This activated satellite cells and thus proliferation. This population of satellite cells were isolated and established as the C2 cell line [32]. The C2C12 cell line is a subclone of C2 myoblasts commonly used for differentiation studies and behave similar to activated satellite cells present in muscle fibers. Although both C2 and C2C12 cell lines have shared origins it was shown that these cells have different differentiation potential [33]. Despite their differences, both cell lines provide insight to atrophy (loss of muscle mass) and hypertrophy (gain of muscle mass), and thus muscular disorders/diseases and regeneration. In addition, C2C12 cells express Transforming growth factor beta 1 (TGF-β) superfamily receptors (including ActRIIb) and are also used for examining TGF-β and BMP (Bone Morphogenetic Proteins) -mediated Small Mothers Against Decapentaplegic (SMAD) signaling. Therefore, in my project, I will be using C2C12 as an *in vitro* cell culture model to study the function of microRNAs in muscle cells.

1.5 Post-natal myogenesis

Muscle regeneration is generally divided into 3 phases (Figure 1.4) [34]. Destruction phase: necrosis and rupture of myofibers, hematoma formation and inflammatory reaction. Repair phase: Dead tissue from damaged muscle is phagocytosed. Remodeling phase: Maturation of regenerated myofibers, re-organization of scar tissue and regaining muscle capabilities.

The destruction phase begins upon injury and lasts for 3 days post-injury. The presence of necrosis marks the initiation of muscle regeneration. During this phase, muscle degeneration and inflammation occurs. Macrophages residing at the injury area are activated and these cells start releasing chemoattractants. Neutrophils and monocytes are recruited to the site of injury via these chemotactic

signals. Leucocytes can also be recruited to the injury site through the action of growth factors, including hepatocyte growth factor (HGF), fibroblast growth factor (FGF) and TGF-β. Macrophages phagocytose dead tissue produced from necrosis and also secrete growth factors (FGF and TGF-β) and proteases to break down the extracellular matrix (ECM) which allows remodeling to occur. Any delay in the inflammatory response for example in the muscle atrophy mice model, Duchenne Muscular Dystrophy (DMD) [35], and phagocytosis will delay myogenesis [36]. The duration of inflammatory response depends on the extent of injury [37]. In response to the necrotic damage, satellite cells residing on myofibers become activated and by 24hrs, they begin to proliferate. They then migrate to the site of necrosis via chemotaxis. After 3.5 days post-injury, small multinucleated cells (myotubes) would have formed due to the fusion of myoblasts [38]. Subsequently, these myotubes fuse further and either replace the damaged myofibers or fuse with damaged segements of myofibers. This occurs within a week post-injury and is completed at the end of 2 weeks post-injury [39, 40]. As mentioned earlier, inflammation is a key step in the initiation of muscle regeneration. Therefore, the inability of inflammation to occur due to various reasons such as impaired recruitment of inflammatory cells can lead and might be a cause of impaired regeneration. This can be further explained by the requirement of phagocytes to clear necrotic tissues to allow the migration of satellite cells to site of damage so that myogenesis can begin. An example to illustrate the importance of inflammation is in autografts of whole muscle grafts which undergo myonecrosis and normal muscle is formed by the 5th day. However, by blocking TNF-α (Tumor necrosis factor), an inflammatory cytokine, regeneration was impaired due to the delayed inflammatory cell migration and therefore initiation of myogenesis [41].

Fibrosis, the deposition of ECM (extra-cellular matrix) such as collagens and fibronectin, occurs in response to inflammation following necrosis. In the case when the area of damage is large and angiogenesis is impaired, this prevents revascularisation of skeletal

muscles to re-establish blood supply. When angiogenesis is delayed and when large portions of damaged muscle fibers undergo ischemia, fibrosis occurs instead of myogenesis and this leads to scar tissue formation. Thus, the extent of fibrosis reflects the efficiency of angiogenesis [36, 42].

1.6 Satellite cells and post-natal regeneration

In adults, myogenesis begins from a self-renewing population of myogenic progenitors, known as satellite cells. Satellite cells are also known as the classic myogenic precursor cells (myoblasts) in post-natal or adult vertebrate skeletal muscle. Evidence for satellite cells in myogenesis and regeneration emerged when these cells were transplanted into skeletal muscle, and their function and myogenic fate assayed; satellite cells are able to contribute myoblasts for both growth and repair *in vivo* [43-46].

Satellite cell numbers in muscles decreases with age coupled with loss of muscle mass, sarcopenia [47, 48] and in muscle dystrophies associated with muscle wasting [49]. In contrast, exercise increases satellite cell numbers in young and aged mice [50, 51].

In adult skeletal muscle, quiescent satellite cells expresses Pax7 [28], M-cadherin [52] and saliomucin, CD34 [53], and many others [54]. In addition, Myf5 was also shown using Myf5nlacZ/1 mouse [48, 53, 55] and several transgenic mouse lines [56] to be activated in quiescent satellite cells. Satellite cells are known to have differing characteristics. For example, upon injury, satellite cells either proliferate giving rise to more daughter satellite cells or become committed to differentiation. Another sub-population of satellite cells have been considered to be committed precursor cells that do not proliferate [57]. Lastly, a subset of satellite cells is thought to exist in a deep quiescent state. These deeply quiescent satellite cells are resistant to high doses of radiation and are activated upon onset of extreme trauma [58].

Satellite cells are commonly present in a quiescent state. However, in response to several stimuli these stem cells become activated, for example, in the event of acute injury [45, 46, 59], hepatocyte growth factor [60], exercise [61] and denervation [62]. The activation of satellite cells involves several signaling pathways.

One example is the Notch signaling pathway where quiescent satellite cells transit to activated state and begin proliferating [63]. This expands the myoblast population. Regeneration by satellite cells requires Notch signaling. Self-renewal in satellite cells is reduced when Notch signaling is absent and this also results in reduction of quiescent satellite cell pool [64, 65] and this would lead to an impairment of muscle regeneration. Furthermore, inhibition of Notch signaling via the hairy and enhancer of split-related (HESR) family of bHLH transcriptional repressors, such as Hesr1 and Hesr3, results in satellite cell differentiation, reduced self-renewal, satellite cell pool depletion and impairment of muscle regeneration [66]. Besides molecular proteins involved in Notch signaling, miRNAs in satellite cells have been reported to contribute to regeneration. In Pax7$^{CreER/+}$:Dicer$^{flox/flox}$ mice when mature miRNAs processing was inhibited via inactivation of the processing enzyme Dicer, this caused satellite cells to undergo apoptosis and muscle regeneration did not occur even after 6 months post Dicer inactivation [67]. This study suggests the importance of miRNAs during muscle regeneration.

Activation of quiescent satellite cells is a complex process [68] and it involves signaling of several factors such as FGFs, HGF, Myostatin (member of TGF-β superfamily), nitric oxide and mechanical stretch [69, 70]. Hepatocyte growth factor/scatter factor (HGF/SF) has also been linked to satellite cell activation [60, 71]. Activated satellite cells are known as myoblasts. Skeletal muscle specific transcription factors, including MyoD and Myf5, which belong to the myogenic regulatory factor (MRF) family of bHLH transcription factors, are upregulated in these cells (see below). This positively regulates proliferation of

myoblasts. Several growth factors play a role in inducing proliferation of myoblasts. These factors include LIF, HGF, FGF, PDGF and insulin-like growth factor (IGF I and II). Satellite cells are also able to be activated in response to other FGF growth factors as these cells express all known FGF receptors [71, 72]. Some factors like TGF-β and bFGF [73] induce proliferation whilst inhibiting differentiation to allow myoblast numbers to obtain adequate density for myotube formation. Recent studies have showed that these growth factors mediate its effects via Notch, Wnt signaling, miRNAs, Pair-box transcription factors Pax3 and Pax7, and MRF factors (MyoD, Myf5 and myogenin), resulting in gene transcription of myogenes [74].

During post-natal myogenesis, activated satellite cells begin to express MRFs (MyoD and Myf5) in a manner similar to embryonic myogenesis. The activation of satellite cells into myoblasts involves rapid activation of MyoD expression [75-77] and these satellite cell-derived myoblasts express the same myogenic markers as myoblasts during development stages (Figure 1.5). The differentiation of myotubes involves several MRFs such as MyoD, Myf5 and myogenin. These bHLH transcription factors heterodimerize with E-proteins and act in a temporal manner to mediate the activation of target genes. Following MyoD expression, CD34 isoform switch occurs but Pax7, M-cadherin and Myf5 expression levels are maintained. Myoblasts begin dividing and start to express cell cycle genes such as PCNA. Subsequently, myogenic differentiation begins due to the onset of Myogenin expression which marks the initiation of myogenic differentiation [75-79]. The temporal expression of MRF4 is still controversial as it has been reported that the expression of MRF4 could be either after or before myogenin expression [80, 81]. In addition, other regulatory factors and structural muscle genes such as myosin light and heavy chains are expressed during the course of differentiation. Muscle progenitor cells either fuse with themselves to form myotubes and eventually form primary myofibers, or they could fuse with damaged muscle fibers during injury [82].

Using *in vitro* satellite cell cultures and 3D time lapse analysis it was shown that satellite cells are highly motile in response to a chemotactic signaling molecule, SDF-1 [83]. In addition, chemotactic molecules such as MOR23 (an odorant receptor), CXCR4 (chemokine receptor), angiotensin II and Eph/Ephrin also have an effect on satellite cell motility and migration [84-86]. *In vivo* analysis has also revealed that satellite cells in non-injured soleus of mice are immotile while satellite cells are motile in an injured muscle [87].

Evidence for the ability for self-renewal in satellite cells was derived from lineage tracing experiments conducted in muscle. When an isolated myofiber together with a few satellite cells were transplanted into adult skeletal muscle, there was amplification of donor-derived satellite cells [43]. Similarly, when a single satellite cell separated by fluorescence-activated cell sorting (FACS) was transplanted into a host skeletal muscle, many donor-derived satellite cells could be obtained [88]. In addition, satellite cells transplanted and amplified in the host could be isolated, transplanted and recovered again several times [89]. In Pax7$^{-/-}$ mice, satellite cell numbers are reduced (<80%) and muscles display fibers of smaller caliber consisting of few myonuclei which results in muscle weakness [17, 28, 90]. In addition, Pax7$^{-/-}$ mice displayed no obvious phenotype at birth [91] but had retarded growth and only survived to 2 weeks of age [28]. In a study using inducible Pax7-Cre null allele (Pax7^{CE}) mice, when tamoxifen was administered at different stages of post-natal growth [92], regeneration was compromised up to day 21 post treatment. These experiments demonstrated the requirement of satellite cells during post-natal muscle growth. The self-renewal potential of satellite cells displayed in these studies termed these cells myogenic stem cells. In addition, MyoD$^{-/-}$ mice had increased satellite cell numbers, abnormal myoblast proliferation was observed and muscle differentiation factors such as MRF-4 and myogenin failed to be upregulated [93]. These studies

displays the ability for satellite cells to self-renew and differentiate and therefore shows that these cells possess stem cell properties.

Although an *In vitro* study provided evidence for satellite cell contribution to osteogenic and adipogenic lineages and therefore multipotency in satellite cells [94], the differentiation capability of satellite cells are however limited to unipotentcy as suggested by several recent studies. Through recombination-based lineage tracing, lipid accumulation was observed when satellite cells were stimulated but was unable to undergo *in vitro* terminal adipogenic differentiation [86]. Furthermore, inhibition of myogenic differentiation in satellite cells by BMP did not affect the osteogenic lineage greatly [95].

1.7 bHLH transcription factors

There are 2 classifications of bHLH transcription factors. Class I bHLH transcription factors are E-proteins, such as HEB/HTF4, E2-2/ITF-2, and E12/E47 and class II bHLH transcription factors include MRFs which can either homodimerize (with another MRF) or heterodimerize with class I bHLH transcription factors. The expression of Class II transcription factors is ubiquitous and controlled in a temporal manner during the course of development. The domains of E-proteins often include a basic region which is required for DNA binding and a HLH domain which is the region that dimerizes with other bHLH proteins [96]. Evidence of an E-protein required for myogenesis is HEB also known as Transcription factor 12; TCF12. It was shown to be localized in the nucleus in differentiating L6 and C2C12 myoblasts. However, in adult muscle tissue (Soleus, TA and heart), there is no expression. Furthermore, the expression of HEB in C2C12 myotubes gradually decreases during differentiation from day 2 through day 6 [97]. In addition, the knockdown of HEB resulted in decreased MyoD and myogenin expression levels and that the co-expression of HEB and MyoD enhanced the transcription of myogenin [98]. This suggests HEB plays an important role as a co-activator of MyoD during the initiation of differentiation.

Another E-protein E2A encodes for 2 alternatively spliced variants, E12 and E47. These E-proteins can form hetero-oligomers with specific bHLH proteins via the HLH domain such as MyoD. It was demonstrated that the heterodimerization of E12 and MyoD lead to increased affinity and tighter binding on the MEF1 site on muscle creatine kinase, where MyoD or E12 alone binds weakly [99]. In addition, MyoD-E12/E47 association functions as an activation point for downstream regulators (i.e. myogenin). Homodimer/heterodimer bHLH proteins recognize a consensus sequence (CANNTG) which is known as an E-box sequence. It was demonstrated *in vitro* that MRFs can heterodimerize with any E-protein to bind E-box sequences to activate transcription of target genes [100]. For example, MyoD and Myf5 can interact with E-proteins (a subfamily of bHLH proteins) such as E2-2/TCF4, HEB/TCF12, and E2A/TCF3 to form heterodimers and function as transcriptional activators. These E-proteins and MyoD can heterodimerize or homodimerize with the protein Id (a HLH protein) and Musculin (MSC) or MyoR (a bHLH protein) to form inhibitory dimers [101, 102]. This results in repression of MyoD activity.
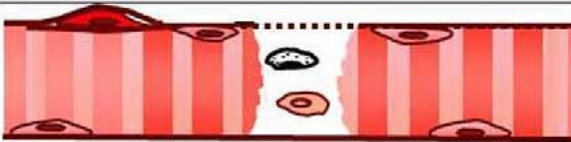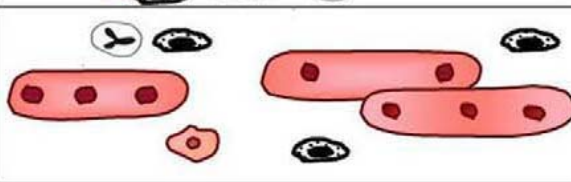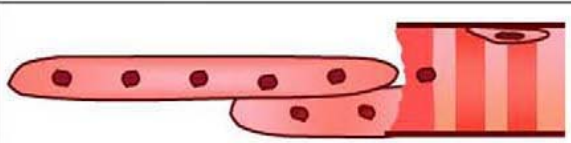
	~ Day	Activity	Schematic representation
Inflammation & proliferation	0	Injury - membrane damage. Necrosis and myoblast activation	
Inflammation & proliferation	1-7	Inflammation and myoblast proliferation	
Formation, growth and maturation of myotubes and myofibres	3-7	Myoblasts differentiate and form myotubes. Myotubes fuse together	
Formation, growth and maturation of myotubes and myofibres	7-10	Myotubes fuse with end of damaged myofibres	
Formation, growth and maturation of myotubes and myofibres	7-21+	Growth and maturation of regenerated portion of myofibre	

Figure 1.4. Stages of muscle regeneration during skeletal muscle post-injury. *The table above shows the sequence of events/stages that occurs during muscle regeneration follow injury. After 1 day post-injury/damage, necrosis becomes obvious and fragmented sarcoplasm and inflammatory cells are observed. Between 3-7 days post-injury, myoblasts become activated, proliferate and eventually fuse to for differentiated myotubes. Between days 7-10 post-injury, myoblasts*

fuse with the damaged muscle fibers. Following this, the newly formed fibers mature into adult myofibers by 3 weeks post-injury.
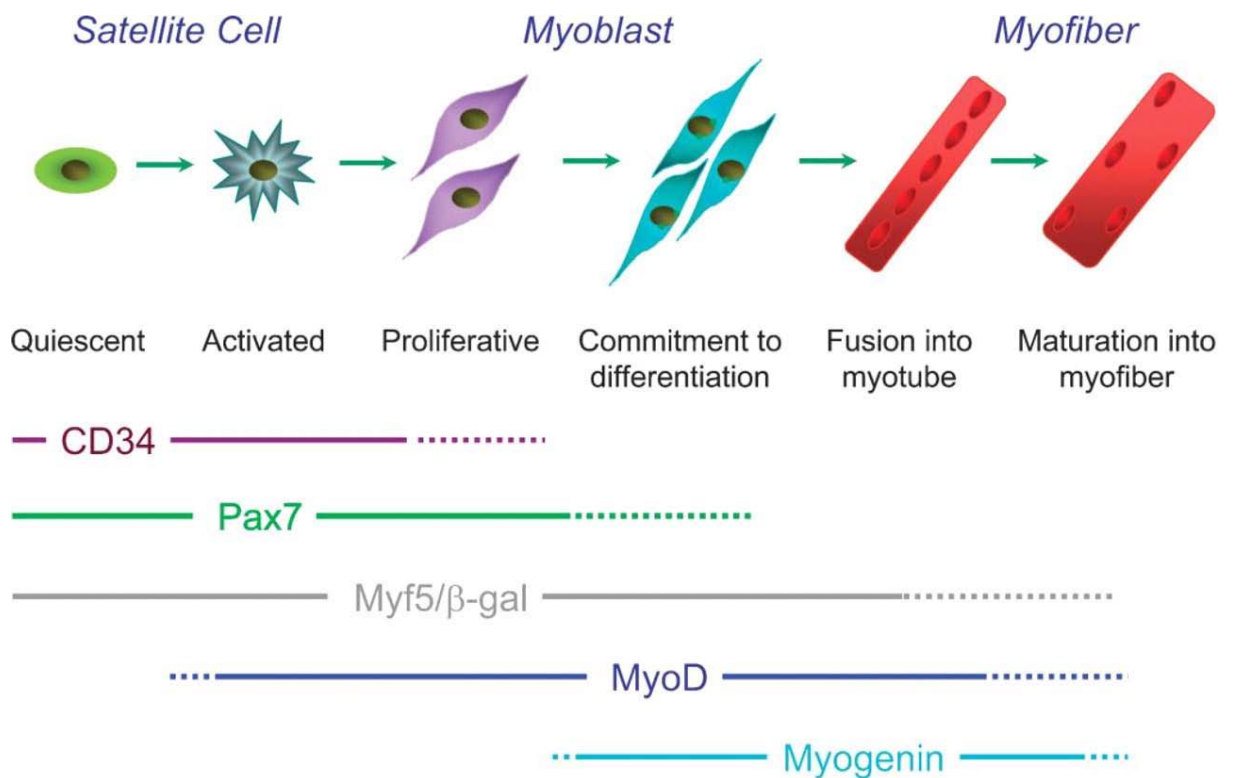
Figure 1.5*: **Key markers involved in formation of nascent myofibers originating from quiescent satellite cells.** Myf5/beta-gal represents the fusion protein product expressed in Myf5nlacZ/1 mouse [55]. Quiescent satellite cells express CD34, Pax7 and Myf5. The expression of these markers diminishes as satellite cells commit to differentiation. In response to stimuli, satellite cells begin to express*

MyoD and become activated, which results in the expression of Myogenin and the commitment of myoblasts to differentiate. Fusion of myoblasts into myotubes then ensues, with new myofibers eventually formed.

1.8 Growth factors involved in myogenesis

Over the past 2 decades, various factors have been discovered which have been shown to be involved in myogenesis.

1.8.1 Insulin-like growth factor

Insulin-like growth factors (IGFs) exert anabolic effects on skeletal muscle as well as many other tissues [103]. The effects of IGFs include increased glucose uptake, cell proliferation, increased amino acid uptake, incorporation of uridine and thymidine into nucleic acids, etc. In addition, IGFs also inhibits protein degradation of proteins [104] and were demonstrated to induce myogenic differentiation as observed by biochemical (CK activity) assays in L6 muscle cell lines [104]. Besides *in vitro* stimulation of myogenesis, IGFs were shown to induce chick embryo muscle cells [105] and L6 (Rat myoblasts) satellite cells [106] to differentiate.

1.8.2 Transforming growth factor (TGF-β)

TGF-β was shown in 4 different cell lines, L6AI, L6E9, C2 and BC3HI, as a potent inhibitor of myogenic differentiation [107, 108]. In these cell lines, TGF-β mediated its inhibition by blocking fusion and elevating creatine kinase activity. Also, the acetylcholine receptor expression and transition from β- and γ- to α-actin was observed in the presence of TGF-β in a concentration dependent manner. In addition, TGF-β was shown to inhibit satellite cell differentiation of rat skeletal muscle, and primary myoblast cell cultures isolated from rat and quail embryos [109].

1.8.3 Fibroblast growth factor (FGF)

FGFs are mitogenic factors that have been demonstrated to inhibit myogenic differentiation. For example, in BC3H1 quiescent satellite cells, FGF caused G_0 exit from the cell cycle [110] and increased the expression of oncogenes c-myc and c-fos which led to inhibition of myogenic differentiation [111]. In addition, FGF was shown to inhibit expression of MyoD [112] and myogenin [113].

1.8.4 Myostatin (Mstn)

Mstn is a member of the TGF-β superfamily of secreted growth factors. Myostatin, also known as growth and differentiation factor 8 (GDF8), has been extensively characterized as a potent inhibitor of skeletal muscle myogenesis.

Mstn was first discovered in mice where muscle mass was observed to exhibit enhanced growth [114] and the same phenomenon was later also observed in Belgian blue and Piedmontese cattle [115]. During embryogenesis, Mstn is specifically expressed in the myotome. However, at late stage development and in adults, Mstn is expressed at varying levels in different skeletal muscles types and lower levels in other tissues [116]. $Mstn^{-/-}$ mice are larger than wild type mice in size with 30% more muscle mass. Individual muscles are about 200-260% larger than wild type and this is the result of muscle hypertrophy and hyperplasia [117]. On the contrary, introduction of recombinant MSTN *in vitro* reduced myotube diameter which suggests anti-anabolic or catabolic effects mediated by Mstn [118]. Shortly after the discovery of Mstn, its homologues were identified in several mammalian species [114]. For example, a mutation in the Mstn gene in Belgium Blue cattle resulted in enhanced muscle growth [119]. Similarly, a naturally occurring mutation in the Mstn gene and the heterozygous mutant in whippet dogs resulted in excessive muscle growth [120]. Muscle atrophy induced by reduced food intake in sheep showed an increase in Mstn levels [121]. These findings demonstrate that the role of Mstn in mammals is conserved.

The link between Mstn and human diseases (muscle and non-muscle) has been reported by several groups. In disuse atrophy, when a 25 day bed rest experiment was conducted to mimic microgravity effects, a negative correlation was observed between body mass and serum Mstn levels [122]. In another disuse atrophy model, hip arthroplasty, Mstn mRNA levels were elevated 5 days post-surgery [123]. Furthermore, liver cirrhosis in rat was observed to have increased Mstn protein expression and decreased myosin heavy chain and MyoD in the gastrocnemius muscle [124].

Mstn is a secreted endocrine hormone which is synthesized as an inactive form and further processed to its active form via cleavage of its propeptide domain. The C-terminus of Mstn is the active domain which forms homodimers [125] and is released from the cell where it functions in an autocrine or paracrine fashion [126].

Mstn binds to the activin receptor type IIB (ActRIIB) resulting in homodimerization of ActRIIB, which leads to subsequent recruitment and phosphorylation of either activin receptor-like kinase-4 or -5 (activin type 1 receptors; ALK4 or ALK5). The phosphorylation of ALK4/5 activates and further leads to phosphorylation and activation of SMAD2 and SMAD3 transcription factors (R-SMADs) (Figure 1.6). This in turn allows binding with SMAD4 (Co-SMAD). The transcription factor trimer complex then translocates into the nucleus to promote target gene expression with the help of DNA and nuclear proteins [127]. One of the effects is the inhibition of MyoD and myogenin expression [128, 129] via MEK/Erk1/2 signaling pathway which results in the inhibition of myoblast fusion and proliferation. Another SMAD protein (SMAD7), which functions as an inhibitory SMAD, is also activated by Mstn. However, it functions as a negative feedback inhibitor in Mstn signaling pathway by interfering with the association of the heterodimer SMAD2 and SMAD3 [130, 131]. In another study, the expression of Mstn was found to be regulated by SMAD3 proteins in an auto-regulatory

mechanism [132] where Mstn increased SMAD3 expression and in turn miR-27a/b. This led to the direct inhibition of Mstn and reduced SMAD3 levels. These results were consistent with studies performed in SMAD3^{-/-} mice where an increase in Mstn levels was observed which resulted in impaired satellite cell activation and muscle atrophy [133].

Another signaling event which occurs in response to Mstn is the inhibition of AKT phosphorylation [134]. This was seen in MSTN treated myotubes where AKT phosphorylation was observed to be reduced [135]. As a result, FOXO1 and FOXO3 transcription factors are unphosphorylated allowing their translocation into the nucleus activating E3-ubiquitin ligases, MAFbx (Atrogin-1) and MuRF-1 [136, 137], which promote protein degradation through the proteasomal pathway [138]. AKT is a potent anabolic signaling protein and the activation of AKT activity enhances protein synthesis pathways. Active AKT leads to inhibition of glycogen synthase kinase 3 (GSK3), increased mTOR activity which phosphorylates and inactivates 4E-BP1, and it also results in the activation of the ribosomal protein p70 S6 kinase (p70S6K) [139, 140]. This allows the eukaryotic translation initiation factor (eIF4E) to mediate protein synthesis as its suppression is relieved [129]. Studies on $Mstn^{-/-}$ mice and cattle revealed an upreglation of AKT/mTOR pathway [141, 142] which affirms that in addition to enhancing proteasomal degradation, Mstn also inhibits protein synthesis via the potent anabolic signaling protein, AKT [143].

Proteins to be degraded are tagged with ubiquitin and are either degraded via the proteasomal pathway or autophagy pathway. The treatment of Mstn (10µg/ml) in C2C12 cells resulted in reduced myotube diameter (57%). This was a result of upregulated Atrogin (150% compared to control) but not Murf1. Atrogin and MurF1 are ubiquitin ligases which function to catalyze the addition of ubiquitin molecules to proteins destined to be degraded. Although MSTN treatment results in a lack in AKT phosphorylation which results in

increased atrogin and MurF1, upregulation of these E3 ubiquitin ligases could also occur in an AKT-independent manner as seen in $AKT^{-/-}$ mice [144].

Mstn has been shown to inhibit the proliferation of myoblasts in a dose-dependent manner. Upon treatment of Mstn in myoblasts, p21 (Waf1, Cip1) a cyclin-dependent kinase inhibitor, is upregulated. This is coupled with the decrease in Cdk2 levels and activity which leads to an accumulation of hypophosphorylated Rb protein. Cells were also observed to be arrested in the G1/S and G2/M cell cycle phases [145]. In addition, both DNA and protein synthesis was inhibited in these cells [125].
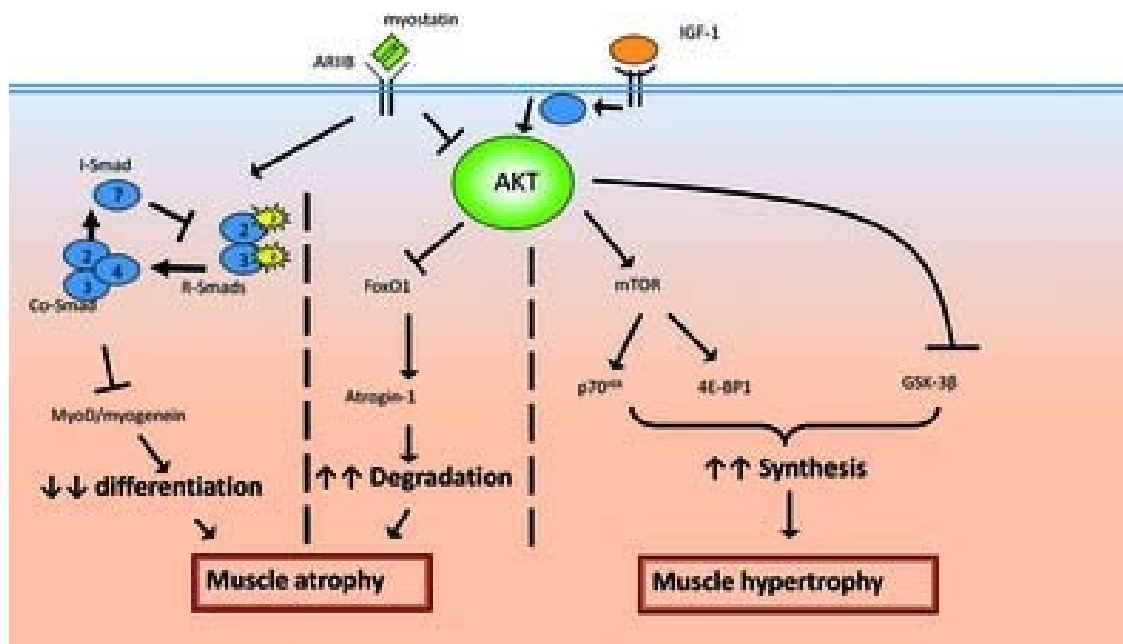
Figure 1.6. Mstn signaling pathway initiates protein degradation and inhibition of protein synthesis. The degradation pathways begins upon Mstn interaction with its receptor (ActRIIb), afterwhich the transcription factors SMAD2 and SMAD3 (R-SMAD) are phosphorylated, resulting in the dimerization and recruitment of the Co-SMAD, SMAD4. The resulting heterotrimer complex represses the transcriptional activation of MRFs, such as MyoD and myogenin leading to inhibition of myoblast differentiation. Molecular mechanisms through which Mstn produces muscle atrophy is through the inhibition of AKT signaling. Mstn-mediated inhibition of AKT phosphorylation prevents the phosphorylation of the transcription factor FOXO1, resulting in enhanced translocation of FOXO1 into the nucleus to activate FOXO1 target genes, such as E3-ubiquitin ligases, MAFbx (Atrogin-1) and MuRF-1. The inhibition of AKT phosphorylation also prevents protein synthesis. Also depicted in this figure is the IGF-1 signaling pathway, which promotes muscle hypertrophy, where IGF-1R interaction results in the phosphorylation of AKT leading to the activation of mTOR and subsequently p70S6 kinase and 4E-BP1, and the inhibition of GSK-3β.

Mstn also has the ability to inhibit the fusion of myoblasts to form myotubes. This was demonstrated in Mstn overexpressing stable cells which had decreased differentiation response [146]. Consistently in another study, the treatment of Mstn blocked the differentiation of myoblasts and was demonstrated to have reduced MyoD, Mfy5 and Myogenin levels [147]. MyoD is an important transcription factor and is a rate-limiting regulator of myoblasts differentiation [148] which suggests that MyoD is a pivotal factor during differentiation of myoblasts where its lack affects downstream MRFs and their functions. One of the ways Mstn regulates MyoD is via SMAD3 and was shown to be mediated by SMAD3 phosphorylation which induces SMAD3-MyoD association therefore interfering with MyoD activity and function [147]. This was further shown in a rescue experiment where recombinant MSTN treated C2C12 myoblasts in the presence of dominant-negative SMAD3 could still activate MyoD promoter reporter (Reviewed in [129]).

In a recent study, human Mstn was also shown to have conserved functions as their mouse homologues. Human myoblasts treated with human Mstn accumulated at G1 boundary of the cell cycle, and were observed to have increased p21 and decreased CDK2 levels [149]. These observations are consistent in prior studies in Mstn treated C2C12 cells [125]. In addition, differentiation of myotubes was inhibited as shown by the decrease in myogenin, myosin heavy chain, myosin light chain and MyoD expression level. Increased Notch signaling pathway during differentiation was observed and Notch was shown to complex with SMAD3 upon Mstn treatment [149]. Similar findings were also observed in a previous study of Mstn treatment in C2C12 cells [147].

Evidence of Mstn function in satellite cells was demonstrated in a study performed on aged (Sarcopenic) mice where the blockade of Mstn led to enhanced muscle regeneration following notexin-induced injury in

these aged mice [150]. This was indicated by increased Pax7 and MyoD levels, improved macrophage and myoblasts migration. In a related study, notexin injured muscle regeneration in *Mstn*^{-/-} mice displayed accelerated recruitment of macrophages and myogenic cells after 48hr post-injury at the site of injury. These results indicated enhanced inflammatory response and also suggest that satellite cell activation was more pronounced in *Mstn*^{-/-} muscle. In addition, at day 28 post-injury, reduced fibrosis and increased decorin (a myokine involved in promoting myogenesis) mRNA was observed which implies enhanced muscle regeneration in the *Mstn*^{-/-} genotype [151].

1.9 Epigenetic regulation of myogenesis

1.9.1 microRNAs

MicroRNAs (miRNA) are short non-coding RNAs (~22nt) that post-transcriptionally regulate genes. MicroRNAs are transcribed by RNA pol II to form a stem-loop structure known as the primary miRNA. Following transcription, a microprocessor complex consisting of Drosha (a RNase III endonuclease) and DGCR8 cleaves the primary miRNA to liberate the precursor miRNA (pre-miRNA) [152]. The pre-miRNA translocates into the cytoplasm with the help of Ran-GTP, which is converted to Ran-GDP, and Exportin-5 [153, 154] and is further cleaved by TRBP-Dicer (another RNase III endonuclease) complex to release the stem from its loop. Subsequently, Argonaute (AGO1-4) proteins and HSC70-HSP90 chaperones form a complex known as the Pre-RISC (Pre-RNA-induced silencing complex) allowing the double stranded RNA to unwind. A mature RISC complex results after unwinding where one strand of the RNA duplex is incorporated. Here the target mRNA is incorporated. The RISC complex consists of Argonaute (AGO1-4) proteins which has endonuclease activity towards mRNA that bind stably with miRNA. AGO proteins also function to recruit factors to induce translational repression, mRNA deadenylation and mRNA decay [155-157]. miRNA's complementarity is often between 5` end of the miRNA towards the 3` untranslated region (UTR) of mRNA and could have multiple binding sites within the 3` UTR. The

base pairing of positions 2-7 nucleotide of the miRNA is essential for target recognition and is known as the seed region. However, the positions of other nucleotides are also of importance such as nucleotide 8 and less importantly 13-16.

1.9.1.1 microRNAs, myogenesis and muscle regeneration

Muscle-specific miRNAs (MyomiRs) miR-1, miR-133 and miR-206 have been identified and have been studied extensively during muscle development [158]. MyomiRs have been named so due to their prevalent expression in skeletal and cardiac muscle [159-161] and more importantly myomiRs play crucial roles in muscle development (myogenesis) and muscle remodeling [162-164]. For example, the injection of miR-1, miR-133 and miR-206 in atecollagen-mediated rat injury model displayed enhanced muscle regeneration and reduced fibrosis [165]. In addition, exogenous administration of all 3 myomiRs induced protein and mRNA expression levels of MyoD, myogenin as well as Pax7 at days 3 and 7 post-injury [165]. Consistent with this, treatment of miR-1, miR-133 and miR-206 in C2C12 resulted in increased myogenic markers MyoD, myogenin and Pax7, thereby promoting myotube differentiation [165].

Both miR-1 and miR-133 have 2 isomers (miR-1a/b and miR-133a/b). The gene cluster miR-1 and miR-133a are expressed in skeletal and cardiac muscle [162, 163, 166] while miR-133b and miR-206 gene cluster is expressed in developing skeletal muscle [158]. Interestingly, miR-1 and miR-206 targets signalling pathways which have opposing functions to the signalling pathways targetted by miR-133a/b; miR1 and miR-206 act to promote myogenic differentiation while miR-133 functions to promote cell proliferation and maintain the undifferentiated state of myoblasts. Examples of myomiR functions and their targets are as follows: miR-1 have been shown to induce myogenic differentiation via downregulation of Histone deacetylase 4 (HDAC4) which represses gene expression transcriptionally [167]. miR-133 represses Serum Response Factor (SRF) thereby enhancing myoblast proliferation

[167]. miR-206 directly targets the the largest subunit of DNA polymerase α (Pola1) resulting in the inhibition of DNA synthesis which is a requirement for the differentiation of myotubes [168]. In addition, a recent finding displayed miR-206 directly targets Twist1 [169] which led to enhanced myogenic differentiation. MyomiR gene targets and the consequence of downregulating these targets in muscle are summarized in Table 1.1.

In addition to the regulation of genes via miRNA-mRNA interactions, myomiRs have also been shown to interact with other signalling pathways. One example is the IGF-1 signalling pathway which promotes myogenesis via the PI3K/AKT pathway. IGF-1 binds to its receptor IGF-1R and induces myogenesis by indirectly activating myogenin. This in turn activates miR-133. In order to maintain the balance of IGF-1 signalling pathway, IGF-1R is downregulated in a negative feedback loop by miR-133 resulting in the inhibition of AKT pathway [170].

myomiR	Target	Function	Reference
miR-1	IGF-1	IGF-1 signalling and miR-1 interacts via a feedback loop to regulate differentiation of myoblasts	[171]
	RhoA	Upregulates Zebrafish muscle gene expression and regulates sarcomeric actin organization	[158]
	Dll-1	Mouse and human ES cells differentiates into muscle	[172]
	Spred1	Angiogenic differentiation	[173]
	Cyclin D1	Muscle regeneration	[174]
	HDAC4	Promotes proliferation and differentiation of skeletal muscle	[163]

miR-133	RhoA	Upregulates Zebrafish muscle gene expression and regulates sarcomeric actin organization	[175]
	SRF	Enhances myoblast proliferation	[163]
	IGF-1R	IGF-1 signalling and miR-133 interacts via a feedbackloop to regulate differentiation of myoblasts	[170]
	Utrophin A	Skeletal muscle differentiation	[176]
	FGFR1	Downregulates ERK1/2 signalling pathway inducing C2C12 differentiation	[177]
	PP2AC	Downregulates ERK1/2 signalling pathway inducing C2C12 differentiation	[177]
	Hand2	Inhibits cardiac muscle development	[178]
	Snail1	Inhibits cardiac reprogramming	[179]
	Caspase9	Inhibtion of apoptosis in rat cardiomyocytes	[180]
	KLF15	Reduces GLUT4 and controls metabolism in cardiomyocytes	[181]
	CTGF	Cardiac myocardium structural changes	[182]
	Bim	Prevents apoptosis	[183]
	Bmf	Prevents apoptosis	[183]
miR-206	Id1-3	Mouse skeletal muscle differentiation	[184]
	BDNF	C2C12 myoblast differentiation	[185]
	Fstl1	Skeletal muscle differentiation	[186]
	Utrn	Skeletal muscle differentiation	[186]
	Utrophin A	Skeletal muscle differentiation	[176]

Table 1.1: List of myomiRs, their targets and function upon downregulation. This list includes validated targets known to date and is not exhaustive.

Subsequently, other non-muscle specific miRNAs were discovered to play a role in myogenesis, such as miR-208a and b, -499, -27b and -486 [187]. It was demonstrated that the overexpression of miR-208a in the heart resulted in hypertrophy of cardiac muscle. This was mediated by inhibition of Mstn and thyroid hormone-associated protein 1, both negative regulators of myogenesis. In addition, it was also shown that miR-208a is required for normal functioning of cardiac electrical conduction and cardiac-specific transcription factor expression [188]. Similarly, work on miR-499 has shown its importance in human cardiomyocyte progenitor cells (CMPC) as it was observed to have higher levels in differentiated cardiomyocytes. Furthermore, the overexpression of miR-499 reduced proliferation and enhanced the differentiation of embryonic stem cells and CMPCs into cardiomyocytes [189].

During skeletal embryonic myogenesis, miRNAs have been shown to regulate both Pax7 and Pax3 expression. For example, the overexpression of miR-27b *in vivo* in Pax3-positive cells in the embryo downregulates Pax3 expression thereby interfering with the migration of muscle progenitor cells and resulting in premature differentiation. Consistently, the inhibition of miR-27b results in continued expression of Pax3 expression and increased proliferation and delayed differentiation with smaller fibers [190]. Myogenesis has also been shown to be induced by miR-1, miR-486 and miR-206 by downregulating Pax7 in C2C12 cell culture models, suggesting a potential role for these miRNAs in satellite cell activation. It was also demonstrated that the inhibition of these miRNAs results in continued Pax7 expression which led to delayed differentiation. In addition, it was also found that miR-486 levels were upregulated during myotube differentiation and promoted cell cycle quiescence [191, 192]. In an *in vivo* study during muscle regeneration, it was found miR-206 was highly expressed in satellite cells upon muscle injury and that overexpressing miR-206 led to increased satellite cell differentiation and fusion of myofibers thus enhancing skeletal muscle regeneration.

Consistently, the inhibition of miR-206 in WT mice delayed regeneration and in DMD mice models, deteriorated the dystrophic phenotype [193].

miR-148a was recently shown to be upregulated during myogenesis in both primary myoblasts cultures and C2C12 myoblasts. It was found that miR-148a promotes myotube differentiation by inhibiting its downstream target, ROCK1 [194]. ROCK1 is a Rho-associated serine/threonine kinase activated by RhoA GTPases. It is involved in actin cytoskeletal arrangement, focal and stress fiber formation, cell adhesion, motility and smooth muscle contraction. This suggests that the regulation of myogenic structural proteins could also be mediated by miRNAs.

Another miRNA involved in myogenesis is miR-29c which was previously shown that in mice primary myoblasts and in the C2C12 myoblast cell line, myogenesis was induced by inhibition of HDAC4 (an inhibitor of myotube differentiation), Ring1 and YY1-binding proteins (a negative regulator of skeletal myogenesis) [195-197]. Besides having a role in myogenesis, miR-29c was also noted to be decreased in human quiescent satellite cells and thus is thought to be required for satellite cell activation [198]. Conversely, miRNAs play a role in the maintenance of quiescent satellite cells. For example, miR-31 was found to target Myf5 sequestering its target mRNA in mRNA granules, thereby inhibiting activation of satellite cells [199].

The function of miRNAs during muscle regeneration is beginning to be elucidated. Exogenous expression of miR-26a demonstrated to promote differentiation of myotubes [200]. This is consistent with prior studies where miR-26a was induced during differentiation by targeting the epigenetic regulator Ezh2 (an inhibitor of myogenesis) [201]. In addition, during myoblast differentiation and muscle regeneration, miR-26a was also found to directly target transcription factors involved in TGF-β/BMP signalling pathway such as SMAD 1 and SMAD 4 which

are negative regulators of myogenesis. In the Notexin (NTX) induced-injury model, the expression of miR-26a was observed to increase gradually from day 1 through 14 post-injury [200]. This suggest miR-26a is required for myoblast differentiation and therefore the formation of nascent myofibers during muscle regeneration.

In another study, miRNAs from uninjured and injured muscle were compared from day 1 through day 21 post injury. A total of 298 miRNAs were observed to be differentially expressed during the course of muscle regeneration and 86 miRNAs had >10 fold difference as compared to uninjured skeletal muscle. Of note was the expression levels of miR-1, miR-133a and miR-499 which decreased following injury and was upregulated at later stages of regeneration [202] suggesting a role in satellite cell activation and nascent myofiber formation.

Another miRNA shown to be involved in muscle regeneration and substantially characterized is miR-351. Its expression is, however, unlike miR-26a. During C2C12 differentiation, miR-351 expression increases and peaks at 48hrs of differentiation and falls subsequently. Similarly, miR-351 levels peaked at day 4 post-injury which gradually fell as myofibers became fully regenerated [202]. When the expression of miR-351 was inhibited in myogenic precursor cells (MPC), proliferation of these cells were significantly lower. Furthermore, the cell cycle gene E2f3 was shown to be a direct target of miR-351 which suggests cell proliferation was enhanced by miR-351 via E2f3 [202].

Taken together, the function of miRNAs in myogenesis have begun to be unraveled and provide potential therapeutics for future treatments in muscle atrophy or ageing.

1.10 Myostatin and miRNAs

Several miRNAs function to regulate the expression of Mstn. This was initially suggested by a single base pair mutation in Belgian Texel sheep at the 3` UTR of Mstn mRNA which generated binding sites for

miR-206 and miR-1 [203] and resulted in hypertrophy. In another discovery, miR-208a and b (heart specific miRNA) was shown to target 3` UTR of Mstn by luciferase reporter assay [204]. This was also shown *in vivo* where miR-208a overexpression in heart of mice inhibited Mstn. In addition, a recent study demonstrated the inhibition of Myostatin 3` UTR by miR-27a and b resulting in the increase in proliferation [205]. Consistent with this, a study conducted by our group also showed that antagomiR-27a treatment led to increased expression of Mstn, impaired myoblast proliferation, reduced activation of satellite cells and the induction of skeletal muscle atrophy [132]. Interestingly, the negative regulation of Mstn by miR-27a/b was demonstrated to be part of an auto-regulatory feedback mechanism where Mstn upregulated SMAD3 signalling, which promoted increased miR-27a/b expression and a subsequent reduction in Mstn levels [132].

1.11 Aims and objectives

Several studies have reported the regulation of miRNAs by growth factors. For example, in human smooth muscle cells, TGF-β and BMP proteins were able to enhance the processing of miR-21 by SMAD proteins such as SMAD3 and SMAD5 [206]. In another study, BMP-2 was shown to mediate the maturation of miR-206 via SMAD proteins in C2C12 cell cultures [207]. A microRNA array performed on IGF-1 treated ER$^+$ MCF7 human breast cancer cell line displayed direct regulation of tumor suppressive and oncogenic miRNA [208]. In addition, TGF-β has been previously shown to upregulate miR-155 expression in murine mammary gland epithelial cells, which leads to reduced RhoA protein levels and as a result contributes to epithelial-mesenchymal transition (EMT) [209]. These findings suggest growth factors are able to modulate miRNA expression to mediate their functions.

Our laboratory has a long standing interest in understanding the mechanisms through which the growth factor Myostatin regulates skeletal muscle myogenesis. To date, several published reports have characterized genetic pathways controlled by Myostatin during myogenesis. In addition, recent work has revealed that Myostatin can potentially regulate non-coding RNAs, such as microRNAs. The expression of the muscle-specific miRNAs (MyomiRs) miR-1, miR-133a/b and miR-206 were shown to be increased in pectoralis muscle tissues isolated from $Mstn^{-/-}$ mice when compared to wild type [210]. In addition, it was also recently reported that miR-486 expression is elevated in $Mstn^{-/-}$ mice and that increased Mstn signalling repressed miR-486 at the transcriptional level [211]. This results in reduced P-Akt and PTEN protein levels and therefore decreased protein synthesis. A recent study from our lab has demomstrated direct regulation of miRNAs by Mstn. Specifically, this study revealed that Mstn promotes the expression of miR-27a/b via Smad3. Interestingly, Mstn-mediated upregulation of miR-27a/b in turn leads to repressed Mstn expression, forming the basis of a novel negative auto-regulatory loop [132].

Although Mstn regulation of miRNAs is beginning to be unravelled, a comprehensive screen has not been undertaken to identify miRNAs regulated by Mstn and the result of this regulation in controlling myogenesis. Given the evidence provided from previously published studies I hypothesize that Mstn can regulate myogenesis through regulation of miRNA expression. To prove this hypothesis, I propose to identify specific miRNAs regulated by Mstn. In addition, I also propose to perform functional studies on these identified miRNAs to elucidate their roles in Mstn-mediated regulation of myogenesis with the following aims:

1   Identify the miRNAs that are regulated by Mstn during myogenesis.
2   Determine if these identified miRNAs are able to mimic Mstn function and its mechanism of action
3   Determine downstream targets of these miRNAs that are regulated by Mstn during myoblast differentiation and muscle regeneration/satellite cell activation

2. Materials and Methods

2.1 Materials

2.1.1 Enzymes

Enzymes	Source
T4 DNA ligase	New England Biolabs (NEB)
Taq DNA polymerase	Thermo Scientific
Collagenase Type 1A	Sigma
Trypsin	Gibco
Not1	New England Biolabs (NEB)
Xho1	New England Biolabs (NEB)
BamH1	New England Biolabs (NEB)
KAPA HiFi DNA polymerase	KAPA biosystems

2.1.2 Antibodies

The following antibodies listed below were used for western blot in this thesis.

Primary antibody	Source	Dilution
Anti-MyoD	Santacruz Biotechnology Inc	1:400
Anti-Myogenin	Santacruz Biotechnology Inc	1:400
α-Tubulin	Sigma-Aldrich	1:10,000
GAPDH	Santacruz Biotechnology Inc	1:10,000
TCF12	Santacruz Biotechnology Inc	1:400
p21	BD pharmingen	1:200
Notch1	Santacruz Biotechnology Inc	1:400
NF-κB(p65)	Santacruz Biotechnology Inc	1:1000
Notch1	Santacruz Biotechnology Inc	1:400

Secondary antibody	Source	Dilution
Goat Anti-Rabbit IgG HRP	Bio-Rad	1:5000
Goat Anti-Mouse IgG HRP	Bio-Rad	1:5000

The following antibodies listed below were used for immunocytochemistry staining in this thesis.

Primary antibody	Source	Dilution
Anti-MyoD	Santacruz Biotechnology Inc	1:50
Anti-Pax7	Developmental Studies Hybridoma Bank (DSHB)	1:100

Secondary antibody	Source	Dilution
Sheep Anti-Mouse IgG Biotinylated	Abnova	1:300
Goat Anti-Rabbit IgG Alexa Fluor® 594 conjugated	Invitrogen	1:300

Tertiary antibody	Source	Dilution
Streptavidin, Alexa Fluor® 488 conjugated	Invitrogen	1:400

2.1.3 Plasmid DNA

Plasmids listed below were used in this thesis. They were either purchased, cloned or gifts.

Plasmid DNA	Vector Size (bp)	Source
Psicheck2	6273	Daniel J. Hodson[1] (Hodson et al., 2010)
Psicheck2-TCF12 3`UTR	8558	Cloned
Psicheck2-TCF12 3`UTR (Mut)	8558	Cloned
Psicheck2-Notch1 3`UTR	7902	Daniel J. Hodson[1] (Hodson et al., 2010)
pGL3 basic	4818	Promega
pGL3b-miR34aPMT	6084	Addgene
pGL3b-miR34aPMT Truncation 1	5791	Cloned
pGL3b-miR34aPMT Truncation 2	5763	Cloned
pGL3b-miR34aPMT Truncation 3	5398	Cloned
pMEV (pEM157)	4248	Biomyx Technology
pMEV-miR-34a	4752	Cloned
pEM791	8000	Cloned
pEM791-shNF-κB	8064	Cloned

[1]Hodson DJ, Janas ML, Galloway A, et al. Deletion of the RNA-binding proteinsZfp36l1 and Zfp36l2 leads to perturbed thymic development and T-lymphoblastic leukaemia. Nature immunology. 2010;11(8):717-724. doi:10.1038/ni.1901.

2.1.4 Chemicals

All the chemicals used in this thesis are listed below. The companies from where they were purchased are also listed below.

Chemical	Source
Matrigel	Corning
Penicillin and Streptomycin (P/S)	Life Technologies
Fetal Bovine Serum (FBS)	Life Technologies
Horse Serum (HS)	Life Technologies
Chicken Embryo Extract (CEE)	Biomed Diagnostics
Phenylmethanesulfonylfluoride (PMSF)	Sigma-Aldrich
Nonidet P-40 (NP40)	Fluka
Protease Inhibitor (PI)	Roche
LB broth	BD biosciences
4x LDS Sample loading dye	Life Technologies
1kb plus DNA ladder	Invitrogen
Lipofectamine 2000 (LF2000)	Invitrogen
SeeBlue Plus2 Protein ladder	Invitrogen
Ponceau S	Sigma-Aldrich
Tryphan blue solution	Life Technologies
Neomycin (G418); Geneticin	Life Technologies
Ampicillin	Sigma-Aldrich
Sodium Borate	Sigma-Aldrich
Methylene blue	Sigma-Aldrich
NaCl	1st Base
37% Formaldehyde	Sigma-Aldrich
Sodium Bicarbonate	Sigma-Aldrich
HCl	Merck Millipore
Ethanol (EtOH)	Merck Millipore
Tris	1st Base
Ethylenediaminetetraacetate(EDTA)	1st Base
Magnesium Sulfate	Sigma-Aldrich
Hematoxylin	Merck Millipore
Eosin	Merck Millipore
Paraformaldehyde	Sigma-Aldrich
Acetic acid	Sigma-Aldrich
Xylene	Sigma-Aldrich
Propidium Iodide	Sigma-Aldrich
Sodium Fluoride	Sigma-Aldrich
DAPI	Molecular Probes
Pro-long gold anti-fade mounting medium	Invitrogen
Normal Goat Serum (NGS)	Sigma-Aldrich
Normal Sheep Serum (NSS)	Sigma-Aldrich
Carrageenan λ	Sigma-Aldrich
Methanol	Merck Millipore
Glycine	Biorad

SsoFast EvaGreen	Biorad
50x Tris-acetate EDTA buffer	1st Base
DPX Mountant	Sigma-Aldrich
B-Mercaptoethanol (β-ME)	Sigma-Aldrich
Skim Milk	Sigma-Aldrich
Triton-X 100	Promega
Tween 20 (Molecular Biology Grade)	Promega
Dulbecco's Modified Eagle Medium (DMEM)	Life Technologies
Sodium Azide	Sigma-Aldrich
Sodium orthovanadate (Na_3VO_4)	Sigma-Aldrich
Sodium dodecyl sulfate (SDS)	Sigma-Aldrich
Ethidium Bromide (EtBr)	Biorad
Bovine Serum Albumin (2mg/ml)	Biorad
Bio-rad protein assay dye reagent concentrate (5x)	Biorad
NuPAGE® MES running buffer	Life Technologies
Sucrose	Usb Corporation
Ketamine	Parnell Pharmaceuticals
Xylazine	Troy Laboratories
DMEM, no methionine, no glutamine, no cysteine	Life Technologies
Glutamine	Sigma-Aldrich
Cysteine	Sigma-Aldrich
Luciferase assay reagent II (LARII)	Promega
Stop and Glo Substrate and Buffer	Promega

2.1.5 Solutions

The compositions of solutions and their concentrations used in this thesis are listed below.

Solution	Composition
Tris-buffered Saline with Tween-20 (TBST) Buffer	0.5M Tris-HCl, 1.5M NaCl, 1% Tween-20
Scott's tapwater	Sodium Bicarbonate 3.5%, Magnesium Sulfate 20%
10% Formal saline	0.17% saline, 10% formaldehyde
Protein lysis buffer	50mM Tris-HCl pH 7.5, 250mM NaCl, 5mM EDTA, 1% NP40, 1x Protease inhibitor, 10mM NaF, 1x PMSF, 0.28mM Na_3VO_4
20:2:1 fixative	70% Ethanol, 37% Formaldehyde, acetic acid (20:2:1 v/v)
Transfer buffer	Glycine 75g, Tris 15.1g, 20%

	Methanol
Methylene blue	1% methylene blue, 0.01M borate buffer, pH 8.7
Borate buffer	0.01M Sodium borate, pH 8.5
10x DNA loading dye	10x TAE buffer, 4% Sucrose, 0.1% Bromophenol blue
ChIP lysis buffer	50 mM HEPES-KOH pH 7.5, 140 mM NaCl, 1 mM EDTA pH8, 1% Triton X-100, 0.1% Sodium Deoxycholate, 0.1% SDS, Protease Inhibitors (add fresh each time)
RIPA buffer (ChIP)	50 mM Tris-HCl pH 8.0, 150 mM NaCl, 2 mM EDTA pH 8.0, 1% NP-40, 0.5% Sodium Deoxycholate, 0.1% SDS, Protease Inhibitors (add fresh each time)
Low Salt wash buffer	0.1% SDS, 1% Triton X-100, 2 mM EDTA, 20 mM Tris-HCl pH 8.0, 150 mM NaCl
High Salt wash buffer	0.1% SDS, 1% Triton X-100, 2 mM EDTA, 20 mM Tris-HCl pH 8.0, 500 mM NaCl
LiCl wash buffer	0.25 M LiCl, 1% NP-40, 1% Sodium Deoxycholate, 1 mM EDTA, 10 mM Tris-HCl pH 8.0
Elution buffer	1% SDS, 100mM $NaHCO_3$

2.1.6 Kits

Extraction and purification kits including their source of purchase used in this thesis are listed below.

Kit	Source
QIAquick® Gel extraction kit	Qiagen
miRNeasy mini kit	Qiagen
QIAprep Spin Miniprep Kit	Qiagen
QIAGEN Plasmid maxiprep	Qiagen
miScript® SYBR® Green PCR Kit	Qiagen

2.1.7 Instruments

Consumables and instruments/machines used to perform experiments in this thesis are listed below.

Consumables and Instrument/Machine	Company
NuPAGE® Novex 4–12% Bis-Tris	Life Technologies

gels	
Countess automated cell counter	Invitrogen
XCell II™ Blot Module	Life Technologies
Trans-Blot Nitrocellulose membrane	Biorad
GloMax® 96 Microplate Luminometer	Promega
FACSAriaII	BD Biosciences
CFX96™ Real-Time PCR Detection System	Biorad
DNA engine peltier thermal cycler (PTC200)	Biorad

2.1.8 Bacterial strains

The *Escherichia coli* bacterial strain (DH5α), was used in the thesis for the transformation of plasmid DNA. The bacteria was purchased from Invitrogen.

2.1.9 Oligonucleotides

Name of primer/oligonucleotide	Sequence (5`-3`)
Scrambled	CUUGUACUACACAAAAGUACUG
AntagomiR-34a	ACAACCAGCUAAGACACUGCCA
Mmu-miR-34a (Qiagen)	UGGCAGUGUCUUAGCUGGUUGU
RNU6B (Qiagen)	Qiagen
Notch1-F	GGTCGCAACTGTGAGAGTGA
Notch1-R	TTGCTGGCACATTCATTGAT
Hes1-F	CCCACCTCTCTCTTCTGACG
Hes1-R	AGGCGCAATCCAATATGAAC
Bcl2-F	TGCAGCGGAAGAGGGGACCA
Bcl2-R	CACCGCAGCGGGGCAAAAG
GAPDH-F	ACAACTTTGGCATTGTGGAA
GAPDH-R	GATGCAGGGATGATGTTCTG
Caspase3-F	TGCAGCATGCTGAAGCTGTA
Caspase3-R	GAGCATGGACACAATACACG
TCF12-3`UTR-F	TCGCTCGAGACATCAGCCAGTTCCAGAGTC
TCF12-3`UTR-R	CCAGCGGCCGCGGATGGCACATTTATTGCTAC
TCF12-3`UTR-Mut	TGAACATAAGCCGGATCCTGGCCT
Psicheck2-Xho1-F	AGATGTTCATCGAGTCCGAC
Psicheck2-Not1-R	CGAGGTCCGAAGACTCATTT
NF-κB p65-F	CGAGTCTCCATGCAGCTACG
NF-κB p65-R	GCGCTTCTCTTCAATCCGGT

p65 sh1-F	TGCTGTACTCTTGAAGGTCTCATAGGGTTT TGGCCACTGACTGACCCTATGAGCTTCAA GAGTA
p65 sh1-R	CCTGTACTCTTGAAGCTCATAGGGTCAGTC AGTGGCCAAAACCCTATGAGACCTTCAAGA GTAC
p65 sh2-F	TGCTGAACTCATCAAAGTTGATGGTGGTTT TGGCCACTGACTGACCACCATCATTTGATG AGTT
p65 sh2-R	CCTGAACTCATCAAATGATGGTGGTCAGTC AGTGGCCAAAACCACCATCAACTTTGATGA GTTC
p65 sh3-F	TGCTGCTGAGTTGTCCACAGATGCCAGTTT TGGCCACTGACTGACTGGCATCTGGACAA CTCAG
p65 sh3-R	CCTGCTGAGTTGTCCAGATGCCAGTCAGT CAGTGGCCAAAACTGGCATCTGTGGACAA CTCAGC
p65 sh4-F	TGCTGTCACCAGGCGAGTTATAGCTTGTTT TGGCCACTGACTGACAAGCTATATCGCCT GGTGA
p65 sh4-R	CCTGTCACCAGGCGATATAGCTTGTCAGTC AGTGGCCAAAACAAGCTATAACTCGCCTG GTGAC
miR34aPMT-Trun1	CTCGAGCGGAAGGGTCGCGATGGC
miR34aPMT-Trun2	CTCGAGGGGACCTCGGCTCTGGGT
miR34aPMT-Trun3	CTCGAGAGCTCCCCGGATCCCGGG
mmu-miR-34a-F	CCGCGGGCCTCC TTGTGGAAGCCGGAAG
mmu-miR-34a-R	ACTAGTGCCCCCGT AAACATGCTCCCC
MyoG-Chip-F	AAAGGAGAGGGAAGGGGAAT
MyoG-Chip-R	ATATAGCCAACGCCACAGAAA
TCF12-α-F	TGATGAGTCCTCCCAGAAAGA
TCF12-α-R	GCTCTCTGGCATTGTTAGCC
TCF12-β-F	GCAAGCTCCTTCATCTCCAA
TCF12-β-R	CCATTCGAGACTGCTCACAG

2.1.10 Mammalian cell lines

The mammalian cell lines used in this thesis were the mouse muscle secondary cell line (C2C12) and human muscle primary cell line (36C15Q). Stable cell lines were established in the C2C12 cell line. C2C12 cell lines were purchased from American Type Culture Collection (ATCC, Manassas VA, USA) and frozen and stored in Dulbecco's Modified Eagle Medium (DMEM) with 10% Fetal bovine serum (FBS), 5% Dimethyl Sulfoxide (DMSO) in liquid nitrogen. Human

primary myoblasts (36C15Q) was a gift from Drs. Vincent Mouly and Gillian Butler-Browne (Institut de Myologie, France).

2.1.11 Recombinant human Myostatin expression and purification

Human recombinant Myostatin protein used was cloned and amplified from *Escherichia coli* as described in [212].

2.1.12 C57BL6 wild type mice

C57BL6 wild type mice were obtained from Biological Resource Centre (BRC), A*STAR, Singapore. Mice were held at Animal Research Facility (ARF), Nanyang Technological University, School of Biological Sciences (NTU, SBS), Singapore. Mice experiments were carried out with an approved IACUC protocol granted by the NTU IACUC committee.

2.2 Methods

2.2.1 Cloning of DNA plasmids

2.2.1.1 Polymerase chain reaction using KAPA HiFi DNA polymerase

PCR reactions carried out using KAPA HiFi DNA polymerase were according to manufacturer's protocol. PCR reaction mix consisted of 10µl 5x KAPA HiFi buffer, 0.3µM Forward/Reverse primer, 0.3mM dNTP mix and 1U HiFi DNA polymerase (1U/µl) in a total volume of 50µl including 50ng Template DNA. PCR was carried out in a thermocycler (Bio-Rad DNA engine PTC-200 Thermal Cycler). Genomic DNA from quadriceps muscle was used as a template DNA for the amplification of TCF12-3`UTR/Notch1-3`UTR. Specific primers were designed with incorporation of restriction enzymes Xho1 (Forward primer) and Not1 (Reverse primer) for cloning purposes. Primer sequences are listed in section 2.1.9. PCR reaction was carried out with the following conditions: Initial denaturation at $95^{o}C$ for 3mins, denaturation at $98^{o}C$ for 20s, annealing at $65^{o}C$ for 15s and extension at $72^{o}C$ for 2 mins for 35 cycles followed by final extension at $72^{o}C$ for 5mins.

2.2.1.2 Polymerase chain reaction using Taq DNA polymerase

Polymerase chain reactions (PCR) with Taq DNA polymerase were performed following manufacturer's protocol. PCR reaction mix consisted of 2.5µl 10x Taq polymerase buffer ($(NH_4)_2(SO_4)$-$MgCl_2$), 1µl (5U/µl) Taq polymerase, 0.4µM dNTPs, 0.4µl Forward/Reverse primers and 1.5mM $MgCl_2$ in a total volume of 25µl including template DNA. All PCR reactions were carried out in a thermocycler (Bio-Rad MJ Research PTC-200 Thermal Cycler) following PCR conditions specific for each insert. To amplify the mutant TCF12 3`UTR, the initial PCR reaction mix consisted of primers specific for mutant sequence (TCF12-3`UTR-Mut) and wild type reverse sequence (TCF12-3`UTR-R). Psicheck2-TCF12-3`UTR (10ng) was used as template DNA. PCR conditions were as follows: Initial denaturation at $90^{o}C$ for 1min, denaturation at $90^{o}C$ for 20s, annealing at $50^{o}C$ for 45s and extension

at 72°C for 30s for 10 cycles followed by final extension 72°C for 5mins. Forward primer (TCF12-3`UTR-F) was added in to the reaction mix to a final concentration of 0.5 µM and the PCR reaction was carried out for another 20 cycles. Following this, the reverse primer (TCF12-3`UTR-R) was added in to the reaction mix to a final concentration of 0.5 µM and the PCR reaction was carried out for 20 cycles. Primers were designed with restriction enzyme Xho1 incorporated into the forward primer (TCF12-3`UTR-F) and Not1 into the reverse primer (TCF12-3`UTR-R). The mutant primer (TCF12-3`UTR-Mut) contained a 4 bp substituition (ACUG -> GCAT) which, introduced a BamH1 restriction enzyme site used for validation of the mutant sequence. miR-34a promoter truncation constructs were PCR amplified following conditions mentioned above. Primers contained Xho1 and Not1 restriction enzyme sites. Subsequently, the PCR product was ligated into pGL3b (basic) vector. miR-34a overexpression constructs were generated by cloning miR-34a coding region (504bp) in to pMEV (pEM157). Primers were designed with incorporating restriction enzyme sites SpeI and SacII. Primer sequences are listed in section 2.1.9.

2.2.1.3 Cloning of shRNA NF-κB

Single stranded shRNA (shNFkb 1-4) were annealed in annealing buffer (10mM Tris, pH 8, 1mM EDTA and 100mM NaCl) by heating at 95°C for 5 minutes and allowing the reaction to cool to room temperature. The mixture was then used directly for ligation to pGEM652 (see section 2.2.1.4).

2.2.1.4 Restriction digestion and ligation of insert to vector

Following PCR, the reaction mix was purified using QIAquick® gel extraction kit (Qiagen), see section 2.2.1.4. The insert and vector were digested with restriction enzymes overnight at 37°C in the following mix: 1µl of restriction enzymes each, 1x NEB buffer and entire purified digestion mix to a total volume of 50µl. Subsequently, the digestion mix was purified once more using QIAquick® gel extraction kit (Qiagen).

The insert and vector was ligated at a molar ratio of 3:1 (Insert:vector) in a reaction mix consisting of 1µl T4 DNA ligase (NEB) and 1x T4 DNA ligase buffer (NEB) to a total volume of 20µl and incubated overnight at 16°C.

2.2.1.5 DNA Agarose gel electrophoresis

DNA agarose gels were made by boiling agarose powder (1st base, Biotechnology grade) with 1x TAE (1st base, Ultra pure grade) buffer till fully dissolved. The mixture was allowed to cool for 5mins and EtBr was added to a final concentration of 0.2-0.5µg/ml. The gel was poured into the template and allowed to solidify before loading the samples. Loading buffer was added into the samples to a final concentration of 1x and the contents were loaded into the gel. Gel running conditions were 80-110V for 30-45mins.

2.2.1.6 QIAquick$^®$ gel extraction kit (Qiagen)

The DNA band of interest was excised on a trans-illuminator under long wavelength UV exposure briefly. Three volumes of buffer QG was added to 1 volume of gel slice (e.g. For 100mg gel, add 100µl). The gel slice was heated at 50°C for 10mins or until it was completely dissolved. One volume of isopropanol was added to the sample to precipitate DNA and the mixture was quickly loaded on to a QIAquick spin column in a 2ml collection tube. The column was spun and the flow-through was discarded. Buffer QG (500µl) was added to the column and centrifuged to remove flow-through. The column was washed with 750µl Buffer PE and centrifuged. A final spin was performed and the DNA fragment was eluted in dH$_2$O.

2.2.1.7 Transformation of competent cells

DNA plasmids were transformed into competent bacterial cells (DH5α) by heat shock. Competent cells (50µl) were incubated with ligation mix (3µl) on ice for 30 mins. Subsequently, the cells underwent heat shock at 42°C for 45s to allow inclusion of DNA plasmids and was allowed to grow in 450µl LB broth at 37°C for 90 mins with gentle shaking. The

cells were then spread on antibiotic LB agar plates (Ampicillin: 100µg/ml) and incubated at 37°C for 16 hrs.

2.2.1.8 QIAprep Spin miniprep kit (Qiagen)

A single colony was inoculated into 5ml of LB broth containing the required antibiotic (Ampicillin: 100µg/ml) and was allowed to grow overnight (12-16hrs) at 37°C with vigourous shaking. Bacteria cells were pelleted by centrifugation at 8000rpm for 3mins followed by resuspension in cold P1 buffer. Buffer P2 was added to lyse the cells and pre-chilled buffer N3 was added to neutralise the reaction. Cell debris were pelleted at 13000rpm for 10mins and the supernatant transferred on to a QIAprep spin column. The column was washed with Buffer PB and PE and the DNA was eluted in appropriate volumes of dH$_2$O.

Upon acquiring DNA plasmids, they were all validated for the appropriate insert (size and sequence) by restriction digestion (see section 2.2.1.3) and sequencing (1st base). Selected DNA plasmids were further propagated and purified by Qiagen plasmid maxi kit (see section 2.2.1.8) for transfections.

2.2.1.9 Qiagen plasmid maxi kit (Qiagen)

Bacterial cells were inoculated from glycerol stocks into 200ml LB broth with antibiotic (Ampicillin: 100µg/ml) and grown overnight (12-16hrs). Bacteria cells were pelleted at 6000g for 15mins at 4°C. The pellet was resuspended in cold buffer P1 and lysed with buffer P2 for 5mins at room temperature. The reaction was neutralized with pre-chilled buffer P3 on ice for 20mins to accelerate precipitation of genomic DNA, proteins and cell debris which was pelleted by centrifugation at 20000g for 30mins at 4°C. The supernatant was further centrifuged for another 15mins and the DNA was loaded onto an equilibrated QIAGEN-tip. The column was washed with Buffer QC twice and DNA eluted with buffer QF. DNA was precipitated with isopropanol and pelleted by centrifugation at 15000g for 30mins at 4°C immediately. The DNA

pellet was washed with 70% ethanol and removed by centrifugation at 15000g for 10mins. The pellet was air-dried and resuspended in appropriate volumes of dH$_2$O.

2.2.2 Cell cultures

C2C12 or 36C15Q cell cultures were used as *in vitro* muscle models as they behave similarly to myoblasts and myotubes *in vivo*. These cells were grown in proliferation media consisting of DMEM, 10% FBS and 1% P/S (C2C12) or DMEM, 20% FBS, 10% Horse Serum, 1% Chick Embryo Extract (CEE), 1% Penicillin/Streptamycin (P/S) (36C15Q and mouse muscle primary cultures) at 37°C, 5% CO$_2$.

2.2.3 Maintenance, trypsinisation or harvesting of mammalian cells

Cells were passaged or harvested as follows: The media was firstly removed followed by washing with phosphate buffered saline (PBS). Cells were treated with trypsin and incubated at 37°C for ~2 mins. This will cause cells to detach from the culture dish. Fresh media was added to resuspend the cells and counted to be passaged, seeded or frozen at the required densities. Cells were counted using an automated counter (Countess automated cell counter, Invitrogen) after diluting the cell stock with tryphan blue (1:1). Cells to be frozen were centrifuged at 500rpm for 3 mins and supernatant was discarded. Cells were resuspended to 1 million cells per ml and frozen with 5% DMSO in liquid nitrogen. Cells to be harvested were washed with PBS once and scraped into protein lysis buffer (1M Tris-HCl pH 7.5, 5M NaCl, 0.5M EDTA, 1% NP40, 1x Protease inhibitor, 10mM NaF, 1x PMSF, 0.28mM Na$_3$VO$_4$) or QIAzol lysis reagent (Qiagen) for protein analysis or RNA extraction respectively.

2.2.4 Mammalian cell transfections

Cells were seeded at a density of 15,000 cells/cm^2 in 6well or 10cm dishes with prolifieration media. After overnight (16hrs) attachment,

cells were transfected with 2µg (6 well) or 12.5µg (10cm) of DNA plasmid or oligonucleotides (200nm). DNA plasmid/oligonucleotides were incubated with 800µl DMEM. In another tube, 8µl (6 well) or 40µl (10cm) of Lipofectamine 2000 (Invitrogen) was incubated with 800µl DMEM. Both mixtures were incubated at room temperature for 5mins. Following this, the plasmids/oligonucleotides were mixed with the Lipofectamine mix and incubated for 20 mins at room temperature. This allows the formation of Lipofectamine-plasmid complexes. The entire contents were transferred onto seeded cells dropwise and cultures were incubated at 37°C, 5% CO_2 for 16hrs. Fresh media was added to the cells and left for a further 24hrs before harvesting or seeding for differentiation.

2.2.5 Selection of stable transfected cell lines

C2C12 cells were transfected as described in section 2.2.4 for 36hrs. Cells were passaged and allowed for attachment before addition of Neomycin containing media (0.6mg/ml). To determine complete death of cells, Neomycin was added onto untransfected C2C12 cells which were used as control. After 5-7days, untransfected cells would have died and selected transfected cells were seeded at 10,000 cells per plate in 10cm dishes. Colonies were picked and expanded in 24 wells and eventually to 10cm dishes and frozen down with 5% DMSO.

2.2.6 Selection of stable transfected cell lines using HiLo RMCE

The HiLo RMCE method used to overexpress shNF-κB is a known protocol and is published [213]. C2C12 acceptor cell lines were co-transfected with pEM784 (150ng) and pEM784-shNF-κB (3850ng) or solely pEM784 (control). The plasmid pEM784 was designed to express nlCre recombinase (N-terminal nuclear localization signal to the Cre protein). After 24hrs of transfection, fresh media was replaced and after a further 24hrs, 0.5µg/ml puromycin was added to select transfected cells. Puromycin concentration was doubled to 1µg/ml 24hrs later and cells were left for 2-3 days to allow cells to die.

Puromycin resistant colonies were then allowed to proliferate and were trypsinized for freezing or harvested for molecular analysis.

2.2.7 Proliferation assay (Methylene blue photometric end-point assay)

C2C12 cells were seeded at a density of 1000 cells/well in 96 wells in replicates of 8. Following overnight attachment, media was removed and fresh proliferation media was added. This is the 0hr time point. Plates were collected and fixed at 24 and 48hrs time points by removal of media followed by 3x washes with PBS and addition of 10% Formal saline (0.17% saline, 10% formaldehyde). Cells were allowed to fix overnight. Following fixation, the fixative was removed and cells were washed with PBS 3x. Methylene blue (1% methylene blue, 0.01M borate buffer, pH 8.7) was added and incubated for 30 mins at room temperature. After incubation, stain was removed and cells were washed with Borate buffer (0.01M Sodium borate buffer, pH 8.5) 4x followed by addition of 0.1M HCl:100% Ethanol (1:1). Absorbance reading was taken at 655nm which reflects the final cell number at the various time points.

2.2.8 Differentiation assay

C2C12 cells were seeded at a density of 25,000 cells/cm^2 in 24 well plates containing coverslips and allowed for overnight attachment. Following attachment, media was removed and changed to differentiation media (DMEM, 2% HS, 1% P/S). Cells were collected at 0, 24, 48, 72 and 96hrs time points, fixed and stained with H & E (Hematoxylin and Eosin) as follows: Media was removed and cells were washed with PBS once and fixed with 20:2:1 fixative (70% Ethanol, 37% paraformaldehyde, acetic acid) for 30s and washed with PBS 3x. PBS was removed and Hematoxylin was added for 3 mins at room temperature. Subsequently, 0.1% HCl was added and removed quickly and cells were washed with Scotts tapwater (Sodium Bicarbonate 0.35%, Magnesium Sulfate 2%) 5x, 1 min each and Eosin was added. 100% Ethanol was added for 5mins 3x each and coverslips

were placed in xylene for dehydration. Coverslips were mounted with DPX on microscope slides and allowed to dry before observing under the microscope.

2.2.9 Protein extraction and Bradford assay

Media was removed and cells were washed with PBS once followed by addition of protein lysis buffer. Cells were scraped in protein lysis buffer with a cell scraper and syringed 20x using a 26G needle. The supernatant was recovered following centrifugation at 12,000 rpm for 15mins at 4°C. Protein estimation was performed by Bradford Assay to provide protein concentration estimations of the lysates. The Bradford reagent was dilued 5x with Mili-Q water to a working concentration of 1x and 1.2ml was added into total protein lysate (98µl + 2µl protein lysate). The contents were mixed and absorbance measured at 595nm by a UV Spectrophotometer. A standard curve was constructed with BSA (Bovine Serum Albumin) at concentrations from 0 - 10µg and the concentration of unknown protein samples calculated.

2.2.10 SDS-PAGE and western blot

Following protein estimation by Bradford assay, samples were prepared according to protein amounts required and boiled for 5 mins in 4x LDS loading dye, 1x β- mercaptoethanol (β-ME). Samples were loaded onto NuPage 4-12% gradient Bis-Tris pre cast polyacrylamide gels (Invitrogen) and proteins were separated in SDS-PAGE gels in 1x NuPage MES SDS running buffer. SeeBlue Plus2 Pre-Stained Standard (Invitrogen) was loaded alongside the samples and used as a marker of the size of proteins on the gel. Following electrophoresis, the proteins were transferred to Trans-Blot (Bio-Rad) Nitrocellulose membranes by electroblotting using the XCell II Blot Module (Invitrogen) in transfer buffer (Glycine 75g, Tris 15.1g, 20% Methanol). The membranes were then blocked overnight at 4°C in 5% low fat milk (Sigma) in TBST. After blocking, membranes were probed with primary antibodies at respective dilutions for 3hrs at room temperature and secondary antibodies (conjugated to horseradish peroxidase; HRP) were incubated for 1hr at room temperature. The protein levels were detected by using Western Lightning (PerkinElmer) Western Blot Chemiluminescence Reagent.

2.2.11 RNA extraction and qPCR

At each time point, cells were harvested in 700µl Qiazol and RNA was extracted using miRNESY mini kit (Qiagen), see section 2.2.12. Quantitation of miRNAs was performed first by reverse transcription using the miScript RT II kit (Qiagen) followed by miScript primer assay kit (Qiagen) for quantitative PCR according to the company's protocol (see section 2.2.13 and 2.2.14). Reverse transcription of mRNAs was performed with iScript cDNA synthesis kit (Biorad), see section 2.2.15. and the qPCR was subsequently performed with SYBR Green (SsoFast Evagreen Supermix, Biorad) which consists of a dye having the same properties as SYBR Green (see section 2.2.16). However, the mix excludes primers and template.

2.2.12 miRNeasy mini kit (Qiagen)

Cells in QIAzol lysis buffer were homogenized by vortexing for 1 min and placed at room temperature for 5 mins. Chloroform (140µl) was added and the homogenate was mixed vigourously for 15s. The mixture was allowed to stand at room temperature for 2-3 mins and centrifuged at 12,000xg 15 mins at $4^{o}C$. Subsequently, the upper phase was collected into a fresh eppendorf tube (1.5ml) and 1.5 volumes of 100% ethanol was added to precipitate the nucleotides. The sample was quickly loaded onto a spin column (RNeasy mini spin column) and centrifuged at 8000xg for 15s. The column was washed with 700µl of buffer RWT followed by 500µl buffer RPE twice where the last wash was performed at 8000xg for 2mins. The column was spun a final time to remove residual ethanol and RNA was eluted in 40µl dH_2O.

2.2.13 Reverse transcription using miScript II RT kit (Qiagen)

Reverse transcription was performed according to manufacturer's protocol. The reverse transcription reaction was performed with the following mix: 1x HiFlex buffer, 1x miScript Nucleics mix, 1x miScript reverse transcriptase mix to a total volume of 20µl. The reaction mix was incubated at $37^{o}C$ for 60 mins followed by $95^{o}C$ for 5 mins to

59

inactivate reverse transcriptase. The cDNA was then diluted as required for real-time quantitative PCR. Duplicate reverse transcription reactions was performed for each sample.

2.2.14 Real-time quantitative PCR (qPCR) using miScript primer assay (Qiagen)

Real-time quantitative PCR (qPCR) was performed in the following reaction mix: 1x SYBR Green, 1x miScript Universal primer, 1x miScript primer (mmu-miR-34a/Hsa-miR-34a or RNU6B) with 1µl of cDNA template (diluted) to a total volume of 10µl. Each reaction was loaded on to a 96-well plate. The plate was spun at 1000rpm for 1min and placed in a thermal cycler (Bio-Rad MJ Research PTC-200 Thermal Cycler). The real-time quantitative PCR conditions are as follows: Initial activation at $95^{o}C$ for 15mins, denaturation at $94^{o}C$ for 15s, annealing at $55^{o}C$ for 30s, extension at $70^{o}C$ 30s (Data acquicision after this step) for 40 cycles. Ramp rate was $1^{o}C/s$

2.2.15 Reverse transcription using iScript cDNA synthesis kit (Biorad)

The components for reverse transcription using iScript cDNA synthesis were as follows: 1µg of RNA template, 1µl iScript reverse transcriptase, 1x iScript reaction mix and dH_2O added to final volume of 20µl. The reaction mix was incubated at $25^{o}C$ for 5 mins, $42^{o}C$ for 30 mins, $85^{o}C$ for 5 mins and held at $4^{o}C$. The cDNA was appropriately diluted according to the abundance of the gene.

2.2.16 Real-time quantitative PCR of mRNA with SYBR green (SsoFast™ EvaGreen)

Quantitative measurement of mRNA was carried out using SYBR green (SsoFast™ EvaGreen, Biorad). SsoFast EvaGreen is a 2x PCR mix consisting of dNTPs, Sso 7d fusion polymerase, MgCl2, EvaGreen dye and stabilizers. The reaction mix consists of 1x SsoFast™ EvaGreen, 0.25µM Forward and Reverse primers and 3µl of diluted cDNA in a final volume of 10µl.

2.2.17 Murine primary myoblast extraction

Four to six week old mice (C57BL6 wild type and $Mstn^{-/-}$) were sacrificed and the hindlimb muscles were dissected and primary myoblasts were cultured. Muscles were minced and digested in 0.2% collagenase type-1A (Sigma) for about 90 mins with gentle shaking at $37^{o}C$. After digestion was complete, the muscle tissue was pelleted and washed with PBS. Following this, the muscle tissues were vigorously broken further into smaller pieces for 5 mins and the slurry filtered through a 100µM cell strainer and centrifuged and the pellet was resuspended in primary myoblast proliferation medium. The mixture was then plated onto uncoated plates to enrich for myoblasts for 3hrs. Following this, the unattached cells were transferred onto Matrigel (BD; Becton Dickinson, Franklin Lakes, NJ) coated plates to allow myoblasts attachment for 16hrs. Myoblasts were cultured on Matrigel coated plates in proliferation medium which consists of DMEM, 20% FBS (Fetal bovine serum, invitrogen), 10% HS, 1% CEE and 1% P/S at $37^{o}C$, 5% CO_2. Following overnight attachment of myoblasts (PP2), the supernatant was transferred to freshly matrigel coated plates (PP3). Attached cells were trypsinized and seeded at a density of 15,000 cells/cm^2 in 10cm dishes and allowed to proliferate for 36hrs before extraction of RNA. PP3 cells were seeded at a density of 25,000 cells/cm^2 in 10cm dishes in proliferation media and allowed for overnight attachment. The media was subsequetly changed to differentiation media (DMEM, 2% HS, 1% P/S) and cells were allowed to differentiate for 48hrs before RNA extraction. This is a well established method in our laboratory and it yields high proportion of myogenic cells.

2.2.18 microRNA microarray

Changes in microRNAs expression in samples were determined by performing microRNA microarray (Exiqon Services, Denmark) as follows: 650 ng total RNA from sample and reference was labeled with Hy3™ and Hy5™ fluorescent label, respectively, using the miRCURY

LNA™ microRNA Hi-Power Labeling Kit, Hy3™/Hy5™ (Exiqon, Denmark) following the procedure described by the manufacturer. The Hy3™-labeled samples and a Hy5™-labeled reference RNA sample were mixed pair-wise and hybridized to the miRCURY LNA™ microRNA Array 7'th GEN (Exiqon, Denmark), which contains capture probes targeting all microRNAs for human, mouse or rat registered in the miRBASE 18.0. The hybridization was performed according to the miRCURY LNA™ microRNA Array Instruction manual using a Tecan HS4800™ hybridization station (Tecan, Austria). After hybridization the microarray slides were scanned and stored in an ozone free environment (ozone level below 2.0 ppb) in order to prevent potential bleaching of the fluorescent dyes. The miRCURY LNA™ microRNA Array slides were scanned using the Agilent G2565BA Microarray Scanner System (Agilent Technologies, Inc., USA) and the image analysis was carried out using the ImaGene 9.0 software (BioDiscovery, Inc., USA). The quantified signals were background corrected (Normexp with offset value 10, see Ritchie et al. 2007) and normalized using quantile normalization method, which produces the best between-slide normalization to minimize the intensity-dependent differences between the samples.

2.2.19 Muscle injury and RNA extraction from muscle

Six week old male wild type mice (C57BL6) were anaesthetized (10mg/ml ketamine and 1mg/ml xylazine dissolved in PBS) via intraperitoneal injections and injury was induced into the Tibialis anterior (TA) muscle of the left hindlimb with Notexin (10µg/ml in 0.9% sterile saline). Notexin injury and adenovirus (Ctrl or miR-34a OE) administration was performed via injection of Notexin with 1×10^8 pfu virus particles. Mice were sacrificed at 1, 2, 3, 5, 7, 10 and 28 days post-injury. Muscles were either embedded in optimal cutting temperature compound (OCT) and frozen at -80^oC or RNA was extracted (miRNESY mini kit, Qiagen) from the injured TA and its corresponding uninjured TA muscle and the expression of genes were

quantified (see section 2.2.12 – 2.2.14). TA muscles were sectioned to 0.2μM thickness and stained for histological analysis.

2.2.20 Luciferase assay

Luciferase assay was performed using Dual-Luciferase® Reporter (DLR™) Assay system (Promega). Cells were transfected with reporter genes for 24hrs and subsequently lysed in passive lysis buffer as indicated in the manufacturer's protocol. Cells were incubated with lysis buffer for 5 mins room temperature with gentle shaking. Following this, the lysate was collected and aliquoted in to 96 well plates in volumes of 20μl and placed in the GloMax® 96 Microplate Luminometer. Briefly, 100μl of Stop and Glo buffer (1:50 Stop and Glo reagent: Stop and Glo buffer) and 100μl of Luciferase assay reagent II (LARII) were injected in to each well and the fluorescence measured. Renilla or firefly luciferase was used for normalization as according to the design of vector.

2.2.21 Propidium iodide staining and Flow cytometry Cell Sorter (FACS)

Approximately 1 million cells/ml were washed in cold PBS twice in a 5ml round-bottom tube (BD Pharmigen). Cells were centrifuged at 1000g for 5 mins and supernatant discarded. With gentle vortexing, ice-cold 70% ethanol was added to fix the cells and was stored at -20°C overnight. To stain cells, cells were centrifuged at 1000g for 10mins, ethanol was removed and propidium iodide (10ml water; 100μl propidium iodide (10mg/ml) and 50μl RNAse (10mg/ml)) was added and incubated at 4°C for 1hr. Staining solution was removed by centrifugation at 1000g for 5mins and cells were washed with ice-cold PBS twice leaving a final volume of 1ml per sample. FACS was performed using FACSAria II and cell cycle profile was analyzed using Modfit.

2.2.22 TUNEL assay

Tunel assay was performed with In situ cell death detection kit, Fluorescein kit (Roche). Cells were fixed at appropriate time points with 4% Paraformaldehyde in PBS, pH 7.4 for 1hr at Room temperature (RT). Subsequently, cells were rinsed with PBS and permeabilized with 0.1% Triton X-100 in 0.1% Sodium Azide for 10mins with gentle shaking at RT. Cells were washed and Tunel reaction mixture (1:50 dilution; Enzyme solution: Labeling solution) was added and the slide was incubated in a humidified chamber for 1hr at 37°C in the dark. Cells were washed with PBS 3x and stained with DAPI (1:1000 in PBS) with gentle shaking for 5mins at RT. After washing with PBS, slides were mounted with Prolong gold mounting media and left to dry overnight before viewing under microscope.

2.2.23 *In vitro* induced quiescence in C2C12 myoblasts

Proliferating C2C12 myoblasts were cell cycle arrested at G0 phase following the method described by Kitzmann et al [214]. Briefly, methionine-free media was added into proliferating C2C12 myoblasts for 36hrs. After which, cells would exit the cell cycle enter in to G0 phase. Cells were either harvested or released into G1 phase by replacing existing media with fresh media (DMEM, 10%FBS, 1% P/S) and incubated for 10hrs. Cells were then harvested in protein lysis buffer or Qiazol for molecular analysis.

2.2.24 Generation of adenovirus

Pre-miR-34a was amplified including 100bp flanking sequences incorporating restriction enzyme sites BamH1 and Nhe1. The PCR product was cloned into pacAd5 miR-GFP/Puro shuttle vector (VPK-253, Cellbiolabs). Subsequently, pacAd5 containing pre-miR-34a or GFP control and pacAd5 9.2-100 vector was linearized with Pac1 restriction enzyme and purified using phenol and chloroform. pacAd5 (pre-miR-34a) or pacAd5 (GFP) was co-transfected with pacAd5 9.2-100 vector backbone in a ratio of 4:1 in to HEK293AD cells. After 24hrs

of transfection, fresh media was supplied and the culture was left for about 7 days. When viral plaques were observed, the crude virus was collected. The crude virus was lysed with repeated freeze-thaw cycles as follows: 30mins at 37°C followed by rapid freezing in dry-ice soaked with methanol. Cycles were repeated 3 times and the viral lysate was used for further propagation.

2.2.25 Determination of virus titer

HEK293AD cells were seeded into 96 well plates at a density of 30,000 cells per well and allowed to attach overnight. Fresh media was replaced and the viral lysate was added in serial dilutions (10^{-1}, 10^{-2}, 10^{-3}, 10^{-4}, 10^{-5}, 10^{-6}, 10^{-7}, 10^{-8}, 10^{-9}, 10^{-10}) and allowed to incubate for 10 days. Following this, the viral titer was calculated based on Cytopathic effect (CPE) observed on cells at all dilutions using the formula: Titer (pfu/ml) = $10^{(1 + Z (X - 0.5))}$, where Z is Log 10 of the starting dilution (= 1 for a ten-fold dilution) and X is the sum of the fractions of CPE-positive wells.

2.2.26 Isolation of satellite cells for adenovirus infection and immunocytochemistry (ICC) staining

Satellite cells were isolated as mentioned in section 2.2.17 and seeded in to 8 well chamber slides at a density of 10,000 cells per well. After 3 hrs of attachment, adenovirus (Ctrl or miR-34a OE) was added at a MOI of 8 and infection was allowed to occur for 48hrs. Subsequently, cells were fixed with 20:2:1 fixative and stained for MyoD as follows: Cells were washed with 1x PBS once and permeabilized with 0.1% Triton-X 100 in PBS for 10 mins at RT with gentle shaking. Cells were washed with 1x PBS for 5 mins and incubated in 5% Normal Goat Serum (NGS) with 5% Normal Sheep Serum (NSS) in 0.35% Carrageenan (cλ) in PBS for 1 hr at RT for blocking. Following this, primary antibody (MyoD, 1:100 in 5% NGS with 5% NSS in 0.35% cλ in PBS) was added and incubated overnight at 4°C. Cells were washed with TBST 3x for 5 mins each and the secondary antibody was added

(Goat Anti-Rabbit IgG Alexa Fluor® 594 conjugated, 1:300 in 5% NGS with 5% NSS in 0.35% cλ in PBS) and incubated for 1 hr at RT in the dark. Cells were washed with TBST 3x for 5 mins each and incubated with DAPI (1:1000 in PBS) for 5 mins at RT and finally rinsed with PBS once. Slides were mounted with Prolong gold anti-fade reagent (Invitrogen).

2.2.27 Immunohistochemistry (IHC) staining of muscle sections

Muscle tissue sections were fixed with 4% PFA for 5 mins and washed with 1x PBS for 3 times, 5 mins each. Cells were permeabilized with 0.1% Triton-X 100 in PBS for 10 mins at RT with gentle shaking. Cells were washed with 1x PBS for 5 mins and incubated in 5% Normal Goat Serum (NGS) with 5% Normal Sheep Serum (NSS) in 0.35% Carrageenan (cλ) in PBS for 1 hr at RT for blocking. Following this, primary antibody (MyoD, 1:50 in 5% NGS with 5% NSS in 0.35% cλ in PBS) was added and incubated overnight at 4^oC. Cells were washed with TBST 3x for 5 mins each and the secondary antibody was added (Goat Anti-Rabbit IgG Alexa Fluor® 594 conjugated, 1:300 in 5% NGS with 5% NSS in 0.35% cλ in PBS) and incubated for 1 hr at RT in the dark. Cells were washed with TBST 3x for 5 mins each and incubated with DAPI (1:1000 in PBS) for 5 mins at RT and finally rinsed with PBS once. Slides were mounted with Prolong gold anti-fade reagent (Invitrogen).

2.2.28 H & E staining of muscle tissue sections

Muscle tissue sections were stained with Haematoxylin and Eosin (H & E) for histological analysis. Sections were initially stained with Haematoxylin for 1 min and excess stain was washed away with tap water. Next, the sections were washed with Scotts tap water for 2 mins followed by staining with Eosin for 2 mins. Excess Eosin was washed away with tap water. Sections were then dehydrated with successive increment of Ethanol dilutions; 50% Ethanol, 70% Ethanol, 95% Ethanol for 2 mins and finally 100% Ethanol 2x for 2 mins. Sections were then placed in xylene for 5 mins 2x and mounted with DPX.

2.2.29 Chromatin immunoprecipitation (ChIP)

ChIP was performed following X-ChIP protocol (abcam) C2C12 cells were treated with formaldehyde (0.75% final concentration), drop-wise, in to the media and allowed to incubate for 10mins at RT with gentle shaking to cross-link proteins to DNA. Glycine (125mM final concentration) was added and incubated further for 5 mins at RT. Cells

were washed with cold PBS twice and scraped in to 5 ml of PBS. Cells were pelleted by centrifugation at 1000g for 5mins at 4°C. The cell pellet was then resuspended in ChIP lysis buffer (50 mM HEPES-KOH pH 7.5, 140 mM NaCl, 1 mM EDTA pH8, 1% Triton X-100, 0.1% Sodium Deoxycholate, 0.1% SDS, Protease Inhibitors (add fresh each time), 750µl per 1 x 10^7 cells).. The genomic DNA was sonicated to a range of 200-700bp sized fragments and pelleted by centrifugation at 8000g for 30s at 4°C. The supernatant was collected for immunoprecipitation. Equal amounts of DNA were used for each IP. DNA was incubated with primary antibodies (MyoD and TCF12) at 4°C for 1 hr. Preparation of Protein A and G was performed by washing 3 times in RIPA buffer (50 mM Tris-HCl pH 8.0, 150 mM NaCl, 2 mM EDTA pH 8.0, 1% NP-40, 0.5% Sodium Deoxycholate, 0.1% SDS, Protease Inhibitors (add fresh each time)) and blocked with single stranded herring sperm DNA at a final concentration of 75ng/µl of beads and BSA to a final concentration of 0.1 µg/µl of beads. RIPA buffer was added at twice bead volume and incubated for 30mins RT. Beads were washed with RIPA buffer and twice the bead volume of RIPA buffer was added. Blocked beads (60µl) were added to all IP samples and incubated overnight with rotation at 4°C. The mixture was then centrifuged at 2000g for 1 min and the supernatant removed. Beads were washed once in low salt buffer (0.1% SDS, 1% Triton X-100, 2 mM EDTA, 20 mM Tris-HCl pH 8.0, 150 mM NaCl), followed by high salt buffer (0.1% SDS, 1% Triton X-100, 2 mM EDTA, 20 mM Tris-HCl pH 8.0, 500 mM NaCl) After each wash, beads were centrifuged at 2000g for 1 min and supernatant was removed. DNA was eluted from the beads by addition of elution buffer (1% SDS, 100mM NaHCO$_3$) and vortexed gently for 15 mins at 30°C. The mixture was centrifuged at 2000g for 1 min and 2µl RNase A (10mg/ml) was added, and incubated overnight at 65°C. The DNA was then purified using PCR purification kit (Qiagen) and PCR was performed using primers specific for myogenin promoter.

2.2.30 Statistical analysis

Statistical method used for all experiments conducted in this thesis was the Student's T-test. Statistical analysis was performed using Microsoft Excel. P values calculated in microRNA array were based on moderated t-statistics and further adjusted with Benjamini and Hochberg multiple testing adjustment method. P value < 0.05 was considered significant for all experiments.

3. Results

3.1 microRNAs (miRNAs) involved in myogenesis

To identify miRNAs regulated by Myostatin (Mstn), RNA was isolated from primary myoblasts and myotubes from Wild type (WT) and $Mstn^{-/-}$ mice. In addition, RNA was also isolated from WT primary myoblasts and myotubes treated without or with recombinant MSTN protein. RNA from these samples were used for miRNA microarray which was performed as described in section 2.2.18. Subsequent bioinformatics analysis identified 62 microRNAs to be upregulated and 88 microRNAs to be downregulated during myogenic differentiation of myoblasts into myotubes (Table 3.1). In MSTN treated primary myoblasts, 22 miRNAs were observed to be upregulated and 18 miRNAs downregulated, when compared to control treated myoblasts (Table 3.2). In $Mstn^{-/-}$ primary myoblasts, 6 miRNAs were found to be upregulated while 15 miRNAs were found to be downregulated as compared to WT primary myoblasts (Table 3.3). Sixteen miRNAs were observed to be upregulated in MSTN treated myotubes and 10 miRNAs downregulated (Table 3.4), when compared to control treated primary myotubes. Lastly, 15 miRNAs were found to be upregulated and 11 miRNAs dowregulated in $Mstn^{-/-}$ primary myotubes, as compared to WT primary myotubes (Table 3.5).

miRNAs upregulated during myotube differentiation		
miRNA	**FC**	**P.value**
mmu-miR-1a-3p	7.99	2.24E-07
mmu-miR-503-5p	5.91	2.24E-07
mmu-miR-133a-3p	5.46	2.24E-07
mmu-miR-133a-5p	4.75	2.24E-07
mmu-miR-133b-3p	3.80	1.96E-06
mmu-miR-1a-1-5p	3.46	5.37E-06
mmu-miR-669c-3p	3.26	4.52E-07
mmu-miR-298-5p	2.92	4.52E-07
mmu-miR-128-3p	2.43	1.37E-06
mmu-miR-210-3p	2.40	1.33E-05
mmu-miR-322-5p	2.36	3.18E-06
mmu-miR-206-3p	2.30	3.18E-06
mmu-miR-1a-2-5p	2.23	3.10E-06
mmu-miR-351-5p	2.09	3.18E-06
mmu-miR-542-3p	2.05	2.79E-05
mmu-miR-199a-3p/mmu-miR-199b-3p	2.00	2.06E-05
mmu-miR-378b	1.97	3.78E-05
mmu-miR-378-3p	1.92	4.82E-05
mmu-miR-501-5p	1.85	2.06E-05
mmu-miR-214-3p	1.78	3.04E-04
mmu-miR-5100	1.66	3.29E-03
mmu-miR-34a-5p	1.65	1.46E-03
mmu-miR-500-3p	1.64	2.29E-04
mmu-miR-362-3p	1.63	2.32E-05
mmu-miR-483-5p	1.62	3.17E-04
mmu-miR-365-3p	1.62	6.35E-05
mmu-miR-181b-5p	1.62	1.06E-04
mmu-miR-206-5p	1.58	3.70E-05
mmu-miR-199a-5p	1.58	5.94E-04
mmu-miR-188-5p	1.57	3.33E-04
mmu-miR-33-5p	1.53	6.49E-04
mmu-miR-149-5p	1.53	3.70E-05
mmu-miR-532-5p	1.50	8.76E-05
mmu-miR-34b-5p	1.50	1.15E-03
mmu-miR-301a-3p	1.49	3.83E-04
mmu-miR-133b-5p	1.48	1.31E-03
mmu-miR-181d-5p	1.47	2.62E-04
mmu-miR-350-3p	1.46	1.31E-03
mmu-miR-489-5p	1.45	4.00E-04
mmu-miR-199b-5p	1.41	2.01E-04
mmu-miR-378-5p	1.41	1.15E-03

miRNA	FC	P.Value
mmu-miR-501-3p	1.40	3.33E-04
mmu-miR-181a-5p	1.35	4.46E-04
mmu-miR-675-3p	1.32	8.34E-03
mmu-miR-34c-5p	1.31	3.33E-03
mmu-miR-136-5p	1.30	9.50E-03
mmu-let-7f-5p	1.29	1.78E-02
mmu-miR-290-5p	1.28	1.02E-03
mmu-miR-5097	1.26	2.75E-02
mmu-miR-487b-3p	1.26	3.08E-02
mcmv-miR-M23-1-5p	1.25	3.08E-02
mmu-miR-3107-5p/mmu-miR-486-5p	1.24	7.58E-03
mmu-miR-431-5p	1.24	4.07E-02
mmu-miR-208a-5p	1.20	3.04E-02
mmu-miR-24-1-5p	1.19	7.67E-03
mmu-miR-450a-1-3p	1.19	2.78E-02
mmu-miR-744-5p	1.18	1.84E-02
mmu-miR-693-5p	1.16	3.26E-02
mmu-miR-503-3p	1.14	3.42E-02
mmu-miR-31-3p	1.12	3.54E-02
mmu-miR-466d-3p	1.11	4.07E-02
mmu-miR-465b-5p	1.10	4.52E-02

miRNAs downregulated during myotube differentiation

miRNA	FC	P.Value
mmu-miR-466b-5p/mmu-miR-466o-5p	0.89	1.84E-02
mmu-miR-19a-3p	0.89	2.57E-02
mmu-miR-1196-5p	0.88	2.53E-02
mmu-miR-669k-5p	0.88	4.54E-02
mmu-miR-882	0.88	2.76E-02
mmu-miR-17-5p	0.87	1.78E-02
mmu-miR-677-3p	0.87	3.82E-02
mmu-miR-1843-3p	0.87	1.76E-02
mmu-miR-669d-5p	0.87	1.33E-02
mmu-miR-99a-5p	0.86	1.65E-02
mmu-miR-320-3p	0.86	4.56E-02
mmu-miR-26b-5p	0.86	2.57E-02
mmu-miR-669b-3p	0.86	2.53E-02
mmu-miR-710	0.86	8.34E-03
mmu-miR-466a-5p/mmu-miR-466p-5p	0.85	3.63E-02
mmu-miR-151-5p	0.85	3.08E-02
mmu-miR-466q	0.85	3.82E-02
mmu-miR-300-5p	0.85	8.06E-03
mmu-miR-669a-3-3p	0.85	1.59E-02
mmu-miR-302a-3p	0.84	1.01E-02
mmu-miR-1957	0.84	3.42E-02
mmu-miR-204-5p	0.84	8.06E-03

mmu-miR-93-5p	0.84	2.78E-02
mmu-miR-290-3p	0.84	3.29E-02
mmu-miR-143-3p	0.83	2.34E-02
mmu-miR-30c-5p	0.83	1.70E-02
mmu-miR-467g	0.83	2.13E-03
mmu-miR-30b-5p	0.83	1.58E-02
SNORD110	0.82	6.99E-03
mmu-miR-466f	0.82	2.30E-03
mmu-let-7i-5p	0.82	2.09E-02
mmu-miR-1897-5p	0.82	7.23E-03
mmu-miR-21-3p	0.82	1.81E-03
mmu-miR-17-3p	0.82	1.31E-03
mghv-miR-M1-8	0.81	1.77E-03
mmu-miR-30e-5p	0.81	1.25E-02
mmu-miR-467e-3p	0.81	4.63E-02
mmu-miR-3069-3p	0.81	1.58E-03
mmu-miR-3103-3p	0.81	2.85E-03
mmu-miR-3572	0.81	1.01E-02
mmu-miR-669n	0.80	1.30E-03
mmu-miR-30a-5p	0.80	2.75E-02
mmu-miR-29a-3p	0.80	8.28E-04
SNORD68	0.80	5.12E-03
mmu-miR-100-5p	0.79	6.04E-04
mmu-miR-145-5p	0.78	9.51E-03
mmu-miR-25-3p	0.78	8.10E-04
mmu-miR-32-3p	0.78	8.10E-04
mmu-miR-7a-5p	0.77	1.06E-02
mmu-miR-3082-5p	0.77	4.58E-03
mmu-miR-23a-3p	0.77	4.00E-04
SNORD3@	0.76	3.63E-02
mmu-miR-712-5p	0.76	1.30E-03
mmu-miR-466i-5p	0.76	2.76E-03
mmu-miR-3084-3p	0.76	8.21E-04
mmu-miR-669c-5p	0.75	2.34E-03
mmu-miR-29c-3p	0.75	6.99E-03
mmu-miR-125a-5p	0.75	4.70E-04
mmu-miR-669p-3p	0.73	8.10E-04
mmu-miR-466f-3p	0.73	4.40E-04
mmu-miR-221-3p	0.72	3.33E-03
mmu-miR-19b-3p	0.70	2.20E-02
mmu-let-7c-5p	0.69	2.29E-04
mmu-miR-26a-5p	0.68	5.10E-05
mmu-let-7b-5p	0.67	2.57E-04
mmu-miR-30d-5p	0.67	8.93E-04
mmu-miR-3096-3p/mmu-miR-3096b-3p	0.66	8.76E-05
mmu-miR-338-3p	0.64	5.30E-05

mmu-miR-1949	0.64	4.76E-05
mmu-miR-101a-3p/mmu-miR-101c	0.63	1.66E-04
mmu-miR-3096-3p	0.63	7.43E-04
mmu-miR-346-3p	0.62	1.97E-05
mmu-miR-5109	0.59	3.55E-04
mmu-miR-222-3p	0.59	9.42E-05
mmu-miR-15b-5p	0.57	2.40E-05
mmu-miR-101a-3p	0.57	2.45E-05
mmu-miR-16-5p	0.56	6.04E-05
mmu-miR-1192	0.56	3.82E-02
mmu-miR-15a-5p	0.55	2.79E-05
mmu-miR-10b-5p	0.50	4.76E-05
mmu-miR-92a-3p	0.47	2.86E-05
mmu-miR-3473b	0.46	2.30E-05
mmu-miR-10a-5p	0.45	2.29E-06
mmu-miR-706	0.44	1.48E-06
mmu-miR-497-5p	0.44	1.33E-05
mmu-miR-126-5p	0.26	2.68E-06
mmu-miR-126-3p	0.24	2.77E-07
mmu-miR-195-5p	0.23	4.52E-07

Table 3.1: Differentially expressed miRNAs during myogenic differentiation of myoblasts into myotubes. All miRNAs listed have P values < 0.05.

miRNAs upregulated upon MSTN treatment of myoblasts		
miRNAs	**FC**	**P.value**
mmu-miR-450a-1-3p	1.68	1.27E-04
mmu-miR-34a-5p	1.35	2.09E-03
mmu-miR-7a-5p	1.30	2.09E-03
mmu-miR-10a-5p	1.27	2.83E-03
mmu-miR-675-3p	1.26	2.83E-03
mmu-miR-195-5p	1.21	4.14E-03
mmu-miR-29c-3p	1.20	2.25E-02
mmu-miR-126-3p	1.19	1.15E-02
mmu-miR-20b-5p	1.18	1.53E-02
mmu-miR-34b-5p	1.16	1.45E-02
mmu-miR-31-3p	1.16	2.65E-02
mmu-miR-125b-5p	1.15	1.45E-02
mmu-miR-26a-5p	1.15	3.50E-02
mmu-miR-10b-5p	1.15	1.53E-02
mmu-miR-126-5p	1.15	2.25E-02
mmu-miR-338-3p	1.14	2.97E-02
mmu-miR-101b-3p	1.13	2.83E-02
mmu-miR-30d-5p	1.13	4.68E-02
mmu-miR-32-5p	1.13	2.25E-02
mmu-miR-27a-3p	1.13	3.51E-02
mmu-miR-21-5p	1.12	2.25E-02
mmu-miR-145-5p	1.12	4.40E-02

miRNAs downregulated upon MSTN treatment of myoblasts		
miRNA	**FC**	**P. value**
mmu-miR-93-5p	0.89	4.41E-02
mmu-miR-669l-3p	0.88	3.50E-02
mmu-miR-501-5p	0.88	3.50E-02
mmu-miR-1a-2-5p	0.86	2.97E-02
mmu-miR-206-3p	0.86	2.25E-02
mmu-miR-706	0.85	2.64E-02
mmu-miR-302a-3p	0.84	4.14E-03
mmu-miR-503-5p	0.82	4.14E-03
mmu-miR-206-5p	0.82	5.48E-03
mmu-miR-1a-1-5p	0.81	3.51E-02
mmu-miR-133b-5p	0.79	2.83E-03
mmu-miR-133a-3p	0.79	2.83E-03
mmu-miR-301a-3p	0.78	3.89E-03
mmu-miR-188-5p	0.78	1.21E-02
mmu-miR-5111-5p	0.77	4.14E-03
mmu-miR-669c-3p	0.72	2.48E-02
mmu-miR-1a-3p	0.69	8.72E-04
mmu-miR-133a-5p	0.57	8.70E-06

Table 3.2: Differentially expressed miRNAs between Control and MSTN treated primary myoblasts. All miRNAs listed have P values < 0.05.

miRNAs upregulated in *Mstn*^{-/-} myoblasts		
miRNA	FC	P. value
mmu-miR-2137	1.80	1.60E-03
mmu-miR-199a-3p/mmu-miR-199b-3p	1.49	3.52E-03
mmu-miR-199a-5p	1.41	1.87E-02
mmu-miR-199b-5p	1.37	2.38E-03
mmu-miR-3473b	1.35	2.68E-02
mmu-miR-3096-5p	1.28	4.03E-02
miRNAs downregulated in *Mstn*^{-/-} myoblasts		
miRNA	FC	P. value
mmu-miR-338-3p	0.76	4.03E-02
mmu-miR-10b-5p	0.75	4.35E-02
mmu-miR-126-3p	0.74	7.22E-03
mmu-miR-31-5p	0.73	3.45E-02
mmu-miR-10a-5p	0.71	3.73E-03
mmu-miR-206-3p	0.69	6.85E-03
mmu-miR-34c-5p	0.68	3.52E-03
mmu-miR-126-5p	0.64	7.84E-03
mmu-miR-133a-5p	0.61	2.99E-03
mmu-miR-133b-3p	0.57	1.99E-03
mmu-miR-133a-3p	0.56	1.22E-03
mmu-miR-34b-5p	0.56	1.90E-03
mmu-miR-210-3p	0.56	1.22E-03
mmu-miR-34a-5p	0.56	2.39E-03
mmu-miR-1a-3p	0.55	1.90E-03

Table 3.3: Differentially expressed miRNAs between WT and *Mstn*^{-/-} primary myoblasts. All miRNAs listed have P.values <0.05.

miRNAs upregulated upon Myostatin treatment in myotubes		
miRNA	**FC**	**P.value**
mmu-miR-503-5p	1.35	1.51E-02
mmu-miR-2137	1.34	1.83E-02
mmu-miR-450a-1-3p	1.32	2.63E-03
mmu-miR-3107-5p/mmu-miR-486-5p	1.23	2.51E-02
mmu-miR-7a-5p	1.20	1.79E-02
mmu-miR-710	1.19	1.51E-02
mmu-miR-126-3p	1.18	3.18E-02
mmu-miR-335-5p	1.18	3.18E-02
mmu-miR-126-5p	1.18	1.79E-02
mmu-miR-222-3p	1.17	2.59E-02
mmu-miR-20a-5p	1.16	3.20E-02
mmu-let-7i-5p	1.15	3.20E-02
mmu-miR-351-5p	1.15	2.51E-02
mmu-miR-100-5p	1.15	3.18E-02
mmu-miR-34a-5p	1.13	4.20E-02
mmu-miR-17-5p	1.12	4.30E-02
miRNAs downregulated in MSTN treated myotubes		
miRNA	**FC**	**P.value**
mmu-miR-706	0.87	3.18E-02
mmu-miR-709	0.86	1.79E-02
mmu-miR-1a-2-5p	0.86	2.51E-02
mmu-miR-1a-1-5p	0.84	2.18E-02
mmu-miR-762	0.80	3.20E-02
mmu-miR-3475	0.78	2.88E-03
mmu-miR-5111-5p	0.70	1.83E-02
mmu-miR-133b-5p	0.70	3.75E-04
mmu-miR-206-5p	0.64	3.75E-04
mmu-miR-133a-5p	0.55	2.63E-03

Table 3.4: Differentially expressed miRNAs between Control and MSTN treated primary myotubes. All miRNAs listed have P.values <0.05.

miRNAs upregulated in *Mstn*^{-/-} myotubes		
miRNA	FC	P. value
mmu-miR-199b-5p	1.72	7.45E-03
mmu-miR-99b-5p	1.71	2.51E-02
mmu-miR-199a-3p/mmu-miR-199b-3p	1.68	1.69E-02
mmu-miR-214-3p	1.58	3.69E-02
mmu-miR-199a-5p	1.54	1.04E-02
mmu-miR-499-5p	1.40	7.45E-03
mmu-miR-128-3p	1.36	9.27E-03
mmu-miR-125a-5p	1.34	4.86E-02
mmu-miR-542-3p	1.31	3.69E-02
mmu-miR-1957	1.26	2.49E-02
mmu-miR-155-5p	1.23	2.48E-02
mmu-miR-99a-5p	1.20	2.48E-02
mmu-miR-29a-5p	1.19	4.91E-02
mmu-miR-139-5p	1.16	2.57E-02
mmu-miR-206-3p	1.15	4.91E-02

miRNAs downregulated in *Mstn*^{-/-} myotubes		
miRNA	FC	P.value
mmu-miR-431-5p	0.82	4.91E-02
mmu-miR-126-5p	0.79	9.27E-03
mmu-miR-706	0.79	9.27E-03
mmu-miR-712-5p	0.76	7.45E-03
mmu-miR-322-5p	0.76	9.27E-03
mmu-miR-136-5p	0.74	9.27E-03
mmu-miR-34c-5p	0.72	9.27E-03
mmu-miR-126-3p	0.71	4.91E-02
mmu-miR-338-3p	0.68	3.31E-03
mmu-miR-298-5p	0.67	3.31E-03
mmu-miR-34b-5p	0.66	3.31E-03

Table 3.5. Differentially expressed miRNAs between WT and *Mstn*^{-/-} primary myotubes. All miRNAs listed have P.values <0.05.

3.2 Myostatin regulates miR-34a

Next the differentially expressed miRNAs were analyzed and filtered, and two miRNAs were identified that were consistently regulated by Mstn; miR-34a and miR-126 (Table 3.6). Given the significant role played by miR-34a and Mstn in cell cycle regulation [125, 215-217], it was speculated that miR-34a could potentially act as a Mstn downstream effector. Therefore, miR-34a was selected for further functional analysis.

Subsequently, the expression of miR-34a was validated using different experimental models. As expected, a significant reduction in miR-34a expression in $Mstn^{-/-}$ primary myoblasts and myotubes was observed, when compared to respective WT controls (Figure 3.1A). Consistent with this, miR-34a expression was significantly increased upon treatment with recombinant MSTN protein in both primary myoblasts and myotubes (Figure 3.1B). Treatment of C2C12 myoblasts with MSTN also resulted in significantly upregulated Precursor miR-34a (Pre-miR-34a) expression (Figure 3.1C). Furthermore, the treatment of C2C12 myoblasts with MSTN upregulated miR-34a expression in both a dose- (Figure 3.1D) and time-dependent (Figure 3.1E) fashion. Similarly, significantly increased miR-34a expression was observed in primary human myoblasts (36C15Q) upon MSTN treatment (Figure 3.1F), which was shown to be time dependent (Figure 3.1G). In order to test if miR-34a-specific blockade would interfere with Mstn-mediated induction of miR-34a, the expression of miR-34a in response to MSTN treatment in the absence or presence of a miR-34a-specific AntagomiR was observed. As shown in Figure 3.1H, miR-34a induction by MSTN was significantly impaired in the presence of a miR-34a-specific AntagomiR (Figure 3.1H). Finally, in agreement with Mstn regulation of miR-34a it was observed that miR-34a expression increased during C2C12 differentiation (Figure 3.1I), which was also associated with increased expression of endogenous $Mstn$ expression (Figure 3.1J). Collectively, these results confirm that excess Mstn induces miR-34a expression in both mouse and human myoblasts and myotubes.

Myoblasts			
Myostatin	miRNA	FC	P.value
+	miR-34a	1.35	0.00209
-		0.56	0.00239
+	miR-126	1.19	0.0115
-		0.74	0.00722
Myotubes			
Myostatin	miRNA	FC	P.value
+	miR-34a	1.13	0.042
-		0.93	0.687
+	miR-126	1.18	0.0318
-		0.71	0.0491

Table 3.6: Two miRNAs (miR-34a and miR-126) were identified to be postively regulated by Mstn, in both myoblasts and myotubes, based on miRNA microarray results. Fold change (FC) is relative to control treated primary cultures.

3.3 Myostatin directly regulates miR-34a via NF-κB (p65)

There are three NF-κB binding sites in the promoter of miR-34a that have been shown to be required for the transcription of miR-34a [218] (Figure 3.2A). As previously demonstrated in our laboratory, Mstn induces the expression and translocation of NF-κB into the nucleus [219]. Therefore, it was hypothesized that Mstn could potentially induce miR-34a expression through activation of NF-κB. Consistent with this hypothesis, NF-κB expression was induced upon MSTN treatment (Figure 3.2B). In addition, shRNA-mediated downregulation of NF-κB expression (Figure 3.2C) significantly reduced miR-34a expression in myoblasts (Figure 3.2D). To assess for direct regulation of miR-34a by Mstn, C2C12 myoblasts were transfected with a 1.3kb miR-34a promoter luciferase reporter construct and subjected to MSTN treatment. Subsequent analysis revealed a dose-dependent increase in miR-34a promoter-reporter luciferase activity in response to treatment with increasing concentrations of MSTN protein (Figure 3.2E). TNF-α has previously been shown to induce NF-κB expression [219]. Consistent with this, increased miR-34a promoter reporter activity was observed upon treatment with increasing concentrations of TNF-α (Figure 3.2F). To characterize the importance of the upstream

NF-κB binding sites in MSTN-regulation of miR-34a promoter, three different truncated miR-34a promoter reporter constructs were generated (Figure 3.2G). Subsequent analysis revealed a significant reduction in MSTN-mediated activation of the miR-34a promoter reporter upon deletion of the two distal most NF-κB binding sites of the miR-34a promoter reporter (Figure 3.2G). Importantly, comparable MSTN-mediated activation of the miR-34a promoter reporter was observed in myoblasts transfected with either PMT-T2 or the miR-34a promoter reporter construct where all three NF-κB binding sites were deleted (PMT-T3). These results suggest that Mstn activates the transcription of miR-34a through a mechanism involving NF-κB.
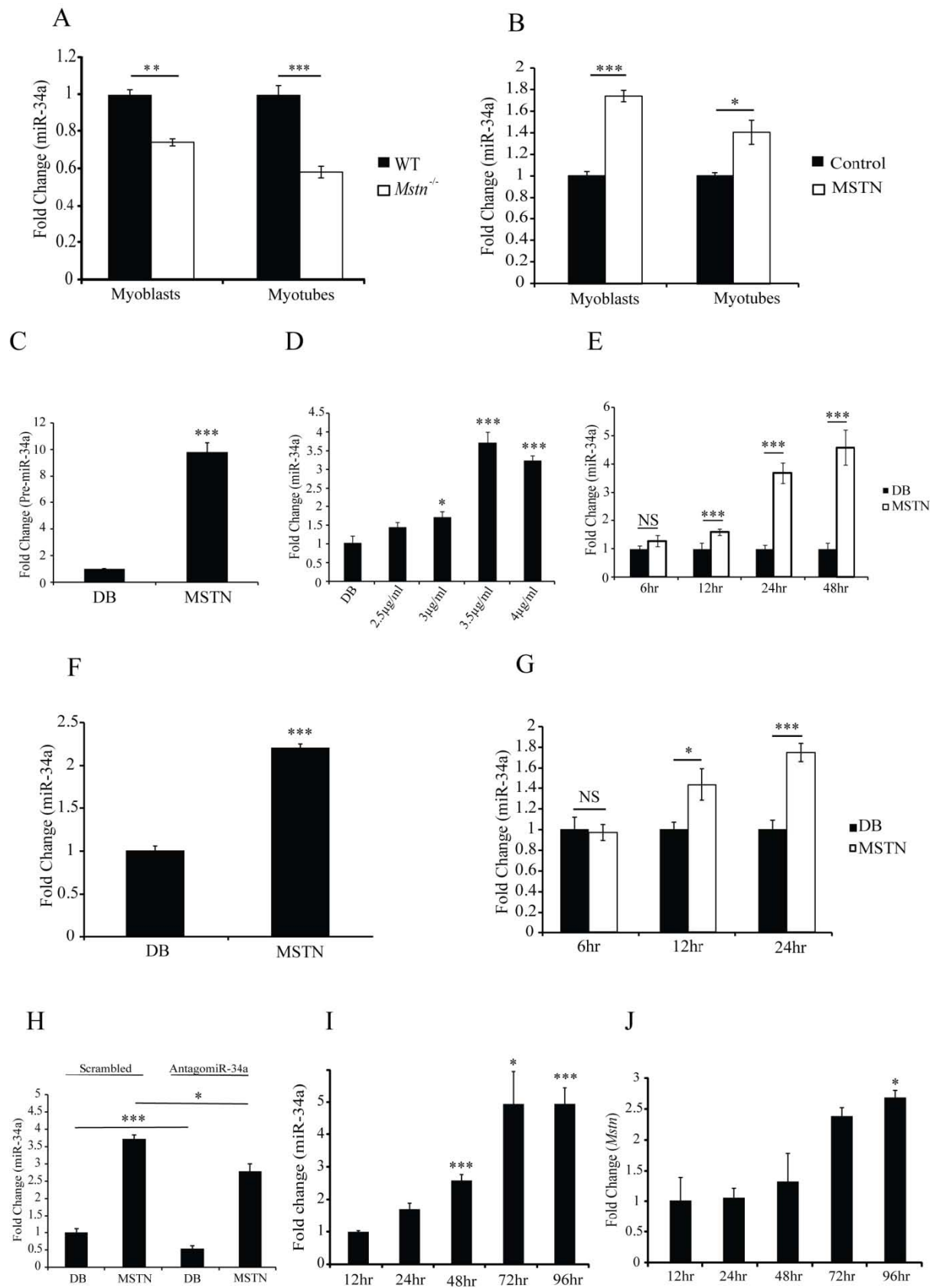
Blank page

Figure 3.1 Myostatin regulates miR-34a. *(A) qPCR analysis of miR-34a expression in primary myoblasts and myotubes isolated from WT and Mstn$^{-/-}$ mice. (B) qPCR analysis of miR-34a expression in Control and MSTN treated (2µg/ml) primary myoblasts and myotubes. (C) qPCR analysis of Pre-miR-34a expression in C2C12 myoblasts treated without (DB) or with MSTN (4µg/ml). (D) qPCR analysis of miR-34a expression in C2C12 myoblasts treated without (DB) or with increasing concentrations (2.5µg/ml, 3µg/ml, 3.5µg/ml and 4µg/ml) of MSTN protein. (E) qPCR analysis of miR-34a expression in C2C12 myoblasts treated with dialysis buffer (DB) or with MSTN for 6, 12, 24 and 48hrs. (F) qPCR analysis of miR-34a expression in 48hrs control (DB) and MSTN treated 36C15Q primary human myoblasts. (G) qPCR analysis of miR-34a expression in 36C15Q primary human myoblasts treated with DB or with MSTN for 6, 12, 24, and 48hrs. (H) qPCR analysis of miR-34a expression in C2C12 myoblasts transfected with either control non-silencing AntagomiR (Scrambled) or miR-34a-specific AntagomiR (AntagomiR-34a), and treated with DB or with 4µg/ml MSTN. qPCR analysis of miR-34a (I) and Mstn (J) expression in C2C12 myoblasts at 12, 24, 48, 72 and 96hrs of myogenic differentiation. All bars represent mean ± s.e.m. P < 0.05 *, P < 0.01 ** and P < 0.005 ***.*
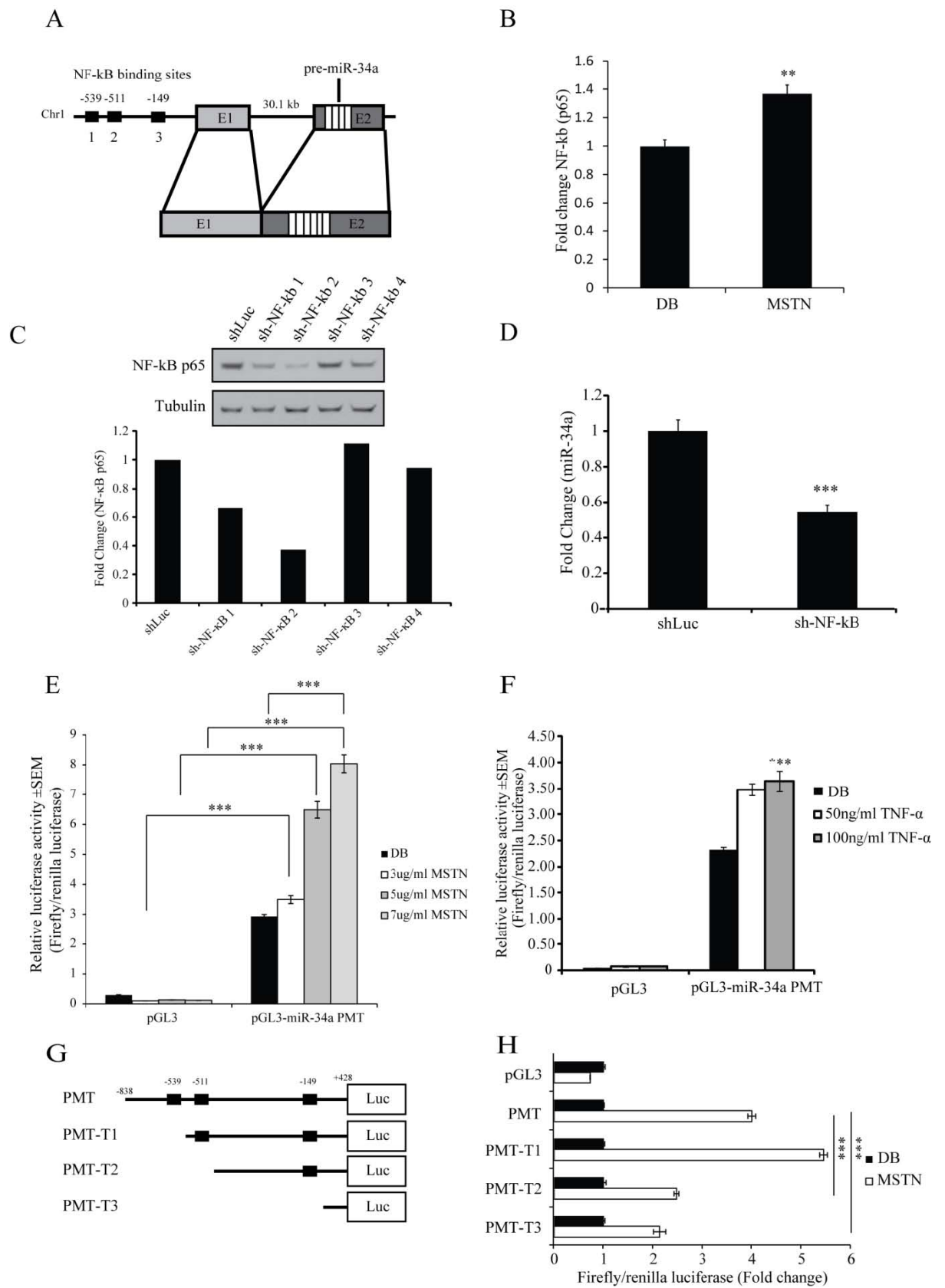
*Figure 3.2 Mstn transcriptionally regulates miR-34a via NF-kB. (A) Schematic diagram of the genomic structure of miR-34a and upstream NF-κB binding sites. miR-34a is transcribed from chromosome 1 and consists of 2 exons (E1 and E2). Upstream of E1 of miR-34a are three NF-κB binding sites at -149, -511, and -539 with respect to the transcription start site. (B) qPCR analysis of NF-κB (p65) expression in C2C12 myoblasts treated with DB or 4μg/ml MSTN. (C) (Top) Western blot analysis of NF-κB (p65) protein levels in stable control (shLuc) and NF-κB (p65) knockdown (sh-NF-κB) myoblasts. (Bottom) Graph showing fold change in NF-κB (p65) protein levels in sh-NF-κB myoblasts, relative to shLuc control, as quantified through densitometric analysis. All values were normalized to Tubulin. (D) qPCR analysis of miR-34a expression in control (shLuc) and NF-κB (p65) knockdown (sh-NF-κB) myoblasts. (E) Luciferase reporter activity in C2C12 cells transfected with either empty vector (pGL3b) or with miR-34a promoter reporter construct (pGL3-miR34a PMT) and treated with DB or increasing concentrations of MSTN (3, 5 or 7μg/ml) for 24hrs. (F) Luciferase reporter activity in C2C12 cells transfected with either empty vector (pGL3b) or with miR-34a promoter reporter construct (pGL3-miR34a PMT) and treated without (DB) or with increasing concentrations of TNF-α (50 or 100ng/ml) for 24hrs. (G) Schematic diagram of miR-34a promoter truncation constructs generated. The full-length promoter (PMT) construct contains 1.3kb of miR-34a upstream sequence and all three NF-κB binding sites. Truncated constructs were generated that contain two (PMT-T1), one (PMT-T2) and no (PMT-T3) NF-κB binding sites. (H) Luciferase reporter activity in C2C12 cells transfected with either empty vector (pGL3b) or with PMT, PMT-T1, PMT-T2 or PMT-T3 and treated with either DB or 4μg/ml MSTN. All firefly luciferase values were normalized to renilla luciferase. All bars represent mean ± s.e.m. P < 0.01 ** and P < 0.005 ***.*

3.4 miR-34a inhibits C2C12 myoblast proliferation

Increased levels of Mstn have been shown to inhibit myoblast proliferation, as such the effect of miR-34a on proliferating myoblasts was investigated. To study this two stable miR-34a over expressing myoblasts clones (miR-34a OE1 and miR-34a OE2) were generated, which displayed a significant ~3-fold increase in miR-34a expression (Figure 3.3A). Subsequent analysis of myoblast proliferation revealed a significant 24% and 35% reduction in myoblast proliferation rate in miR-34a OE1 and miR-34a OE2 myoblasts respectively, when compared to control (Figure 3.3B). Consistent with this, Western blot analysis revealed increased levels of p21 in both miR-34a overexpressing clones, when compared to control (Figure 3.3C). Conversely, AntagomiR-mediated blockade of miR-34a resulted in a significant increase in myoblast proliferation (Figure 3.3D) and in fact was able to rescue Mstn-mediated inhibition of myoblast proliferation (Figure 3.3E). Specifically, addition of miR-34a-specific AntagomiR (AntagomiR-34a) was able to partially rescue impaired myoblast proliferation following treatment with 5µg/ml MSTN and completely rescued the reduced proliferation in response to 2µg/ml MSTN (Figure 3.3E). These results suggest that increased expression of miR-34a inhibits myoblast proliferation and that Mstn-mediated inhibition of myoblast proliferation is dependent on miR-34a function. To rule out increased apoptosis as an explanation for the reduced number of myoblasts observed in response to miR-34a over expression, we performed a TUNEL assay on both miR-34a overexpression clones. As shown in Figure 3.3F, it was observed that there was no significant difference in apoptosis between control and miR-34a overexpressing myoblasts (Figure 3.3F). In addition, the expression of Bcl2 (an anti-apoptotic protein) and Caspase 3 (apoptosis marker) was assessed by quantitative PCR. The results revealed no significant change in the expression of either Bcl2 (Figure 3.3G) or Caspase 3 (Figure 3.3H) between control and miR-34a overexpressing myoblasts. These results indicate that miR-34a does not induce apoptosis and that the

inhibition of proliferation observed upon over expression of miR-34a reflects slower growth rate. To test whether or not overexpression of miR-34a affects cell cycle progression, cell cycle analysis was performed through Propidium iodide staining and flow cytometry (FACSAria II). Results revealed that cells were enriched in the S-phase of the cell cycle, with reduced numbers of cells present in the G0/G1 phases of the cell cycle, upon overexpression of miR-34a (Figure 3.3I). There was no significant difference in the numbers of cells present in G2/M phases of the cell cycle between control and miR-34a overexpressing myoblasts. These data suggest that overexpression of miR-34a may reduce myoblast proliferation through maintaining cells in the S-phase of the cell cycle.

3.5 miR-34a inhibits C2C12 myogenic differentiation

Higher levels of Mstn inhibits myogenic differentiation [147], as such it was next assessed whether or not miR-34a could also mimic the inhibitory effect of Mstn on myoblast differentiation. Control and miR-34a overexpressing clones were differentiated for 48, 72 and 96hrs and subsequently stained with Hematoxylin and Eosin. While Myotubes were seen in the control cell line by 48hrs, no myotubes were observed in both miR-34a overexpression clones (Figure 3.4A and B). Similarly, no myotubes were observed at either 72 or 96hrs differentiation in the miR-34a over expressing clones (Figure 3.4A and B). Subsequent Western blot analysis revealed that Myosin heavy chain (MyHC) and myogenin were undetectable in miR-34a overexpressing clones during differentiation. Also, the levels of MyoD and p21 levels were significantly reduced at all time points (24, 48, 72 and 96hrs) during differentiation (Figure 3.4C). Consistent with these results, AntagomiR-mediated blockade of miR-34a expression in C2C12 myoblasts resulted in improved differentiation and therefore increased number of Myotubes at both 48 and 72hrs differentiation (Figure 3.4D and E). Moreover, increased levels of MyHC and MyoD were noted at 96hrs differentiation upon AntagomiR-34a-mediated inhibition of miR-34a, when compared to control (Figure 3.4F). In order to test if Mstn inhibits

differentiation via miR-34a, C2C12 myoblasts were transfected with either control scrambled or AntagomiR-34a and subjected to differentiationin the absence or presence of MSTN. As predicted, treatment with MSTN resulted in observable myotubular atrophy in scrambled control transfected myoblasts (Figure 3.4G). Consistent with the results presented in Figure 3.4D, it was observed that AntagomiR-34a transfected myoblasts displayed increased myotube size, when compared to control (Figure 3.4G). Importantly, an observable improvement in myogenic differentiation was displayed whereMSTN-induced myotubular atrophy was rescued in AntagomiR-34a transfected myoblasts (Figure 3.4G).
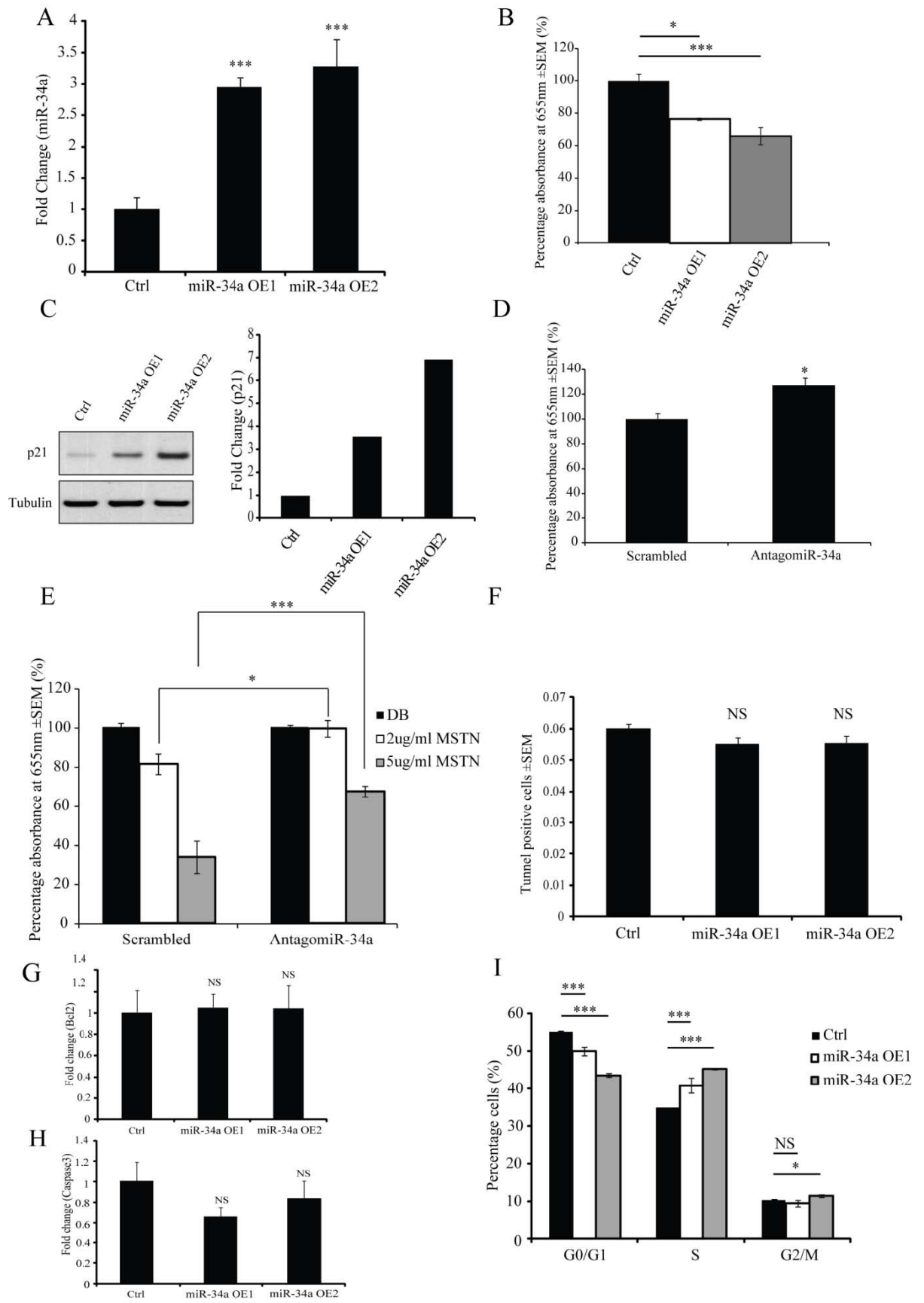
Blank page

Figure 3.3 miR-34a inhibits myoblast proliferation. *(A) qPCR analysis of miR-34a expression in empty vector control (Ctrl) and two stable miR-34a overexpressing clones (miR-34a OE1 and miR-34a OE2). (B) Proliferation analysis of Ctrl, miR-34a OE1 and miR-34a OE2 myoblasts at 48hrs proliferation, as assessed through methylene blue assay, where cell number is proportional to absorbance at 655nm. (C) Western blot analysis of p21 protein levels in Ctrl, miR-34a OE1 and miR-34a OE2 myoblasts at 48hrs proliferation. The levels of Tubulin were assessed to ensure equal loading. Graph shows densitometric analysis of p21 protein levels in Ctrl, miR-34a OE1 and miR-34a OE2 myoblasts, normalized to Tubulin and expressed as fold change relative to Ctrl. (D) Proliferation analysis of scrambled non-silencing control (Scrambled) and AntagomiR-34a transfected myoblasts at 48hrs proliferation, as assessed through methylene blue assay. (E) Proliferation analysis of scrambled non-silencing control and AntagomiR-34a transfected myoblasts at 48hrs proliferation, in the absence (DB) or presence of increasing concentrations of MSTN (2µg/ml and 5µg/ml), as assessed through methylene blue assay. (F). TUNEL assay on Ctrl, miR-34a OE1 and miR-34a OE2 myoblasts at 48hrs proliferation. Positive cells were normalized against total nuclei present in the entire microscope slide and expressed as a percentage. qPCR analysis of Bcl2 (G) and Caspase 3 (H) expression in proliferating Ctrl and miR34a overexpressing clones. (I) Graph showing the percentage of cells in Ctrl, miR-34a OE1 and miR-34a OE2 overexpressing clones in G0/G1, S and G2/M phases of the cell cycle, as assessed through flow cytometry. P < 0.05 *, P < 0.005 ***.*
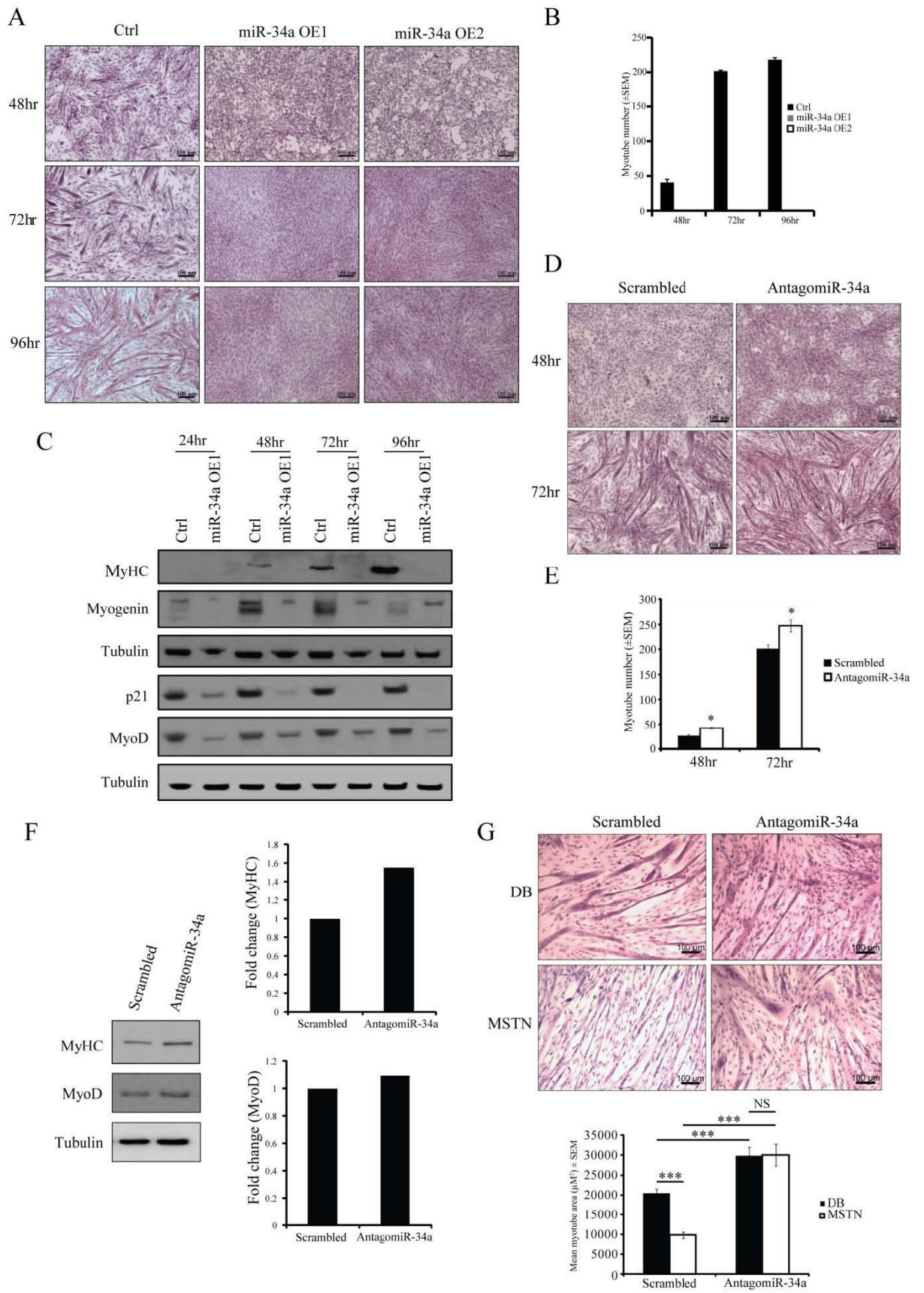
Figure 3.4 miR-34a inhibits myogenic differentiation. (A) Representative images of H & E stained Ctrl, miR-34a OE1 and miR-34a OE2 overexpressing clones at 48, 72 and 96hrs differentiation. Scale bars, 100μm. (B) Graph showing mean myotube number (±SEM) in Ctrl, miR-34a OE1 and miR-34a OE2 overexpressing clones at 48, 72 and 96hrs differentiation. (C) Western blot analysis of MyHC, Myogenin, p21 and MyoD protein levels in Ctrl and miR-34a OE1 at 24, 48, 72 and 96hrs differentiation. The levels of Tubulin were assessed to ensure equal loading on representative blots. (D) Representative images of H & E stained scrambled non-silencing control (Scrambled) and AntagomiR-34a transfected myoblasts at 48 and 72hrs differentiation. Scale bars, 100μm. (E) Graph showing mean myotube number (±SEM) in Ctrl and AntagomiR-34a transfected myoblasts at 48 and 72hrs differentiation. (F) Western blot analysis of MyHC and MyoD protein levels in 96hrs differentiated Scrambled and AntagomiR-34a transfected myoblasts. The levels of Tubulin were assessed to ensure equal loading. Graphs show densitometric analysis of MyHC and MyoD protein levels in Scrambled and AntagomiR-34a transfected myoblasts, normalized to Tubulin and expressed as fold change relative to respective Ctrl. (G) Representative images (Top) and myotube area (bottom) of 72 hrs differentiated H & E stained Scrambled and AntagomiR-34a transfected myoblasts treated without (DB) or with recombinant MSTN protein. A total of 120 myotube areas were measured per treatment. Scale bars, 100μm. $P < 0.05$ *, $P < 0.005$ ***.

3.6 miR-34a directly targets TCF12 to inhibit myogenic differentiation

To elucidate the mechanism of miR-34a-mediated inhibition of C2C12 myogenic differentiation, we performed an *in silico* search for miR-34a predicted targets using miRNA prediction databases (TargetScan and miRDB). Subsequent bioinformatics analysis identified Transcription factor 12 (TCF12) as a potential target of miR-34a. Alignment of miR-34a and TCF12 3`UTR revealed 7-mer base-pair complementarity at nucleotides 2-8 (5`-3`) of the miR-34a seed region, which was conserved between human and mouse (Figure 3.5A). TCF12 has 2 alternatively spliced variants, TCF12-α and -β, and has been shown to play a role in myogenesis [98, 220]. To understand the temporal role TCF12 plays during differentiation, the endogenous levels of TCF12 (-α and -β) during C2C12 differentiation was assessed. Results revealed a steady decrease in TCF12-α expression, but not TCF12-β, from 48 to 96hrs differentiation (Figure 3.5B), which was contrary to the expression of endogenous miR-34a observed during differentiation (Figure 3.1H).

Next the levels of TCF12 during differentiation in miR-34a overexpressing clones were monitored. Results revealed a significant reduction in *TCF12* mRNA expression (both TCF12-α and -β) (Figure 3.5C) and protein levels (Figure 3.5D) upon over expression of miR-34a. Consistent with this, AntagomiR-mediated blockade of miR-34a resulted in an increase in TCF12 protein levels at 72hrs differentiation (Figure 3.5E). To confirm whether or not TCF12 is a direct target of miR-34a, the wild type and a mutant form (where the miR-34a binding site has been mutated) of the mouse 3`UTR of *TCF12* was cloned into the Psicheck2 luciferase reporter vector and transfected into miR-34a overexpressing stable cells. Subsequent reporter analysis revealed significantly reduced *TCF12* 3'UTR reporter activity upon overexpression of miR-34a, which was ablated upon mutation of the miR-34a binding site in the *TCF12* 3'UTR (Figure 3.5F).

Next in order to prove that the inhibition of TCF12 by miR-34a was mediated by Mstn, C2C12 myoblasts were differentiated for 48hrs and subjected to treatment with recombinant MSTN protein. Western blot analysis revealed a reduction in TCF12 levels upon treatment with MSTN (Figure 3.5G); whereas Mstn-mediated inhibition of TCF12 was prevented upon addition of miR-34a-specific AntagomiR (Figure 3.5H) confirming that miR-34a is required for the downregulation of TCF12 by Mstn.

To validate whether or not miR-34a inhibits the association of TCF12 and MyoD to E Box binding sites in the myogenin enhancer region, ChIP analysis was performed. The results revealed binding of MyoD and TCF12 to E Box sites within the myogenin enhancer, which was blocked upon over expression of miR-34a (Figure 3.5I). These results are consistent with the low levels of MyoD and myogenin noted during differentiation of miR-34a overexpressing cells (Figure 3.4C). Taken together, these data demonstrate that miR-34a directly targets TCF12 and that miR-34a-mediated inhibition of TCF12 blocks myogenic differentiation through preventing binding of MyoD to a critical myogenic regulatory factor.
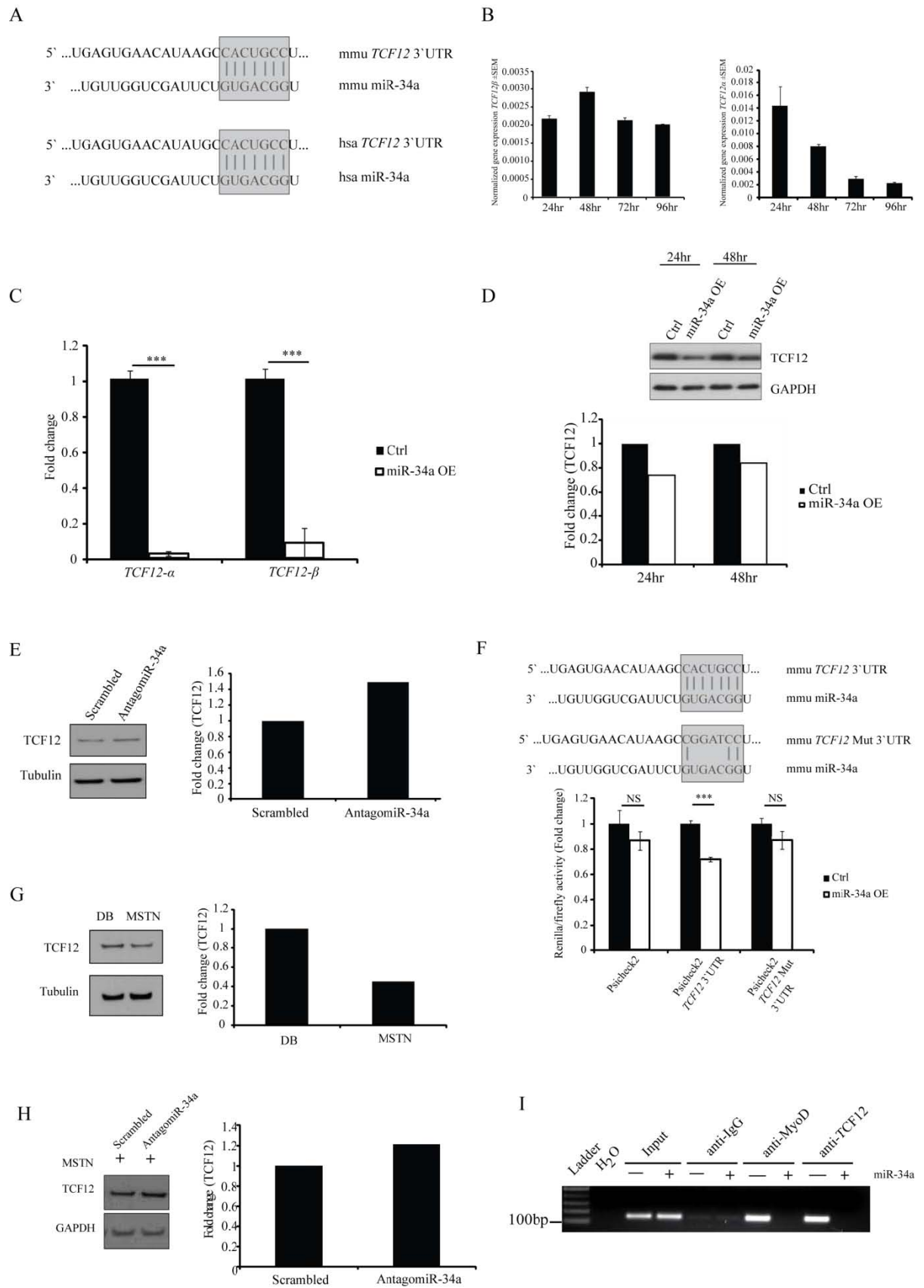
Figure 3.5 miR-34a directly targets TCF12 to inhibit myogenic differentiation. (A) Schematic highlighting 7-mer base-pair complementarity (grey box) between the seed region of mouse (mmu miR-34a) and human (hsa miR-34a) miR-34a and the respective 3'UTR of mouse (mmu TCF12 3'UTR) and human (hsa TCF12 3'UTR) TCF12 gene. (B). qPCR analysis of TCF12-α and TCF12-β expression in C2C12 myoblasts at 24, 48, 72 and 96hrs differentiation. (C) qPCR analysis of TCF12-α and TCF12-β expression in 48hrs differentiated Ctrl and miR-34a OE1 overexpressing myoblasts. (D) Western blot analysis of TCF12 protein levels in 24 and 48hrs differentiated Ctrl and miR-34a OE1 overexpressing myoblasts. The levels of GAPDH were assessed to ensure equal loading. Graph shows densitometric analysis of TCF12 protein levels in Ctrl and miR-34a OE1 overexpressing myoblasts, normalized to GAPDH and expressed as fold change relative to respective Ctrl. (E) Western blot analysis of TCF12 protein levels in Ctrl and AntagomiR-34a transfected myoblasts at 48hrs differentiation. The levels of Tubulin were assessed to ensure equal loading. Graph shows densitometric analysis of TCF12 protein levels in Ctrl and AntagomiR-34a transfected myoblasts, normalized to Tubulin and expressed as fold change relative to Ctrl. (F) (Top) Schematic highlighting base-pair complementarity (grey box) between the seed region of mouse miR-34a (mmu miR-34a) and the wildtype (mmu TCF12 3'UTR) and mutated (mmu TCF12 Mut 3'UTR) TCF12 gene 3'UTR, where the miR-34a binding site has been mutated. (Bottom) Assessment of Psicheck2 luciferase activity in Ctrl and miR-34a OE1 overexpressing myoblasts transfected with either control empty vector (Psicheck2), the TCF12 3'UTR reporter construct (Psicheck2 TCF12 3'UTR) or the mutant TCF12 3'UTR reporter construct (Psicheck2 TCF12 Mut 3'UTR), where the miR-34a binding site has been mutated. Renilla luciferase activity was normalized to Firefly luciferase and expressed as fold change relative to respective control (Ctrl). (G) Western blot analysis of TCF12 protein levels in control (DB) and MSTN treated C2C12 myoblasts differentiated for 48hrs. The levels of Tubulin were assessed to ensure equal loading. Graph shows densitometric analysis of TCF12 protein levels in DB and MSTN treated myoblasts, normalized to Tubulin and expressed as fold change relative to DB. (H) Western blot analysis of TCF12 protein levels in 72hrs differentiated Scrambled and AntagomiR-34a transfected myoblasts treated with MSTN. The levels of GAPDH were assessed to ensure equal loading. Graph shows densitometric analysis of TCF12 protein levels in Scrambled and AntagomiR-34a transfected myoblasts treated with MSTN, normalized to GAPDH and expressed as fold change relative to Ctrl. (I) ChIP assay of TCF12 interaction with the myogenin promoter in Control (-) and miR-34a OE1

cells (+). Input DNA used in the ChIP assay is shown. The micrograph shows amplicons corresponding to a MyoD binding site in the myogenin promoter of Input DNA and following addition of either anti-IgG (Negative Control), anti-MyoD or anti-TCF12 antibodies. P < 0.05 *, P < 0.005 ***.

3.7 miR-34a is highly expressed in quiescent satellite cells and impairs skeletal muscle regeneration

Previous work has revealed that Mstn acts as a negative regulator of muscle stem cell (satellite cell) activation [221]. Therefore, the effect of miR-34a in satellite cell activation was assessed. Initially, quiescent and activated satellite cells were isolated and qPCR performed to quantify endogenous miR-34a in these cells. Subsequent analysis revealed significantly higher expression of both pre-miR-34a and mature miR-34a in quiescent satellite cells as compared to activated satellite cells (Figure 3.6A). Consistent with this, significantly higher expression of both pre-miR-34a and mature miR-34a was noted in a C2C12 myoblast model of induced quiescence, where cells are maintained in the G_0 phase of the cell cycle, when compared to actively proliferating (G1 Phase of the cell cycle) C2C12 myoblasts (Figure 3.6B). As a result of these findings, it is quite possible that the overexpression of miR-34a could delay satellite cell activation. To test this, satellite cells were isolated and infected with either control or miR-34a overexpressing adenovirus and the number of satellite cells positive for MyoD (a marker of activated satellite cells) were quantified (Figure 3.6C). Consistent with the increased miR-34a expression noted in quiescent satellite cells (Figure 3.6A) and the inhibitory role of miR-34a on myogenesis, as shown previously (Figures 3.3 & 3.4), a significant reduction in the numbers of MyoD positive (activated) satellite cells was observed upon adenoviral overexpression of miR-34a, suggesting that increased expression of miR-34a leads to delayed activation of satellite cells *in vitro*. Skeletal muscle satellite cells have critical functions during postnatal skeletal muscle growth and are in fact primarily responsible for maintaining muscle mass in response to injury (Reviewed in [67]). As such, the role of miR-34a during skeletal muscle repair following notexin-induced injury in mice was examnied. Changes in endogenous miR-34a expression post-injury was examined by qPCR which revealed significantly lower expression of miR-34a between days 1-3 post-injury, when compared to uninjured controls. miR-34a expression increased significantly at day 5 and peaked at day

7, when compared to uninjured controls. At day 10, miR-34a expression returned to endogenous levels, with a further reduction of miR-34a expression noted at day 28 post-injury (Figure 3.6D). During the first 3 days post skeletal muscle injury there is a dramatic increase in satellite cell activation to allow for effective repair of skeletal muscle mass (Reviewed in [222]). As the endogenous levels of miR-34a were reduced during the first 3 days post-injury, it was hypothesized that miR-34a may play an inhibitory role in the activation of satellite cells, and as such result in impaired skeletal muscle regeneration. To examine this, TA muscles of mice were injected with control adenovirus or miR-34a overexpressing adenovirus and subjected to notexin-induced injury. Subsequent analysis revealed a significant reduction in MyoD positive activated satellite cells in TA muscles at day 3 post-injury upon adenoviral-mediated overexpression of miR-34a (Figure 3.6E). In addition, histological analysis (H & E) of TA skeletal muscle tissue at day 10 (Figure 3.6F) and day 28 (Figure 3.6G) post-injury revealed an observable reduction in myofiber size, which was associated with reduced myofiber cross sectional area (CSA), following adenoviral-mediated overexpression of miR-34a (Figure 3.6F & 3.6G). Taken together, these results confirm that over expression of miR-34a *in vivo* results in impaired satellite cell activation and muscle regeneration following injury.
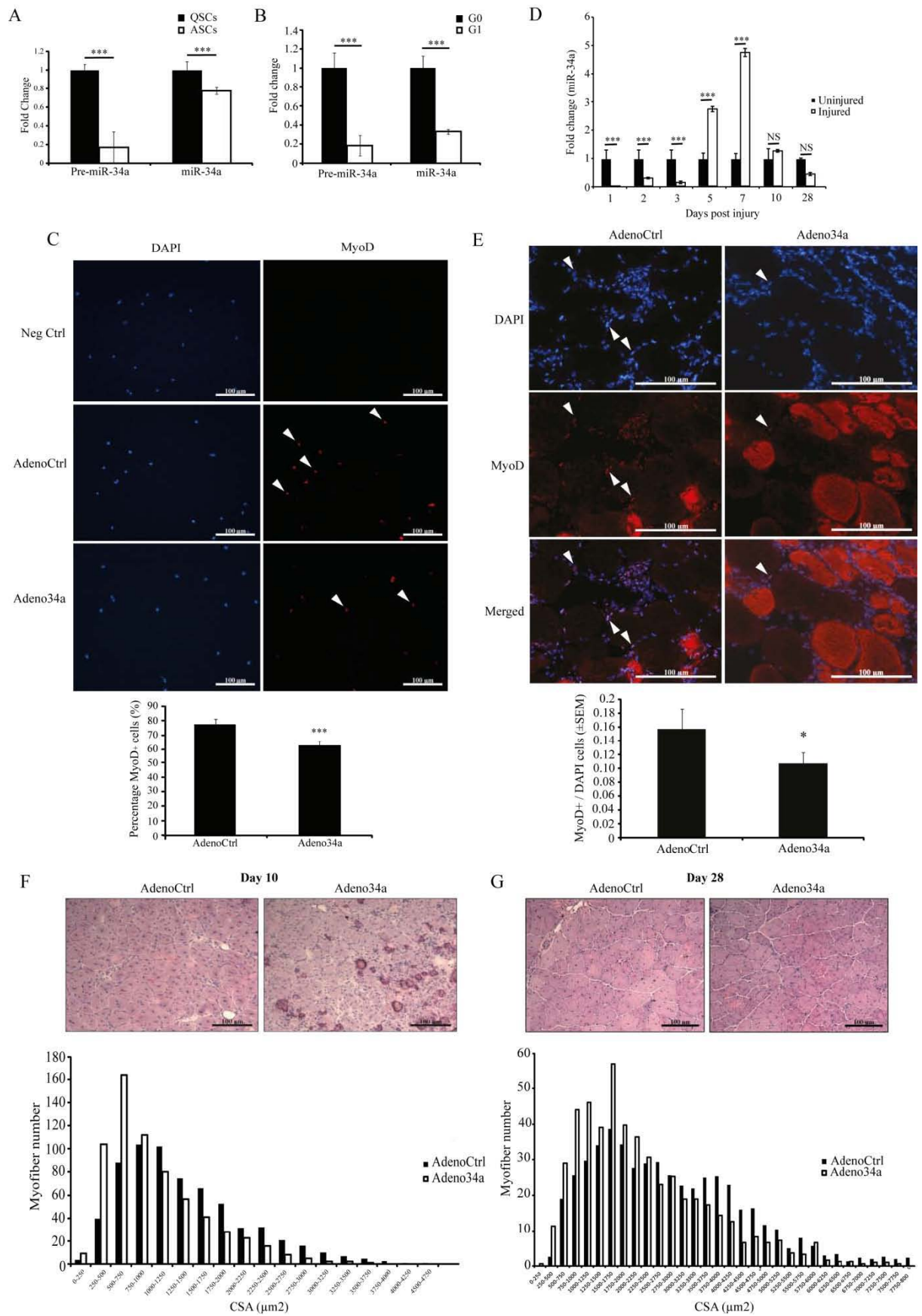
Blank page

104

Figure 3.6 miR-34a is highly expressed in quiescent satellite cells and impairs skeletal muscle regeneration in response to injury. *(A) qPCR analysis of precursor (Pre-miR-34a) and mature (miR-34a) miR-34a expression in quiescent (QSCs) and activated (ASCs) satellite cells. (B) qPCR analysis of precursor (Pre-miR-34a) and mature (miR-34a) miR-34a expression in actively proliferating C2C12 myoblasts (G1) and in C2C12 myoblasts induced to maintain quiescence (G0). (C) (Top) Representative images of MyoD immunofluorescence analysis of primary murine myoblasts infected with either control adenovirus (AdenoCtrl) or miR-34a-specific overexpressing adenovirus (Adeno34a). Images of unstained negative control are also shown. Staining with DAPI was used to identify myonuclei. Scale bars, 100µm. (Bottom) Graph shows quantification of MyoD positive (MyoD+) myoblasts in AdenoCtrl and Adeno34a infected myoblasts expressed as a percentage of total cell number. (D) qPCR analysis of miR-34a expression in TA muscle from mice at days 1, 2, 3, 5, 7, 10 and 28-post Notexin-induced injury. Data is expressed as fold change relative to respective uninjured controls. (E) (Top) Representative images of MyoD IHC staining on day 3 post-injured TA muscle infected with either control (AdenoCtrl) or miR-34a-specific overexpressing adenovirus (Adeno34a). (Bottom) Graph shows quantification of MyoD positive (MyoD+) activated satellite cells in day 3 post-injured AdenoCtrl and Adeno34a infected TA muscle expressed as a percentage of total DAPI positive cells. (F) (Top) Representative images of hematoxylin and eosin (H&E) stained TA muscle cross-sections at day 10-post Notexin-induced injury in mice infected with either AdenoCtrl or Adeno34a adenovirus. Scale bars, 100µm. (Bottom) Frequency distribution of TA muscle fiber cross-sectional area (CSA; $µm^2$) at day 10-post Notexin-induced injury in mice infected with either AdenoCtrl or Adeno34a adenovirus. (G) (Top) Representative images of H&E stained TA muscle cross-sections at day 28-post Notexin-induced injury in mice infected with either AdenoCtrl or Adeno34a adenovirus. Scale bars, 100µm. (Bottom) Frequency distribution of TA muscle fiber cross-sectional area (CSA; $µm^2$) at day 28-post Notexin-induced injury in mice infected with either AdenoCtrl or Adeno34a adenovirus. $P < 0.05$ *, $P < 0.005$ ***.*

3.8 Myostatin and miR-34a downregulate Notch1

During the activation of SCs, Notch1 is upregulated and is required for the expansion of pre-myogenic cells [63]. This suggests Notch1 plays a pivotal role in SC activation. Therefore, it is possible that miR-34a regulates Notch1 and thus SC activation. qPCR analysis revealed significant inhibition of both *Notch1* and its downstream signaling target *Hes1* in miR-34a overexpression stable cells (Figure 3.7A). Subsequent bioinformatics analysis, using miRNA target prediction sites TargetScan and miRDB, identified perfect base pair complementarity between nucleotides 2-8 (5`-3`) of the miR-34a sequence and the 3'UTR of the *Notch1* gene, which was highly conserved between mouse and human *Notch1* gene (Figure 3.7B). In order to confirm direct regulation of *Notch1* by miR-34a, the *Notch1* 3`UTR was cloned into the Psicheck2 reporter vector and *Notch1* reporter luciferase activity in control and miR-34a overexpressing stable cells was assessed. Subsequent *Notch1* 3'UTR reporter analysis revealed significantly reduced *Notch1* 3'UTR reporter activity in miR-34a overexpressing stable cells, when compared to controls, suggesting that miR-34a is able to transcriptionally regulate *Notch1* in myoblasts (Figure 3.7C).

As shown previously that Mstn upregulates miR-34a, the ability for Mstn to regulate *Notch1* transcription was determined. To test this, C2C12 cells were transfected with either the *Notch1* 3`UTR Psicheck2 reporter vector or empty vector control (Psicheck2) followed by treatment with or without recombinant MSTN protein. Much akin to what was observed upon overexpression of miR-34a, the *Notch1* 3`UTR reporter activity was significantly downregulated upon treatment with MSTN (Figure 3.7D). Although repression of Psicheck2 empty vector reporter activity was observed in response to MSTN treatment, a greater reduction in reporter activity was noted in cells transfected with the *Notch1* 3`UTR Psicheck2 reporter (Figure 3.7D). In order to test whether or not Mstn can also downregulate Notch1 protein we treated

C2C12 cells with Mstn and performed western blot analysis for the active Notch1 ICD (intracellular domain). Results identified significant (>50%) inhibition of Notch1 ICD levels upon treatment with MSTN, when compared to control treated cells (Figure 3.7E). Taken together these results reveal that both Mstn and miR-34a are able to downregulate Notch1 and further suggest that Mstn and miR-34a may control SC activation via preceding regulation of Notch1.

A

B

```
5`...AUUUUCCACAGAA ACACUGCC U... mmu Notch1 3`UTR
                   | | | | | | | |
3`...UGUUGGUCGAUUC UGUGACGG U    mmu miR-34a


5`...UUUUCUGGGGAAAG ACACUGCC U... hsa Notch1 3`UTR
                    | | | | | | | |
3`...UGUUGGUCGAUUC UGUGACGG U     hsa miR-34a
```
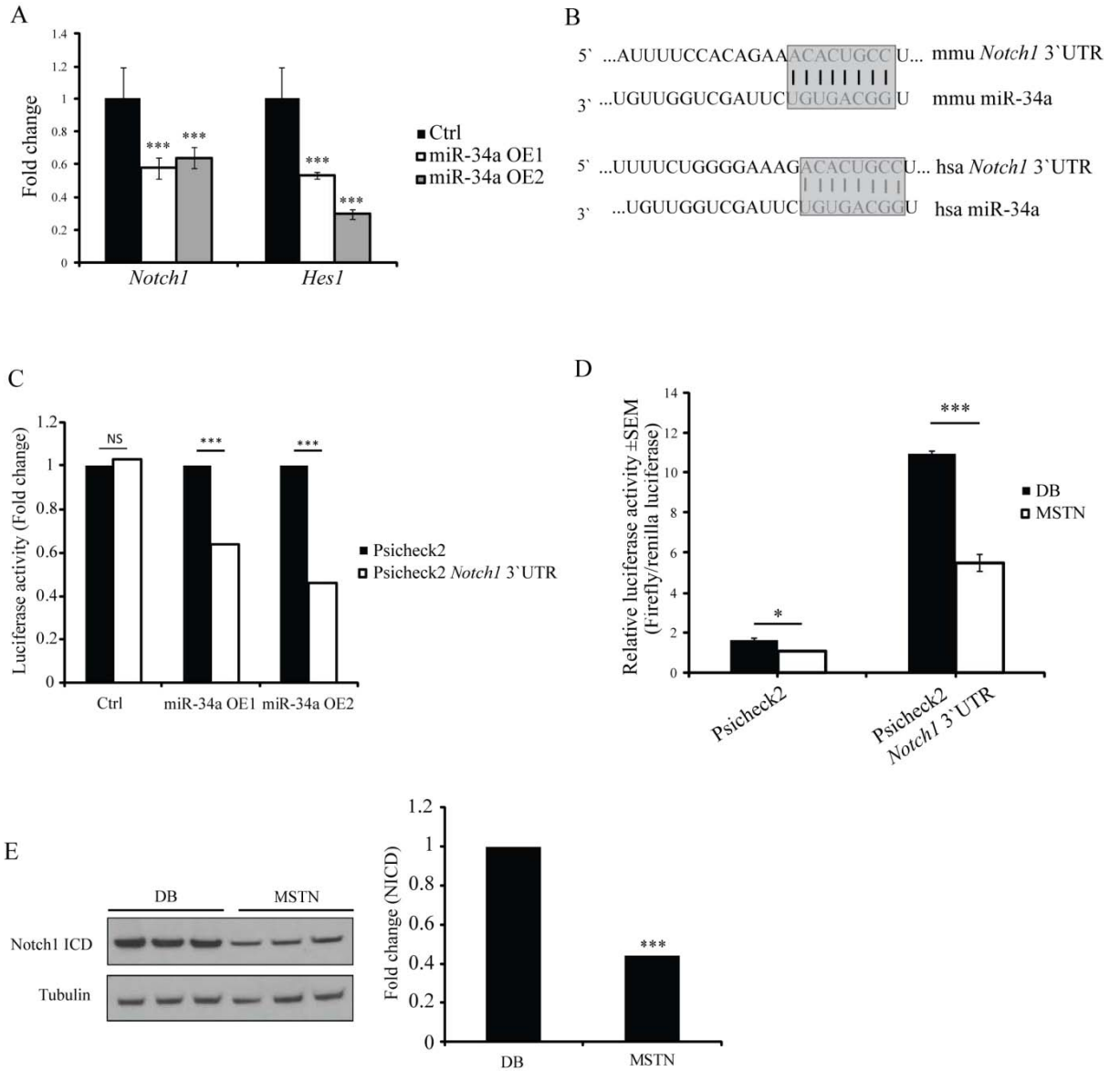
C

D

E

Figure 3.7 Myostatin and miR-34a inhibit Notch1. (A) qPCR analysis of Notch1 and Hes1 expression in Ctrl and miR-34a OE1 and miR-34a OE2 overexpressing clones. (B) Schematic highlighting 8-mer base-pair complementarity (grey box) between the seed region of mouse (mmu miR-34a) and human (hsa miR-34a) miR-34a and the respective 3'UTR of mouse (mmu Notch1 3'UTR) and human (hsa Notch1 3'UTR) Notch1 gene. (C) Assessment of Psicheck2 luciferase activity in Ctrl, miR-34a OE1 and miR-34a OE2 overexpressing clones transfected with either control empty vector (Psicheck2) or Notch1 3'UTR reporter construct (Psicheck2 Notch1 3'UTR). Renilla luciferase activity was normalized to Firefly luciferase and expressed as fold change relative to respective empty vector transfect controls. (D) Assessment of Psicheck2 luciferase activity in C2C12 myoblasts transfected with either control empty vector (Psicheck2) or Notch1 3'UTR reporter construct (Psicheck2 Notch1 3'UTR) and treated without (DB) or with MSTN. Renilla luciferase activity was normalized to Firefly luciferase and expressed as fold change relative to respective DB treated controls. (E) Western blot analysis of Notch1 ICD in C2C12 myoblasts treated without (DB) or with MSTN (4µg/ml). The levels of Tubulin were assessed to ensure equal loading. Graph shows densitometric analysis of Notch1 ICD protein levels in DB and MSTN treated C2C12 myoblasts, normalized to Tubulin and expressed as fold change relative to DB control. P < 0.005 ***.

4. Discussion

Mstn is a potent negative regulator of skeletal muscle growth. Although Mstn signaling and several genetic downstream targets during myogenesis have been identified, epigenetic mechanisms through which Mstn signals have not been well understood so far. Therefore, in this thesis the importance of miRNA in Mstn signaling was characterized. Here it was shown that Mstn regulates myogenesis through a novel miR-34a-TCF12-dependent mechanism. Further, it was also shown that high levels of miR-34a is associated with satellite cell quiescence and that miR-34a overexpression during Notexin-induced skeletal muscle injury results in impaired muscle regeneration.

4.1 Myostatin regulates the expression of several miRNAs during myogenesis

Growth factors play an important role in the regulation of skeletal muscle growth. Previously, several growth factors have been shown to regulate myogenesis by altering the expression of miRNAs. For example, recent miRNA profiling of TNF-α or IGF-1 treated human primary myoblasts and murine cell lines displayed alterations to several myomiRs (miR-1, -133a/b, -206) and non-muscle specific miRNAs. While TNF-α reduced myomiR expression, IGF-1 increased the expression of myomiRs [223]. An independent screen performed during the differentiation of myoblasts demonstrated that TGF-β regulates HDAC4 (an inhibitor of myogenesis) and that this regulation was blocked by miR-206 and miR-29, which translationally represses HDAC4 allowing myogenic differentiation to occur. Furthermore, it was also shown that miR-29 inhibits SMAD3 expression thereby blocking TGF-β mediated inhibition of myogenic differentiation [224]. These results therefore revealed novel miRNA-dependent mechanisms behind growth factor regulation of myogenesis.

Our laboratory has a long-standing interest in Mstn biology and its mechanism of function during myogenesis. To date, the signaling

pathways through which Mstn regulates growth and differentiation of myogenic cells [133, 145, 147] has been characterized extensively. In order to further characterize the epigenetic mechanisms behind Mstn function during myogenesis, a screen was performed for miRNAs regulated by Mstn in skeletal muscle. This study employed both gain- and loss-of-function models, which allowed identification of miRNAs directly regulated by Mstn.

The resulting miRNA microarray profile identified 6 miRNAs that were upregulated and 15 miRNAs that were downregulated in $Mstn^{-/-}$ primary myoblasts (Table 3.3). In addition, 15 miRNAs were upregulated and 11 dowregulated in $Mstn^{-/-}$ primary myotubes, as compared to WT primary myotubes (Table 3.5). Interestingly, several miRNAs were identified to be consistently up- or downregulated in both myoblasts and myotubes in the absence of Mstn. For example, the expression of miR-199a-3p/199b-3p, 199a-5p and miR-199b-5p was consistently elevated when compared to WT controls, in both $Mstn^{-/-}$ myoblasts and myotubes. Conversely, the expression of miR-338-3p, miR-126-3p, miR-126-5p, miR-34c-5p and miR-34b-5p were downregulated, in both $Mstn^{-/-}$ myoblasts and myotubes, when compared to WT controls. In addition to our study, other groups have recently identified miRNAs regulated by Mstn. For example, a study by Javed *et al.* (2014) has identified, similar to what was observed in the current study, elevated expression of miR-199a-3p/199b-3p, miR-499-5p, miR-125a-5p and miR-542-3p in *M. gastrocnemius* muscle of Mstn propeptide overexpressing transgenic mice, where Mstn signaling is inactivated [225].

Next, it was observed that several myomiRs involved in myogenesis, including miR-1a-3p, miR-133a-3p, miR-133b-3p, miR-133a-5p and miR-206-3p were downregulated upon treatment with MSTN in primary myoblasts. Given that miR-1a and miR-206 are known to promote myogenic differentiation [163] and that miR-133 positively regulates myoblast proliferation it is not surprising that excess MSTN, a potent

negative regulator of myogenesis, results in reduced myomiR expression. In agreement with this, elevated expression of the myomiRs miR-1, miR-133 and miR-206 has been previously noted in *Mstn*$^{-/-}$ mice when compared to WT mice [210]. These results suggest that Mstn specifically regulates myomiRs during myogenesis.

In addition to the identified myomiRs our bioinformatics analysis revealed two miRNAs, which are known to play a role in myogenesis, as possible targets of Mstn. Specifically, miR-214 was observed to be upregulated in *Mstn*$^{-/-}$ myotubes (Table 3.5). As miR-214 functions to target and repress a polycomb group protein Ezh2 [226], which is an inhibitor of myogenesis, it is quite possible that increased muscle growth seen in *Mstn*$^{-/-}$ mice could be due to reduced Ezh2 proteins. Another miRNA identified to be upregulated in *Mstn*$^{-/-}$ mice was miR-199a-3p. Previous work has shown that miR-199a-3p is involved in myogenesis and in fact increased expression of miR-199-3p was noted during C2C12 myoblast differentiation [227]. Therefore the increased expression of miR-199a-3p noted in *Mstn*$^{-/-}$ mice could be partially responsible for the increased muscle growth observed in these mice.

Among the many miRNA targets of Mstn identified, miR-34a was chosen to be studied during myogenesis. The expression of miR-34a in humans is relatively ubiquitous. This includes reproductive tissues (e.g. ovary and testes), secretory organs (e.g. salivary and adrenal glands), digestive organs (e.g. stomach and kidney), nervous system (e.g. cortex and spinal cord) and muscle (e.g. skeletal muscle and heart). This suggests that miR-34a functions in several tissues. Indeed, this was evidenced by the overexpression of miR-34a which resulted in enhanced neural progenitor proliferation, reduced migration of neuroblasts and increased neurite outgrowth and complexity [228]. These effects led to increased learning abilities and reduced emotionality in rats. In a recent study, miR-34a expression was shown to be induced during cardiac ageing by targeting PPP1R10 (PNUTS) which reduces telomere shortening, DNA damage response and

cardiomyocyte apoptosis [229]. This suggests miR-34a contributes to the process of ageing in the heart. In adipose tissues, miR-34a was shown to inhibit the browning of adipocytes by downregulation of FGF21 and SIRT1 (activators of fat browning) [230]. The blocking of miR-34a which leads to the upregulation of beige fat-specific marker CD137 and the browning marker UCP1 in all white fat adipose tissues could provide an avenue for the treatment of obesity-related diseases.

The decision to perform functional studies on miR-34a was based on its known functions as a cell cycle regulator in cancer cells as well as the similarity between targets of miR-34a and Mstn. A number of miR-34a targets are required for the progression of cell cycle. For example, miR-34a was shown to directly target cyclin D1 (CCND1) and cyclin E2 resulting in G1 cell cycle arrest [231, 232]. This is consistent with the known function of Mstn, whereby Mstn induces G1-S cell cycle arrest through degrading cyclin D1 [233] and downregulating cyclin E [215]. In addition, both Mstn and miR-34a have been shown to induce the expression of p21 [145, 234]. Another reason for selecting miR-34a was that its functions in muscle remain to be elucidated.

4.2 miR-34a is regulated by Myostatin

Several lines of evidence presented in this thesis confirm that Mstn regulates miR-34a expression. Validation of miR-34a expression levels in murine primary myoblasts and myotubes in the presence or absence of Mstn showed that miR-34a was positively regulated by Mstn (Figure 3.1A and B). More importantly, Mstn induced the expression of both the precursor and mature forms of miR-34a (Figure 3.1C-E). This suggests that regulation of miR-34a by Mstn is at the transcriptional level and further implies the involvement of a transcription factor. Analysis of the upstream sequence of miR-34a revealed the presence of three NF-κB transcription factor binding sites (Figure 3.2A) which was previously reported in a study on the activation of miR-34a by NF-κB in human esophageal cancer cells [218]. Given that previous work in our laboratory revealed that Mstn induces the expression and translocation

of NF-κB into the nucleus [219], it was hypothesized that Mstn could regulate miR-34a expression via NF-κB. Consistent with this, deletion of all 3 NF-kB binding sites in the miR-34a upstream enhancer region prevented the increased miR-34a enhancer-reporter activity observed in response to MSTN treatment (Figure 3.2H). It is noteworthy to highlight that a significantly greater increase in Mstn-mediated activation of the miR-34a enhancer-reporter was noted upon deletion of the distal most (1st) NF-κB binding site, when compared the reporter activation noted upon MSTN treatment of the full-length miR-34a enhancer-reporter construct (with all three binding sites intact) (Figure 3.2H). These data suggest that there may be a transcriptional repression site preceding the 2nd NF-kB binding site in the miR-34a upstream enhancer region. Deletion of the two distal most NF-kB binding sites resulted in a significant reduction in Mstn-mediated activation of miR-34a enhancer-reporter activity, which was comparable to that observed following deletion of all 3 NF-kB binding sites (Figure 3.2H). These data underscores the importance of the 2nd NF-kB binding site (at -511) in Mstn-mediated transcriptional activation of miR-34a. Taken together these data suggests an NF-κB transcription factor-dependent mechanism behind Mstn regulation of miR-34a. Transcriptional regulation of miRNAs by Mstn is not novel, in fact a similar study in our laboratory revealed that Mstn transcriptionally upregulates miR-27a/b, via the transcription factor Smad3 [132]. Based on these studies it is clear that Mstn signals through miRNAs to exert its functions and therefore underscores the importance of miRNAs in the Mstn regulatory pathway during myogenesis. Consistent with the findings presented here, evidence suggests that miR-34a expression may be regulated by Mstn during ageing. In a study on human muscle biopsies from young and aged males, both Mstn protein and RNA was observed to be 2-fold higher in aged muscle [235]. Consistent with this, a genome-wide profiling of Gastrocnemius muscle from mice aged 6 and 24 months revealed a 30% increase in miR-34a levels in aged muscle [236]. Taken together, these data suggest that miR-34a levels

are correlated with Mstn during aging, further supporting a role for Mstn in regulation of miR-34a.

4.3 Myostatin regulates myogenesis via a miR-34a-dependent mechanism

Functional analysis suggests that excess levels of either Mstn or miR-34a results in reduced proliferation and myogenic differentiation of myoblasts into myotubes (Figure 3.3 and 3.4) [145, 147]. Given the fact that miR-34a is transcriptionally and positively regulated by Mstn (Figures 3.1 and 3.2), it is quite possible that Mstn regulates cell cycle progression and differentiation of myoblasts via a miR-34a-dependent mechanism. This hypothesis was reinforced by two rescue experiments performed in this study where Mstn-mediated inhibition of both C2C12 myoblast proliferation and differentiation was prevented upon addition of miR-34a-specific AntagomiR (Figures 3.3E and 3.4G).

Mstn has been previously shown to inhibit cell cycle progression and reduce myoblast proliferation through promoting the levels of the cyclin-dependent kinase inhibitor p21 [215]. Similarly, it was observed that stable overexpression of miR-34a in C2C12 myoblasts led to increased p21 expression during proliferation and a subsequent reduction in C2C12 myoblast proliferation. Several reports have shown that miR-34a promotes cell cycle arrest during the G1-S phase of the cell cycle in cancer cells [231, 232]. However, in a separate study overexpresion of miR-34a was shown to induce cell cycle arrest during both S and G2/M phases of the cell cycle medulloblastoma cells [237]. Here it was shown that overexpression of miR-34a in C2C12 myoblasts leads to accumulation of myoblasts in the S-phase of the cell cycle (Figure 3.3I), suggesting that miR-34a may promote S-phase cell cycle arrest in myoblasts. However, it is important to highlight that previous work from our laboratory has revealed that treatment of C2C12 myoblasts with Mstn promotes cell cycle arrest at the G1-S transition [145]. This diffference suggests that Mstn may regulate cell cycle progression through additional mechanisms independent of miR-34a.

An increased level of Mstn during differentiation leads to inhibition of myogenic differentiation and this was shown to be due to downregulation of MyoD levels [147]. Similarly, overexpression of miR-34a inhibits differentiation, which was confirmed by the complete absence of myotubes even in response to extended periods of myogenic differentiation (Figure 3.4A and B). Subsequent molecular analysis revealed that miR-34a inhibits the expression of the transcription factor TCF12. Specifically, the expression of both *TCF12α* and *-β* in miR-34a overexpressing clones were significantly downregulated(Fig 3.5C), which was consistent with the reduced TCF12 3'UTR-reporter activity observed following overexpression of miR-34a (Fig 3.5F). It is noteworthy to mention that the protein levels of TCF12 were not inhibited to the same extent as *TCF12* mRNA expression. Given the fact that the antibody used in this study does not distinguish between different TCF12 protein isoforms it is possible that the differences observed between TCF12 mRNA and protein levels in miR-34a overexpressing cells could be due to antibody specificity.

TCF12 is an important transcriptional co-activator of MyoD. Specifically, co-transfection of both TCF12 and MyoD resulted in increased activation of a MLC-enhancer-reporter in proliferating conditions and also increased endogenous Myogenin levels during C2C12 differentiation [98]. Furthermore, TCF12 was also found to modulate the binding of MyoD to the Myogenin promoter and MLC enhancer. Therefore, in the absence of TCF12 or in response to reduced TCF12 levels, the ability of MyoD to act as a transcriptional activator is severely reduced [98]. Since MyoD is an important transcriptional regulator of the key myogenic regulatory factor Myogenin, miR-34a-mediated reduction of TCF12 and subsequent impairment of MyoD activity would presumably result in reduced Myogenin expression and inhibition of myogenic differentiation. This hypothesis is consistent with the ChIP results presented here (Figure 3.5I), which shows that overexpression of miR-34a leads to reduced

binding of TCF12 and MyoD to E-box regulatory sequences in the *myogenin* upstream enhancer region (Figure 3.5I).

4.4 miR-34a regulates SC quiescence

Since miR-34a expression is detected in myogenic precursor cells, it would also be important to find out if miR-34a is expressed in muscle stem cells, also known as satellite cells. Our molecular analysis revealed increased miR-34a expression in isolated quiescent satellite cells and in an *in vitro* model of induced quiescence (Figure 3.6A and B). This suggests that elevated levels of miR-34a are associated with quiescence. These data are consistent with the expression of miR-34a noted in Notexin injured muscle, where significantly lower levels of endogenous miR-34a from 1-3 days post-injury was observed, which is the phase when satellite cells become activated during regeneration. Furthermore, adenoviral-mediated overexpression of miR-34a in isolated quiescent satellite cells resulted in reduced numbers of MyoD positive satellite cells, suggesting that ectopic expression of miR-34a results in reduced satellite cell activation. Taken together, these results confirm that high levels of miR-34a impair satellite cell activation. These data, at least in part, explain the low levels of miR-34a detected during early regeneration (Day 1-3 post-injury), which would presumably allow for efficient activation of satellite cells, myoblast proliferation and muscle regeneration. Recently, it was discovered that there exists 2 states of stem cell quiescence; G_0 and G_{alert} [238]. Although quiescent, satellite cells in these states possess different cell cycle kinetics and in fact G_{alert} cells were shown to have enhanced muscle regeneration potential, when compared to cells in G_0. Given that miR-34a plays a role in the maintenance of satellite cell quiescence, it would be interesting to study if miR-34a maintains satellite cells in either a G_{alert} or G_0 state of quiescence, where the findings would be useful to further understand the endogenous function of miR-34a in satellite cells.

Notch1 is an important regulator of satellite cell activation. Notch1 intracellular domain is cleaved upon interaction with its ligand, Delta-like or Jagged. This active form of Notch1 (Notch1*) then translocates into the nucleus where it activates the transcription factor RBP-J resulting in the activation of target genes Hes-1 and Hes-5. The levels of Notch1* increases during satellite cell activation [63] which leads to increased Notch1 signaling. The importance of Notch1 signaling in regulating satellite cell activation is clear. Specifically, previous work from Conboy *et al.* (2003) has shown that while inhibition of Notch signaling during muscle injury resulted in impaired muscle regeneration; activation of the Notch signaling pathway during muscle injury resulted in enhanced muscle regeneration in aged muscles [239]. It has been reported that miR-34a directly targets Notch1 in several cancer cell lines such as MCF7 (Breast cancer cell line) [240] and prostate cancer cells [241] thereby reducing the self-renewal potential of these cancer cell lines. Similarly, here it was shown that Notch1 is directly targeted by miR-34a (Figure 3.7A and C) in C2C12 cells. Therefore it was hypothesize that miR-34a-mediated inhibition of satellite cell activation may result from targeted inhibition of Notch1. However, further experiments are required to elucidate and understand the mechanism through which miR-34a downregulates Notch1 to maintain satellite cell quiescence.

Our laboratory has previously demonstrated that Mstn regulates satellite cell activation and self-renewal [221]. Specifically, addition of exogenous recombinant MSTN protein to single muscle fibre cultures *ex vivo* led to impaired activation of satellite cells [221]. Consistent with this, *Mstn$^{-/-}$* mice displayed improved muscle regeneration as observed by reduced fibrosis, enhanced activation of satellite cells (MyoD+ cells) and an accelerated inflammatory response [151]. Moreover, blockade of Mstn has also been shown to enhance muscle regeneration during aging-related muscle wasting (sarcopenia) [150]. Taken together, these studies suggest that Mstn may negatively regulate satellite cell quiescence and muscle regeneration through miR-34a. We

hypothesize that this could occur via the downregulation of Notch1 signaling, which is consistent with the reduced Notch1* protein levels observed in C2C12 myoblast treated with MSTN. However, further experiments are needed to test if Mstn also reduces Notch1* and its downstream signaling in quiescent satellite cells and, more importantly, whether Mstn signals through miR-34a to induce satellite cell quiescence.

Another interesting aspect discovered in this work is the expression of endogenous miR-34a during muscle regeneration. The expression of miR-34a began to increase between days 5 to 7 post-injury, when nascent muscle fibres are formed. A similar expression pattern of endogenous miR-34a was also observed during C2C12 differentiation (Figure 3.1I). It is possible that the higher levels of miR-34a post-differentiation may help to induce and maintain cell cycle arrest of post-mitotic myotubes.

Consistent with the findings thus far, impaired muscle regeneration was observed in the presence of excess miR-34a, with an observable reduction in muscle fibre size (Figure 3.6F and G). This muscle fibre atrophy could be due to impaired satellite cell activation. Consistent with this there was also reduced MyoD+ positive (activated satellite cells) cells during muscle regeneration (Figure 3.6E). In addition, increased miR-34a expression leads to impaired differentiation of myoblasts (Figure 3.4A and B), therefore it is likely that a combination of both impaired satellite cell acitvation and myogenic differentiation may account for the atrophy phenotype observed in response to overexpression of miR-34a in regenerating skeletal muscle.

4.5 Importance of study to human health and diseases

The functions of Mstn have been well studied where it has been shown to induce muscle atrophy and impair muscle regeneration. In addition, Mstn levels were observed to be elevated during cancer cachexia, ageing and insulin resistance (i.e. Type 2 Diabetes).

4.5.1 Treatment of Mstn-induced muscle atrophy, cancer cachexia and impaired/delayed muscle regeneration

In the muscle wasting condition, cancer cachexia, patients experience loss of body mass, fatigue, loss of strength and muscle atrophy. Interestingly, the loss of Mstn inhibited skeletal muscle wasting in the cancer inducing $Apc^{min/+}$ mice model [242]. Consistent with this, high Mstn mRNA and protein levels were observed in muscular atrophy conditions such as sciatic nerve resection, spaceflight disuse and after chronic disuse [243-245]. In addition, the treatment of excess Mstn to human myogenic primary cultures activated the ubiquitin-proteasome degradation pathway and therefore the degradation of sarcomeric proteins (Myosin Heavy and light chains) [246]. This results in myotube atrophy. To date, high levels of miR-34a have been detected in several primary muscular disorders including Duchenne muscular dystrophy, facioscapulohumeral muscular dystrophy, limb-girdle muscular dystrophies types 2A and 2B, Becker muscular dystrophy, Miyoshi myopathy, nemaline myopathy, dermatomyositis, inclusion body myositis and polymyositis [247]. However, there are currently no known studies on miR-34a in muscle atrophy and cancer cachexia. Based on the findings of this thesis, where it was shown that Mstn directly regulates miR-34a to induce myogenic atrophy, it is possible to block Mstn-induced muscle atrophy via inhibition of miR-34a. In addition, reducing miR-34a levels might also prove to be useful in ameliorating muscular disorders.

Mstn has been suggested to impair muscle regeneration in several studies involving work on $Mstn^{-/-}$ mice. For example, our lab has shown that $Mstn^{-/-}$ mice displayed enhanced muscle healing and reduced

fibrosis [151]. In addition, Mstn was also shown to inhibit satellite cell activation and self-renewal [221]. Although no work has been carried out on muscle regeneration in miR-34a knockout mice, the findings of this thesis suggest that Mstn prevents muscle regeneration via miR-34a. Therefore, miR-34a blockade could be a potential therapeutic option or alternative to Mstn inhibition in the enhancement of muscle regeneration or prevent the delay of muscle loss during ageing.

4.5.2 Treatment of ageing and insulin resistance

During ageing, gradual loss of muscle mass and strength occurs. This phenomenon, known as sarcopenia, has been linked to Mstn. This was observed in muscle tissues of old mice where WT displayed obvious fiber atrophy which was minimal in the $Mstn^{-/-}$ muscle fibers [248]. Furthermore, Mstn serum and mRNA levels were also observed to be increased in old human individuals as compared to young [249], suggesting Mstn may contribute to ageing. Interestingly, miR-34a has also been reported play a role during ageing. For example, miR-34a was demonstrated to induce cardiac ageing and that inhibition of miR-34a reduces cardiomyocyte cell death attributed to ageing [229]. In addition, circulatory miR-34a levels were observed to increase from 2 day old neonates through young adult to old mice (25 months) [250]. This suggests a correlation between Mstn and miR-34a expression levels during ageing which is in agreement with the regulation of miR-34a by Mstn presented in this thesis. Therefore, the inhibition of miR-34a could be a possible therapeutic option in delaying ageing. However, it is important that prior preliminary studies on miR-34a and ageing/sarcopenia be conducted as it is still unclear if miR-34a induces ageing and sarcopenia.

Insulin resistance is a diseased condition where cells fail to respond to insulin resulting in high blood glucose levels. Mstn injected mice were observed to induce insulin resistance and high Mstn levels was detected in insulin-resistant human patients [251]. Consistent with this, a recent study involving the inhibition of Mstn displayed improved

121

insulin sensitivity through Irisin (Fndc5) [252]. Interestingly, Fndc5 has been shown to be directly targeted by miR-34a in our lab and that Fndc5 levels were significantly higher in $Mstn^{-/-}$ mice. Furthermore, it was also discovered that Mstn positively regulates miR-34a which targets Fndc5. Although it is still unknown whether Mstn induces insulin resistance via the miR-34a-Fndc5 axis, the results presented here along with work on Fndc5 suggests a treatment in improving insulin sensitivity via the inhibition of miR-34a.

4.6 Future directions

Much of the studies performed in this thesis have been conducted in vitro using cell culture models. In order to prove the relevance of these studies to human health, muscle-specific miR-34a knockout mice have been generated. Interestingly, body weights of muscle-specific miR-34a knockout mice were significantly reduced as compared to wild type and litter mate control (3 months old) mice. This is in contrast to the studies conducted in this thesis and it is possible that miR-34a signals via an Mstn-independent signaling pathway. Therefore, it would be interesting to decipher the mechanisms involved in the knockout genotype. In particular, I would focus on understanding the effect of muscle-specific miR-34a knockout mice during myogenesis including myogenic regeneration. Another aspect would be to observe the consequence of ablating miR-34a in muscle during ageing.

4.6.1 Muscle-specific miR-34a knockout in Myogenesis and muscle regeneration

Importantly, I will first characterize the phenotypic differences as displayed by reduced body weight in miR-34a knockout mice. Preliminary work would be performed by measuring the weights of the different muscle types (e.g. Tibialis Anterior, Gastrocnemius, Soleus and Extensor digitorum longus) of both wild type control and miR-34a knockout mice. This would provide an indication on the muscular phenotype (hypertrophy or atrophy) and whether the loss of miR-34a

contributes to loss of body weight. Following this, microscopic analysis of the muscle fiber number and area would be performed on different age groups (3, 6, 12, 24 month old mice). In addition, myoblast and myotube primary cultures would be established to assess for the proliferation and differentiation potential in the absence of miR-34a. More importantly, muscle regeneration studies in these knockout mice would be performed to observe the effect of miR-34a deficiency during muscle formation *in vivo*.

In order to further study the function of miR-34a during muscle regeneration, satellite cell-specific miR-34a knockout mice have been generated. This was performed by cross breeding of miR-34a$^{Fl/Fl}$ and Pax7$^{Cre/Cre}$ mice. The mice generated from this mating would be Notexin injured and the regeneration kinetics, recovery rate and mechanisms would be studied. Specifically, satellite cell activation (MyoD+ cells), fibrosis and formation of nascent myosin heavy chain would be assessed. It is expected that the loss of miR-34a would enhance the activation of satellite cells therefore increasing myofiber cross sectional area and improved muscle regeneration.

4.6.2 Muscle-specific miR-34a knockout and ageing

Another area of interest would be to study the effect of muscle-specific miR-34a knockout in ageing or sarcopenia (loss of skeletal mass and strength due to ageing). It is expected that the miR-34a knockout mice would display delayed ageing. In order to study this phenomenon, the muscle phenotype and myogenesis abilities of both young and old mice of WT and miR-34a knockout would be compared. This would be carried out by measuring body and muscle weights (e.g. Tibialis Anterior, Gastrocnemius, Soleus and Extensor digitorum longus) which would provide preliminary information on ageing and muscle-specific loss of miR-34a. Next, histological analysis of myofiber cross-sectional area and myofiber number as well as biochemical analysis of myogenic markers would be performed. These results would help understand the

effect of miR-34a knockout in muscles during ageing. In addition, muscle regeneration studies would also be carried out in both young and old, WT and miR-34a knockout mice. This is to confirm the observations in this thesis where miR-34a overexpression displayed impaired muscle regeneration. To do this, the Notexin-induced muscle injury model would be used to study the muscle regeneration potential of the knockout genotype in both young and old aged mice.

A possible mechanism which links miR-34a to ageing is senescence. This was demonstrated in a recent study where the overexpression of miR-34a induced senescent-like phenotypes as observed by the inhibition of telomerase activity and telomere length [253]. In addition, miR-34a expression has been shown to be elevated during cardiac and brain ageing [229, 250] and is also a senescence-associated miRNA. Therefore, it is possible that miR-34a induces senescence during ageing. To study this, biochemical and histological analysis of senescent markers in miR-34a knockout mice would be performed. In addition, the direct target of miR-34a would also be determined to understand the mechanism of miR-34a mediated ageing. More importantly, whether or not Mstn induces senescence through miR-34a would also be extensively studied.

4.7 Conclusion

In conclusion, the work presented in this thesis described a novel miR-34a-dependnt mechanism through which Mstn regulates myogenesis. Specifically, Mstn transcriptionally upregulates miR-34a via NF-κB. Higher levels of miR-34a results in impaired myoblast proliferation and differentiation. Furthermore, miR-34a-mediated inhibition of differentiation occurs through repression of TCF12 and subsequent blockade of MyoD activity and myogenin expression. miR-34a also demonstrated to play a role in negatively regulating satellite cell activation and skeletal muscle regeneration, via targeting Notch1 signaling. Therefore, taken together this study advances our understanding of Mstn biology and proposes a novel epigenetic mechanism through which Mstn regulates several aspects of myogenesis.

3. References

1.   MacIntosh BR, Gardiner PF & McComas AJ (2006) *Skeletal muscle : form and function / Brian R. MacIntosh, Phillip F. Gardiner, Alan J. McComas*. Champaign, IL : Human Kinetics, c2006.
2nd ed.
2.   Marieb EN (2004) *Human anatomy & physiology / Elaine N. Marieb*. New York : Pearson Education, c2004.
6th ed.
3.   Larsson L, Edstrom L, Lindegren B, Gorza L & Schiaffino S (1991) MHC composition and enzyme-histochemical and physiological properties of a novel fast-twitch motor unit type. *Am J Physiol* **261**, C93-101.
4.   Bottinelli R, Betto R, Schiaffino S & Reggiani C (1994) Maximum shortening velocity and coexistence of myosin heavy chain isoforms in single skinned fast fibres of rat skeletal muscle. *J Muscle Res Cell Motil* **15**, 413-419.
5.   Schiaffino S & Reggiani C (2011) Fiber types in mammalian skeletal muscles. *Physiol Rev* **91**, 1447-1531, doi: 10.1152/physrev.00031.2010.
6.   DeNardi C, Ausoni S, Moretti P, Gorza L, Velleca M, Buckingham M & Schiaffino S (1993) Type 2X-myosin heavy chain is coded by a muscle fiber type-specific and developmentally regulated gene. *J Cell Biol* **123**, 823-835.
7.   Klitgaard H, Bergman O, Betto R, Salviati G, Schiaffino S, Clausen T & Saltin B (1990) Co-existence of myosin heavy chain I and IIa isoforms in human skeletal muscle fibres with endurance training. *Pflugers Arch* **416**, 470-472.
8.   Maier A, Gorza L, Schiaffino S & Pette D (1988) A combined histochemical and immunohistochemical study on the dynamics of fast-to-slow fiber transformation in chronically stimulated rabbit muscle. *Cell Tissue Res* **254**, 59-68.
9.   Patterson MF, Stephenson GM & Stephenson DG (2006) Denervation produces different single fiber phenotypes in fast- and slow-twitch hindlimb muscles of the rat. *American journal of physiology Cell physiology* **291**, C518-528, doi: 10.1152/ajpcell.00013.2006.
10.   Ciciliot S, Rossi AC, Dyar KA, Blaauw B & Schiaffino S (2013) Muscle type and fiber type specificity in muscle wasting. *Int J Biochem Cell Biol* **45**, 2191-2199, doi: 10.1016/j.biocel.2013.05.016.
11.   Aulehla A & Pourquie O (2008) Oscillating signaling pathways during embryonic development. *Curr Opin Cell Biol* **20**, 632-637, doi: 10.1016/j.ceb.2008.09.002.
12.   Parker MH, Seale P & Rudnicki MA (2003) Looking back to the embryo: defining transcriptional networks in adult myogenesis. *Nat Rev Genet* **4**, 497-507, doi: 10.1038/nrg1109
nrg1109 [pii].
13.   Yusuf F & Brand-Saberi B (2006) The eventful somite: patterning, fate determination and cell division in the somite. *Anat Embryol (Berl)* **211 Suppl 1**, 21-30, doi: 10.1007/s00429-006-0119-8.
14.   Kiefer JC & Hauschka SD (2001) Myf-5 is transiently expressed in nonmuscle mesoderm and exhibits dynamic regional changes within the presegmented mesoderm and somites I-IV. *Dev Biol* **232**, 77-90, doi: 10.1006/dbio.2000.0114.
15.   Gros J, Manceau M, Thome V & Marcelle C (2005) A common somitic origin for embryonic muscle progenitors and satellite cells. *Nature* **435**, 954-958, doi: 10.1038/nature03572.

16.   Kassar-Duchossoy L, Giacone E, Gayraud-Morel B, Jory A, Gomes D & Tajbakhsh S (2005) Pax3/Pax7 mark a novel population of primitive myogenic cells during development. *Genes Dev* **19**, 1426-1431, doi: 10.1101/gad.345505.

17.   Relaix F, Rocancourt D, Mansouri A & Buckingham M (2005) A Pax3/Pax7-dependent population of skeletal muscle progenitor cells. *Nature* **435**, 948-953, doi: 10.1038/nature03594.

18.   Goulding MD, Chalepakis G, Deutsch U, Erselius JR & Gruss P (1991) Pax-3, a novel murine DNA binding protein expressed during early neurogenesis. *EMBO J* **10**, 1135-1147.

19.   Jostes B, Walther C & Gruss P (1990) The murine paired box gene, Pax7, is expressed specifically during the development of the nervous and muscular system. *Mech Dev* **33**, 27-37.

20.   Duxson MJ, Usson Y & Harris AJ (1989) The origin of secondary myotubes in mammalian skeletal muscles: ultrastructural studies. *Development* **107**, 743-750.

21.   Zhang M & McLennan IS (1995) During secondary myotube formation, primary myotubes preferentially absorb new nuclei at their ends. *Dev Dyn* **204**, 168-177, doi: 10.1002/aja.1002040207.

22.   Ben-Yair R & Kalcheim C (2005) Lineage analysis of the avian dermomyotome sheet reveals the existence of single cells with both dermal and muscle progenitor fates. *Development* **132**, 689-701, doi: 10.1242/dev.01617.

23.   Schienda J, Engleka KA, Jun S, Hansen MS, Epstein JA, Tabin CJ, Kunkel LM & Kardon G (2006) Somitic origin of limb muscle satellite and side population cells. *Proc Natl Acad Sci U S A* **103**, 945-950, doi: 10.1073/pnas.0510164103.

24.   Buckingham M (1992) Making muscle in mammals. *Trends Genet* **8**, 144-148, doi: 10.1016/0168-9525(92)90373-c.

25.   Ott MO, Bober E, Lyons G, Arnold H & Buckingham M (1991) Early expression of the myogenic regulatory gene, myf-5, in precursor cells of skeletal muscle in the mouse embryo. *Development* **111**, 1097-1107.

26.   Bismuth K & Relaix F (2010) Genetic regulation of skeletal muscle development. *Exp Cell Res* **316**, 3081-3086, doi: 10.1016/j.yexcr.2010.08.018.

27.   Hutcheson DA, Zhao J, Merrell A, Haldar M & Kardon G (2009) Embryonic and fetal limb myogenic cells are derived from developmentally distinct progenitors and have different requirements for beta-catenin. *Genes Dev* **23**, 997-1013, doi: 10.1101/gad.1769009.

28.   Seale P, Sabourin LA, Girgis-Gabardo A, Mansouri A, Gruss P & Rudnicki MA (2000) Pax7 is required for the specification of myogenic satellite cells. *Cell* **102**, 777-786.

29.   Braun T, Rudnicki MA, Arnold HH & Jaenisch R (1992) Targeted inactivation of the muscle regulatory gene Myf-5 results in abnormal rib development and perinatal death. *Cell* **71**, 369-382.

30.   Rudnicki MA, Braun T, Hinuma S & Jaenisch R (1992) Inactivation of MyoD in mice leads to up-regulation of the myogenic HLH gene Myf-5 and results in apparently normal muscle development. *Cell* **71**, 383-390.

31.   Rudnicki MA, Schnegelsberg PN, Stead RH, Braun T, Arnold HH & Jaenisch R (1993) MyoD or Myf-5 is required for the formation of skeletal muscle. *Cell* **75**, 1351-1359.

32.   Yaffe D & Saxel O (1977) Serial passaging and differentiation of myogenic cells isolated from dystrophic mouse muscle. *Nature* **270**, 725-727.

33.   Sharples AP, Al-Shanti N & Stewart CE (2010) C2 and C2C12 murine skeletal myoblast models of atrophic and hypertrophic potential: relevance to disease and ageing? *J Cell Physiol* **225**, 240-250, doi: 10.1002/jcp.22252.

34. Grounds MD (2014) The need to more precisely define aspects of skeletal muscle regeneration. *Int J Biochem Cell Biol* **56**, 56-65, doi: 10.1016/j.biocel.2014.09.010.

35. Mann CJ, Perdiguero E, Kharraz Y, Aguilar S, Pessina P, Serrano AL & Munoz-Canoves P (2011) Aberrant repair and fibrosis development in skeletal muscle. *Skelet Muscle* **1**, 21, doi: 10.1186/2044-5040-1-21.

36. Grounds MD (2001) Regeneration of Muscle. In *eLS*. John Wiley & Sons, Ltd.

37. Moyer AL & Wagner KR (2011) Regeneration versus fibrosis in skeletal muscle. *Curr Opin Rheumatol* **23**, 568-573, doi: 10.1097/BOR.0b013e32834bac92.

38. Abmayr SM & Pavlath GK (2012) Myoblast fusion: lessons from flies and mice. *Development* **139**, 641-656, doi: 10.1242/dev.068353.

39. Jarvinen TA, Jarvinen M & Kalimo H (2013) Regeneration of injured skeletal muscle after the injury. *Muscles Ligaments Tendons J* **3**, 337-345.

40. Robertson TA, Papadimitriou JM & Grounds MD (1993) Fusion of myogenic cells to the newly sealed region of damaged myofibres in skeletal muscle regeneration. *Neuropathol Appl Neurobiol* **19**, 350-358.

41. Grounds MD, Davies M, Torrisi J, Shavlakadze T, White J & Hodgetts S (2005) Silencing TNFalpha activity by using Remicade or Enbrel blocks inflammation in whole muscle grafts: an in vivo bioassay to assess the efficacy of anti-cytokine drugs in mice. *Cell Tissue Res* **320**, 509-515, doi: 10.1007/s00441-005-1102-z.

42. Serrano AL & Munoz-Canoves P (2010) Regulation and dysregulation of fibrosis in skeletal muscle. *Exp Cell Res* **316**, 3050-3058, doi: 10.1016/j.yexcr.2010.05.035.

43. Collins CA, Olsen I, Zammit PS, Heslop L, Petrie A, Partridge TA & Morgan JE (2005) Stem cell function, self-renewal, and behavioral heterogeneity of cells from the adult muscle satellite cell niche. *Cell* **122**, 289-301, doi: 10.1016/j.cell.2005.05.010.

44. Schultz E & Lipton BH (1978) The effect of Marcaine on muscle and non-muscle cells in vitro. *Anat Rec* **191**, 351-369, doi: 10.1002/ar.1091910308.

45. Snow MH (1977) Myogenic cell formation in regenerating rat skeletal muscle injured by mincing. II. An autoradiographic study. *Anat Rec* **188**, 201-217, doi: 10.1002/ar.1091880206.

46. Snow MH (1978) An autoradiographic study of satellite cell differentiation into regenerating myotubes following transplantation of muscles in young rats. *Cell Tissue Res* **186**, 535-540.

47. Collins CA, Zammit PS, Ruiz AP, Morgan JE & Partridge TA (2007) A population of myogenic stem cells that survives skeletal muscle aging. *Stem Cells* **25**, 885-894, doi: 10.1634/stemcells.2006-0372.

48. Shefer G, Van de Mark DP, Richardson JB & Yablonka-Reuveni Z (2006) Satellite-cell pool size does matter: defining the myogenic potency of aging skeletal muscle. *Dev Biol* **294**, 50-66, doi: 10.1016/j.ydbio.2006.02.022.

49. Blau HM, Webster C & Pavlath GK (1983) Defective myoblasts identified in Duchenne muscular dystrophy. *Proc Natl Acad Sci U S A* **80**, 4856-4860.

50. Shefer G, Rauner G, Yablonka-Reuveni Z & Benayahu D (2010) Reduced satellite cell numbers and myogenic capacity in aging can be alleviated by endurance exercise. *PLoS One* **5**, e13307, doi: 10.1371/journal.pone.0013307.

51. Smith HK & Merry TL (2012) Voluntary resistance wheel exercise during post-natal growth in rats enhances skeletal muscle satellite cell and myonuclear content at adulthood. *Acta Physiol (Oxf)* **204**, 393-402, doi: 10.1111/j.1748-1716.2011.02350.x.

52.   Irintchev A, Zeschnigk M, Starzinski-Powitz A & Wernig A (1994) Expression pattern of M-cadherin in normal, denervated, and regenerating mouse muscles. *Dev Dyn* **199**, 326-337, doi: 10.1002/aja.1001990407.

53.   Beauchamp JR, Heslop L, Yu DS, Tajbakhsh S, Kelly RG, Wernig A, Buckingham ME, Partridge TA & Zammit PS (2000) Expression of CD34 and Myf5 defines the majority of quiescent adult skeletal muscle satellite cells. *J Cell Biol* **151**, 1221-1234.

54.   Charge SB & Rudnicki MA (2004) Cellular and molecular regulation of muscle regeneration. *Physiol Rev* **84**, 209-238, doi: 10.1152/physrev.00019.2003.

55.   Tajbakhsh S, Rocancourt D, Cossu G & Buckingham M (1997) Redefining the genetic hierarchies controlling skeletal myogenesis: Pax-3 and Myf-5 act upstream of MyoD. *Cell* **89**, 127-138.

56.   Zammit PS, Carvajal JJ, Golding JP, Morgan JE, Summerbell D, Zolnerciks J, Partridge TA, Rigby PW & Beauchamp JR (2004) Myf5 expression in satellite cells and spindles in adult muscle is controlled by separate genetic elements. *Dev Biol* **273**, 454-465, doi: 10.1016/j.ydbio.2004.05.038.

57.   Zammit P & Beauchamp J (2001) The skeletal muscle satellite cell: stem cell or son of stem cell? *Differentiation* **68**, 193-204.

58.   Heslop L, Morgan JE & Partridge TA (2000) Evidence for a myogenic stem cell that is exhausted in dystrophic muscle. *J Cell Sci* **113 (Pt 12)**, 2299-2308.

59.   Maltin CA, Harris JB & Cullen MJ (1983) Regeneration of mammalian skeletal muscle following the injection of the snake-venom toxin, taipoxin. *Cell Tissue Res* **232**, 565-577.

60.   Tatsumi R, Anderson JE, Nevoret CJ, Halevy O & Allen RE (1998) HGF/SF is present in normal adult skeletal muscle and is capable of activating satellite cells. *Dev Biol* **194**, 114-128, doi: 10.1006/dbio.1997.8803.

61.   Darr KC & Schultz E (1987) Exercise-induced satellite cell activation in growing and mature skeletal muscle. *J Appl Physiol* **63**, 1816-1821.

62.   Snow MH (1983) A quantitative ultrastructural analysis of satellite cells in denervated fast and slow muscles of the mouse. *Anat Rec* **207**, 593-604, doi: 10.1002/ar.1092070407.

63.   Conboy IM & Rando TA (2002) The regulation of Notch signaling controls satellite cell activation and cell fate determination in postnatal myogenesis. *Developmental cell* **3**, 397-409.

64.   Bjornson CRR, Cheung TH, Liu L, Tripathi PV, Steeper KM & Rando TA (2012) Notch Signaling Is Necessary to Maintain Quiescence in Adult Muscle Stem Cells. *STEM CELLS* **30**, 232-242, doi: 10.1002/stem.773.

65.   Mourikis P, Gopalakrishnan S, Sambasivan R & Tajbakhsh S (2012) Cell-autonomous Notch activity maintains the temporal specification potential of skeletal muscle stem cells. *Development* **139**, 4536-4548, doi: 10.1242/dev.084756.

66.   Fukada S, Yamaguchi M, Kokubo H, Ogawa R, Uezumi A, Yoneda T, Matev MM, Motohashi N, Ito T, Zolkiewska A, et al. (2011) Hesr1 and Hesr3 are essential to generate undifferentiated quiescent satellite cells and to maintain satellite cell numbers. *Development* **138**, 4609-4619, doi: 10.1242/dev.067165.

67.   Relaix F & Zammit PS (2012) Satellite cells are essential for skeletal muscle regeneration: the cell on the edge returns centre stage. *Development* **139**, 2845-2856, doi: 10.1242/dev.069088.

68.   Dhawan J & Rando TA (2005) Stem cells in postnatal myogenesis: molecular mechanisms of satellite cell quiescence, activation and replenishment. *Trends Cell Biol* **15**, 666-673, doi: 10.1016/j.tcb.2005.10.007.

69.   Wozniak MA, Desai R, Solski PA, Der CJ & Keely PJ (2003) ROCK-generated contractility regulates breast epithelial cell differentiation in response to the physical properties of a three-dimensional collagen matrix. *J Cell Biol* **163**, 583-595, doi: 10.1083/jcb.200305010.

70.   Yamada M, Tatsumi R, Kikuiri T, Okamoto S, Nonoshita S, Mizunoya W, Ikeuchi Y, Shimokawa H, Sunagawa K & Allen RE (2006) Matrix metalloproteinases are involved in mechanical stretch-induced activation of skeletal muscle satellite cells. *Muscle & nerve* **34**, 313-319, doi: 10.1002/mus.20601.

71.   Sheehan SM & Allen RE (1999) Skeletal muscle satellite cell proliferation in response to members of the fibroblast growth factor family and hepatocyte growth factor. *J Cell Physiol* **181**, 499-506, doi: 10.1002/(sici)1097-4652(199912)181:3<499::aid-jcp14>3.0.co;2-1.

72.   Kastner S, Elias MC, Rivera AJ & Yablonka-Reuveni Z (2000) Gene expression patterns of the fibroblast growth factors and their receptors during myogenesis of rat satellite cells. *J Histochem Cytochem* **48**, 1079-1096.

73.   Bischoff R & Heintz C (1994) Enhancement of skeletal muscle regeneration. *Dev Dyn* **201**, 41-54, doi: 10.1002/aja.1002010105.

74.   Tsivitse S (2010) Notch and Wnt signaling, physiological stimuli and postnatal myogenesis. *Int J Biol Sci* **6**, 268-281.

75.   Fuchtbauer EM & Westphal H (1992) MyoD and myogenin are coexpressed in regenerating skeletal muscle of the mouse. *Dev Dyn* **193**, 34-39, doi: 10.1002/aja.1001930106.

76.   Grounds MD, Garrett KL, Lai MC, Wright WE & Beilharz MW (1992) Identification of skeletal muscle precursor cells in vivo by use of MyoD1 and myogenin probes. *Cell Tissue Res* **267**, 99-104.

77.   Yablonka-Reuveni Z & Rivera AJ (1994) Temporal expression of regulatory and structural muscle proteins during myogenesis of satellite cells on isolated adult rat fibers. *Dev Biol* **164**, 588-603, doi: 10.1006/dbio.1994.1226.

78.   Yablonka-Reuveni Z, Seger R & Rivera AJ (1999) Fibroblast growth factor promotes recruitment of skeletal muscle satellite cells in young and old rats. *J Histochem Cytochem* **47**, 23-42.

79.   Zammit PS, Golding JP, Nagata Y, Hudon V, Partridge TA & Beauchamp JR (2004) Muscle satellite cells adopt divergent fates: a mechanism for self-renewal? *J Cell Biol* **166**, 347-357, doi: 10.1083/jcb.200312007.

80.   Smith TH, Block NE, Rhodes SJ, Konieczny SF & Miller JB (1993) A unique pattern of expression of the four muscle regulatory factor proteins distinguishes somitic from embryonic, fetal and newborn mouse myogenic cells. *Development* **117**, 1125-1133.

81.   Smith TH, Kachinsky AM & Miller JB (1994) Somite subdomains, muscle cell origins, and the four muscle regulatory factor proteins. *J Cell Biol* **127**, 95-105.

82.   Morgan JE & Partridge TA (2003) Muscle satellite cells. *Int J Biochem Cell Biol* **35**, 1151-1156.

83.   Siegel AL, Atchison K, Fisher KE, Davis GE & Cornelison DD (2009) 3D timelapse analysis of muscle satellite cell motility. *STEM CELLS* **27**, 2527-2538, doi: 10.1002/stem.178.

84.   Griffin CA, Apponi LH, Long KK & Pavlath GK (2010) Chemokine expression and control of muscle cell migration during myogenesis. *J Cell Sci* **123**, 3052-3060, doi: 10.1242/jcs.066241.

85.   Pavlath GK (2010) Spatial and functional restriction of regulatory molecules during mammalian myoblast fusion. *Exp Cell Res* **316**, 3067-3072, doi: 10.1016/j.yexcr.2010.05.025.

86.   Starkey JD, Yamamoto M, Yamamoto S & Goldhamer DJ (2011) Skeletal muscle satellite cells are committed to myogenesis and do not spontaneously adopt nonmyogenic fates. *J Histochem Cytochem* **59**, 33-46, doi: 10.1369/jhc.2010.956995.

87.   Ishido M & Kasuga N (2012) In Vivo Real-Time Imaging of Exogenous HGF-Triggered Cell Migration in Rat Intact Soleus Muscles. *Acta Histochem Cytochem* **45**, 193-199, doi: 10.1267/ahc.11058.

88.   Sacco A, Doyonnas R, Kraft P, Vitorovic S & Blau HM (2008) Self-renewal and expansion of single transplanted muscle stem cells. *Nature* **456**, 502-506, doi: 10.1038/nature07384.

89.   Rocheteau P, Gayraud-Morel B, Siegl-Cachedenier I, Blasco MA & Tajbakhsh S (2012) A subpopulation of adult skeletal muscle stem cells retains all template DNA strands after cell division. *Cell* **148**, 112-125, doi: 10.1016/j.cell.2011.11.049.

90.   Kuang S, Charge SB, Seale P, Huh M & Rudnicki MA (2006) Distinct roles for Pax7 and Pax3 in adult regenerative myogenesis. *J Cell Biol* **172**, 103-113, doi: 10.1083/jcb.200508001.

91.   Mansouri A, Hallonet M & Gruss P (1996) Pax genes and their roles in cell differentiation and development. *Curr Opin Cell Biol* **8**, 851-857.

92.   Lepper C & Fan CM (2010) Inducible lineage tracing of Pax7-descendant cells reveals embryonic origin of adult satellite cells. *Genesis* **48**, 424-436, doi: 10.1002/dvg.20630.

93.   Megeney LA, Kablar B, Garrett K, Anderson JE & Rudnicki MA (1996) MyoD is required for myogenic stem cell function in adult skeletal muscle. *Genes & development* **10**, 1173-1183.

94.   Asakura A, Komaki M & Rudnicki M (2001) Muscle satellite cells are multipotential stem cells that exhibit myogenic, osteogenic, and adipogenic differentiation. *Differentiation* **68**, 245-253.

95.   Ono Y, Masuda S, Nam HS, Benezra R, Miyagoe-Suzuki Y & Takeda S (2012) Slow-dividing satellite cells retain long-term self-renewal ability in adult muscle. *J Cell Sci* **125**, 1309-1317, doi: 10.1242/jcs.096198.

96.   Berkes CA & Tapscott SJ (2005) MyoD and the transcriptional control of myogenesis. *Semin Cell Dev Biol* **16**, 585-595, doi: 10.1016/j.semcdb.2005.07.006.

97.   Conway K, Pin C, Kiernan JA & Merrifield P (2004) The E protein HEB is preferentially expressed in developing muscle. *Differentiation* **72**, 327-340, doi: S0301-4681(09)60309-1 [pii]
10.1111/j.1432-0436.2004.07207004.x.

98.   Parker MH, Perry RL, Fauteux MC, Berkes CA & Rudnicki MA (2006) MyoD synergizes with the E-protein HEB beta to induce myogenic differentiation. *Molecular and cellular biology* **26**, 5771-5783, doi: 26/15/5771 [pii]
10.1128/MCB.02404-05.

99.   Lassar AB, Davis RL, Wright WE, Kadesch T, Murre C, Voronova A, Baltimore D & Weintraub H (1991) Functional activity of myogenic HLH proteins requires hetero-oligomerization with E12/E47-like proteins in vivo. *Cell* **66**, 305-315.

100.   Blackwell TK & Weintraub H (1990) Differences and similarities in DNA-binding preferences of MyoD and E2A protein complexes revealed by binding site selection. *Science* **250**, 1104-1110.

101.   Benezra R, Davis RL, Lockshon D, Turner DL & Weintraub H (1990) The protein Id: a negative regulator of helix-loop-helix DNA binding proteins. *Cell* **61**, 49-59.

102.   Lu J, Webb R, Richardson JA & Olson EN (1999) MyoR: a muscle-restricted basic helix-loop-helix transcription factor that antagonizes the actions of MyoD. *Proc Natl Acad Sci U S A* **96**, 552-557.

103.   Baxter RC (1988) The insulin-like growth factors and their binding proteins. *Comp Biochem Physiol B* **91**, 229-235.

104.   Florini JR, Ewton DZ & Roof SL (1991) Insulin-like growth factor-I stimulates terminal myogenic differentiation by induction of myogenin gene expression. *Mol Endocrinol* **5**, 718-724, doi: 10.1210/mend-5-5-718.

105.   Schmid C, Steiner T & Froesch ER (1983) Preferential enhancement of myoblast differentiation by insulin-like growth factors (IGF I and IGF II) in primary cultures of chicken embryonic cells. *FEBS Lett* **161**, 117-121.

106.   Allen RE & Boxhorn LK (1989) Regulation of skeletal muscle satellite cell proliferation and differentiation by transforming growth factor-beta, insulin-like growth factor I, and fibroblast growth factor. *J Cell Physiol* **138**, 311-315, doi: 10.1002/jcp.1041380213.

107.   Massague J, Cheifetz S, Endo T & Nadal-Ginard B (1986) Type beta transforming growth factor is an inhibitor of myogenic differentiation. *Proc Natl Acad Sci U S A* **83**, 8206-8210.

108.   Olson EN, Sternberg E, Hu JS, Spizz G & Wilcox C (1986) Regulation of myogenic differentiation by type beta transforming growth factor. *J Cell Biol* **103**, 1799-1805.

109.   Evinger-Hodges MJ, Ewton DZ, Seifert SC & Florini JR (1982) Inhibition of myoblast differentiation in vitro by a protein isolated from liver cell medium. *J Cell Biol* **93**, 395-401.

110.   Lathrop B, Olson E & Glaser L (1985) Control by fibroblast growth factor of differentiation in the BC3H1 muscle cell line. *J Cell Biol* **100**, 1540-1547.

111.   Gospodarowicz D, Ferrara N, Schweigerer L & Neufeld G (1987) Structural characterization and biological functions of fibroblast growth factor. *Endocr Rev* **8**, 95-114.

112.   Vaidya TB, Rhodes SJ, Taparowsky EJ & Konieczny SF (1989) Fibroblast growth factor and transforming growth factor beta repress transcription of the myogenic regulatory gene MyoD1. *Molecular and cellular biology* **9**, 3576-3579.

113.   Olson EN & Capetanaki YG (1989) Developmental regulation of intermediate filament and actin mRNAs during myogenesis is disrupted by oncogenic ras genes. *Oncogene* **4**, 907-913.

114.   McPherron AC, Lawler AM & Lee SJ (1997) Regulation of skeletal muscle mass in mice by a new TGF-beta superfamily member. *Nature* **387**, 83-90, doi: 10.1038/387083a0.

115.   Kambadur R, Sharma M, Smith TP & Bass JJ (1997) Mutations in myostatin (GDF8) in double-muscled Belgian Blue and Piedmontese cattle. *Genome Res* **7**, 910-916.

116.   Lee SJ & McPherron AC (2001) Regulation of myostatin activity and muscle growth. *Proc Natl Acad Sci U S A* **98**, 9306-9311, doi: 10.1073/pnas.151270098.

117.   Elliott B, Renshaw D, Getting S & Mackenzie R (2012) The central role of myostatin in skeletal muscle and whole body homeostasis. *Acta Physiologica* **205**, 324-340.

118.   McFarlane C, Alex H, Mark T, Erin P, Nicholas L, Mridula S & Ravi K (2007) Research Article: Myostatin signals through Pax7 to regulate satellite cell self-renewal. *Experimental Cell Research* **314**, 317-329, doi: 10.1016/j.yexcr.2007.09.012.

119.   Kambadur R, Sharma M, Smith TP & Bass JJ (1997) Mutations in myostatin (GDF8) in double-muscled Belgian Blue and Piedmontese cattle. *Genome Research* **7**, 910-916.

120.   Mosher DS, Quignon P, Bustamante CD, Sutter NB, Mellersh CS, Parker HG & Ostrander EA (2007) A Mutation in the Myostatin Gene Increases Muscle Mass and

Enhances Racing Performance in Heterozygote Dogs. *PLoS Genetics* **3**, e79-0786, doi: 10.1371/journal.pgen.0030079.

121. Jeanplong F, Bass JJ, Smith HK, Kirk SP, Kambadur R, Sharma M & Oldham JM (2003) Prolonged underfeeding of sheep increases myostatin and myogenic regulatory factor Myf-5 in skeletal muscle while IGF-I and myogenin are repressed. *The Journal Of Endocrinology* **176**, 425-437.

122. Zachwieja JJ, Smith SR, Sinha-Hikim I, Gonzalez-Cadavid N & Bhasin S (1999) Plasma myostatin-immunoreactive protein is increased after prolonged bed rest with low-dose T3 administration. *J Gravit Physiol* **6**, 11-15.

123. Reardon KA, Davis J, Kapsa RM, Choong P & Byrne E (2001) Myostatin, insulin-like growth factor-1, and leukemia inhibitory factor mRNAs are upregulated in chronic human disuse muscle atrophy. *Muscle & nerve* **24**, 893-899.

124. Dasarathy S, Dodig M, Muc SM, Kalhan SC & McCullough AJ (2004) Skeletal muscle atrophy is associated with an increased expression of myostatin and impaired satellite cell function in the portacaval anastamosis rat. *Am J Physiol Gastrointest Liver Physiol* **287**, G1124-1130, doi: 10.1152/ajpgi.00202.2004.

125. Taylor WE, Bhasin S, Artaza J, Byhower F, Azam M, Willard DH, Jr., Kull FC, Jr. & Gonzalez-Cadavid N (2001) Myostatin inhibits cell proliferation and protein synthesis in C2C12 muscle cells. *Am J Physiol Endocrinol Metab* **280**, E221-228.

126. Artaza JN, Bhasin S, Mallidis C, Taylor W, Ma K & Gonzalez-Cadavid NF (2002) Endogenous expression and localization of myostatin and its relation to myosin heavy chain distribution in C2C12 skeletal muscle cells. *Journal Of Cellular Physiology* **190**, 170-179.

127. Derynck R, Zhang Y & Feng XH (1998) Smads: transcriptional activators of TGF-beta responses. *Cell* **95**, 737-740.

128. Xiangyang Z, Stavros T, Li-fang L & Ronald LS (2004) Myostatin signaling through Smad2, Smad3 and Smad4 is regulated by the inhibitory Smad7 by a negative feedback mechanism. *Cytokine* **26**, 262-272, doi: 10.1016/j.cyto.2004.03.007.

129. Rodriguez J, Vernus B, Chelh I, Cassar-Malek I, Gabillard JC, Hadj Sassi A, Seiliez I, Picard B & Bonnieu A (2014) Myostatin and the skeletal muscle atrophy and hypertrophy signaling pathways. *Cell Mol Life Sci* **71**, 4361-4371, doi: 10.1007/s00018-014-1689-x.

130. Forbes D, Jackman M, Bishop A, Thomas M, Kambadur R & Sharma M (2006) Myostatin auto-regulates its expression by feedback loop through Smad7 dependent mechanism. *J Cell Physiol* **206**, 264-272, doi: 10.1002/jcp.20477.

131. Zhu X, Topouzis S, Liang LF & Stotish RL (2004) Myostatin signaling through Smad2, Smad3 and Smad4 is regulated by the inhibitory Smad7 by a negative feedback mechanism. *Cytokine* **26**, 262-272, doi: 10.1016/j.cyto.2004.03.007.

132. McFarlane C, Vajjala A, Arigela H, Lokireddy S, Ge X, Bonala S, Manickam R, Kambadur R & Sharma M (2014) Negative auto-regulation of myostatin expression is mediated by Smad3 and microRNA-27. *PLoS One* **9**, e87687, doi: 10.1371/journal.pone.0087687.

133. Ge X, Vajjala A, McFarlane C, Wahli W, Sharma M & Kambadur R (2012) Lack of Smad3 signaling leads to impaired skeletal muscle regeneration. *Am J Physiol Endocrinol Metab* **303**, E90-102, doi: 10.1152/ajpendo.00113.2012.

134. Yang W, Zhang Y, Li Y, Wu Z & Zhu D (2007) Myostatin induces cyclin D1 degradation to cause cell cycle arrest through a phosphatidylinositol 3-kinase/AKT/GSK-3 beta pathway and is antagonized by insulin-like growth factor 1. *The Journal Of Biological Chemistry* **282**, 3799-3808.

135. McFarlane C, Plummer E, Thomas M, Hennebry A, Ashby M, Ling N, Smith H, Sharma M & Kambadur R (2006) Myostatin induces cachexia by activating the ubiquitin proteolytic system through an NF-kappaB-independent, FoxO1-dependent mechanism. *J Cell Physiol* **209**, 501-514, doi: 10.1002/jcp.20757.

136. Cohen S, Brault JJ, Gygi SP, Glass DJ, Valenzuela DM, Gartner C, Latres E & Goldberg AL (2009) During muscle atrophy, thick, but not thin, filament components are degraded by MuRF1-dependent ubiquitylation. *J Cell Biol* **185**, 1083-1095, doi: 10.1083/jcb.200901052.

137. Zhao J, Brault JJ, Schild A, Cao P, Sandri M, Schiaffino S, Lecker SH & Goldberg AL (2007) FoxO3 coordinately activates protein degradation by the autophagic/lysosomal and proteasomal pathways in atrophying muscle cells. *Cell Metab* **6**, 472-483, doi: 10.1016/j.cmet.2007.11.004.

138. Lokireddy S, McFarlane C, Ge X, Zhang H, Sze SK, Sharma M & Kambadur R (2011) Myostatin induces degradation of sarcomeric proteins through a Smad3 signaling mechanism during skeletal muscle wasting. *Mol Endocrinol* **25**, 1936-1949, doi: 10.1210/me.2011-1124.

139. Ma XM & Blenis J (2009) Molecular mechanisms of mTOR-mediated translational control. *Nat Rev Mol Cell Biol* **10**, 307-318, doi: 10.1038/nrm2672.

140. Hay N & Sonenberg N (2004) Upstream and downstream of mTOR. *Genes Dev* **18**, 1926-1945, doi: 10.1101/gad.1212704.

141. Trendelenburg AU, Meyer A, Rohner D, Boyle J, Hatakeyama S & Glass DJ (2009) Myostatin reduces Akt/TORC1/p70S6K signaling, inhibiting myoblast differentiation and myotube size. *American journal of physiology Cell physiology* **296**, C1258-1270, doi: 10.1152/ajpcell.00105.2009.

142. Chelh I, Picard B, Hocquette JF & Cassar-Malek I (2011) Myostatin inactivation induces a similar muscle molecular signature in double-muscled cattle as in mice. *Animal* **5**, 278-286, doi: 10.1017/s1751731110001862.

143. Goncalves MD, Pistilli EE, Balduzzi A, Birnbaum MJ, Lachey J, Khurana TS & Ahima RS (2010) Akt Deficiency Attenuates Muscle Size and Function but Not the Response to ActRIIB Inhibition. *PLoS ONE* **5**, 1-12, doi: 10.1371/journal.pone.0012707.

144. Goncalves MD, Pistilli EE, Balduzzi A, Birnbaum MJ, Lachey J, Khurana TS & Ahima RS (2010) Akt deficiency attenuates muscle size and function but not the response to ActRIIB inhibition. *PLoS One* **5**, e12707, doi: 10.1371/journal.pone.0012707.

145. Thomas M, Langley B, Berry C, Sharma M, Kirk S, Bass J & Kambadur R (2000) Myostatin, a negative regulator of muscle growth, functions by inhibiting myoblast proliferation. *The Journal of biological chemistry* **275**, 40235-40243, doi: 10.1074/jbc.M004356200.

146. Rios R, Carneiro I, Arce VM & Devesa J (2001) Myostatin regulates cell survival during C2C12 myogenesis. *Biochem Biophys Res Commun* **280**, 561-566, doi: 10.1006/bbrc.2000.4159.

147. Langley B, Thomas M, Bishop A, Sharma M, Gilmour S & Kambadur R (2002) Myostatin inhibits myoblast differentiation by down-regulating MyoD expression. *J Biol Chem* **277**, 49831-49840, doi: 10.1074/jbc.M204291200
M204291200 [pii].

148. Megeney LA, Kablar B, Garrett K, Anderson JE & Rudnicki MA (1996) MyoD is required for myogenic stem cell function in adult skeletal muscle. *Genes & Development* **10**, 1173-1183.

149. McFarlane C, Hui GZ, Amanda WZ, Lau HY, Lokireddy S, Xiaojia G, Mouly V, Butler-Browne G, Gluckman PD, Sharma M, et al. (2011) Human myostatin

negatively regulates human myoblast growth and differentiation. *American journal of physiology Cell physiology* **301**, C195-203, doi: ajpcell.00012.2011 [pii] 10.1152/ajpcell.00012.2011.

150.   Siriett V, Salerno MS, Berry C, Nicholas G, Bower R, Kambadur R & Sharma M (2007) Antagonism of myostatin enhances muscle regeneration during sarcopenia. *Molecular therapy : the journal of the American Society of Gene Therapy* **15**, 1463-1470, doi: 10.1038/sj.mt.6300182.

151.   McCroskery S, Thomas M, Platt L, Hennebry A, Nishimura T, McLeay L, Sharma M & Kambadur R (2005) Improved muscle healing through enhanced regeneration and reduced fibrosis in myostatin-null mice. *J Cell Sci* **118**, 3531-3541, doi: 10.1242/jcs.02482.

152.   Zeng Y & Cullen BR (2003) Sequence requirements for micro RNA processing and function in human cells. *RNA (New York, NY)* **9**, 112-123.

153.   Lund E, Güttinger S, Calado A, Dahlberg JE & Kutay U (2004) Nuclear Export of MicroRNA Precursors. *Science*, 95, doi: 10.2307/3836045.

154.   Yi R, Qin Y, Macara IG & Cullen BR (2003) Exportin-5 mediates the nuclear export of pre-microRNAs and short hairpin RNAs. *Genes & Development* **17**, 3011-3016.

155.   Huntzinger E & Izaurralde E (2011) Gene silencing by microRNAs: contributions of translational repression and mRNA decay. *Nat Rev Genet* **12**, 99-110, doi: 10.1038/nrg2936.

156.   Hutvágner G & Zamore PD (2002) A microRNA in a Multiple-Turnover RNAi Enzyme Complex. *Science*, 2056, doi: 10.2307/3832438.

157.   Zeng Y, Yi R & Cullen BR (2003) MicroRNAs and Small Interfering RNAs Can Inhibit mRNA Expression by Similar Mechanisms. *Proceedings of the National Academy of Sciences of the United States of America*, 9779, doi: 10.2307/3147612.

158.   Mitchelson KR & Qin WY (2015) Roles of the canonical myomiRs miR-1, -133 and -206 in cell development and disease. *World J Biol Chem* **6**, 162-208, doi: 10.4331/wjbc.v6.i3.162.

159.   McCarthy JJ (2011) The MyomiR network in skeletal muscle plasticity. *Exerc Sport Sci Rev* **39**, 150-154, doi: 10.1097/JES.0b013e31821c01e1.

160.   Liu N & Olson EN (2010) MicroRNA regulatory networks in cardiovascular development. *Developmental cell* **18**, 510-525, doi: S1534-5807(10)00148-6 [pii] 10.1016/j.devcel.2010.03.010.

161.   Potthoff MJ, Olson EN & Bassel-Duby R (2007) Skeletal muscle remodeling. *Curr Opin Rheumatol* **19**, 542-549, doi: 10.1097/BOR.0b013e3282efb761 00002281-200711000-00005 [pii].

162.   Care A, Catalucci D, Felicetti F, Bonci D, Addario A, Gallo P, Bang ML, Segnalini P, Gu Y, Dalton ND, et al. (2007) MicroRNA-133 controls cardiac hypertrophy. *Nat Med* **13**, 613-618, doi: nm1582 [pii] 10.1038/nm1582.

163.   Chen JF, Mandel EM, Thomson JM, Wu Q, Callis TE, Hammond SM, Conlon FL & Wang DZ (2006) The role of microRNA-1 and microRNA-133 in skeletal muscle proliferation and differentiation. *Nat Genet* **38**, 228-233, doi: ng1725 [pii] 10.1038/ng1725.

164.   McCarthy JJ (2008) MicroRNA-206: the skeletal muscle-specific myomiR. *Biochim Biophys Acta* **1779**, 682-691, doi: S1874-9399(08)00062-X [pii] 10.1016/j.bbagrm.2008.03.001.

165.   Nakasa T, Ishikawa M, Shi M, Shibuya H, Adachi N & Ochi M (2010) Acceleration of muscle regeneration by local injection of muscle-specific microRNAs

in rat skeletal muscle injury model. *J Cell Mol Med* **14**, 2495-2505, doi: JCMM898 [pii]
10.1111/j.1582-4934.2009.00898.x.

166.   Liu N, Williams AH, Kim Y, McAnally J, Bezprozvannaya S, Sutherland LB, Richardson JA, Bassel-Duby R & Olson EN (2007) An intragenic MEF2-dependent enhancer directs muscle-specific expression of microRNAs 1 and 133. *Proc Natl Acad Sci U S A* **104**, 20844-20849, doi: 0710558105 [pii]
10.1073/pnas.0710558105.

167.   Jian-Fu C, Mandel EM, Thomson JM, Qiulian W, Callis TE, Hammond SM, Conlon FL & Da-Zhi W (2006) The role of microRNA-1 and microRNA-133 in skeletal muscle proliferation and differentiation. *Nature Genetics* **38**, 228-233, doi: 10.1038/ng1725.

168.   Kim HK, Lee YS, Sivaprasad U, Malhotra A & Dutta A (2006) Muscle-specific microRNA miR-206 promotes muscle differentiation. *Journal of Cell Biology* **174**, 677-687.

169.   Koutalianos D, Koutsoulidou A, Mastroyiannopoulos NP, Furling D & Phylactou LA (2015) MyoD transcription factor induces myogenesis by inhibiting Twist-1 through miR-206. *J Cell Sci* **128**, 3631-3645, doi: jcs.172288 [pii]
10.1242/jcs.172288.

170.   Huang MB, Xu H, Xie SJ, Zhou H & Qu LH (2011) Insulin-like growth factor-1 receptor is regulated by microRNA-133 during skeletal myogenesis. *PLoS One* **6**, e29173, doi: 10.1371/journal.pone.0029173
PONE-D-11-09780 [pii].

171.   Elia L, Contu R, Quintavalle M, Varrone F, Chimenti C, Russo MA, Cimino V, De Marinis L, Frustaci A, Catalucci D, et al. (2009) Reciprocal regulation of microRNA-1 and insulin-like growth factor-1 signal transduction cascade in cardiac and skeletal muscle in physiological and pathological conditions. *Circulation* **120**, 2377-2385, doi: CIRCULATIONAHA.109.879429 [pii]
10.1161/CIRCULATIONAHA.109.879429.

172.   Ivey KN, Muth A, Arnold J, King FW, Yeh RF, Fish JE, Hsiao EC, Schwartz RJ, Conklin BR, Bernstein HS, et al. (2008) MicroRNA regulation of cell lineages in mouse and human embryonic stem cells. *Cell Stem Cell* **2**, 219-229, doi: S1934-5909(08)00057-X [pii]
10.1016/j.stem.2008.01.016.

173.   van Mil A, Vrijsen KR, Goumans MJ, Metz CH, Doevendans PA & Sluijter JP (2013) MicroRNA-1 enhances the angiogenic differentiation of human cardiomyocyte progenitor cells. *J Mol Med (Berl)* **91**, 1001-1012, doi: 10.1007/s00109-013-1017-1.

174.   Zhang D, Li X, Chen C, Li Y, Zhao L, Jing Y, Liu W, Wang X, Zhang Y, Xia H, et al. (2012) Attenuation of p38-mediated miR-1/133 expression facilitates myoblast proliferation during the early stage of muscle regeneration. *PLoS One* **7**, e41478, doi: 10.1371/journal.pone.0041478
PONE-D-12-01711 [pii].

175.   Mishima Y, Abreu-Goodger C, Staton AA, Stahlhut C, Shou C, Cheng C, Gerstein M, Enright AJ & Giraldez AJ (2009) Zebrafish miR-1 and miR-133 shape muscle gene expression and regulate sarcomeric actin organization. *Genes Dev* **23**, 619-632, doi: gad.1760209 [pii]
10.1101/gad.1760209.

176.   Basu U, Lozynska O, Moorwood C, Patel G, Wilton SD & Khurana TS (2011) Translational regulation of utrophin by miRNAs. *PLoS One* **6**, e29376, doi: 10.1371/journal.pone.0029376

PONE-D-11-08322 [pii].

177.   Feng Y, Niu LL, Wei W, Zhang WY, Li XY, Cao JH & Zhao SH (2013) A feedback circuit between miR-133 and the ERK1/2 pathway involving an exquisite mechanism for regulating myoblast proliferation and differentiation. *Cell Death Dis* **4**, e934, doi: cddis2013462 [pii]
10.1038/cddis.2013.462.

178.   Zhao Y, Samal E & Srivastava D (2005) Serum response factor regulates a muscle-specific microRNA that targets Hand2 during cardiogenesis. *Nature* **436**, 214-220, doi: nature03817 [pii]
10.1038/nature03817.

179.   Muraoka N, Yamakawa H, Miyamoto K, Sadahiro T, Umei T, Isomi M, Nakashima H, Akiyama M, Wada R, Inagawa K, et al. (2014) MiR-133 promotes cardiac reprogramming by directly repressing Snai1 and silencing fibroblast signatures. *EMBO J* **33**, 1565-1581, doi: embj.201387605 [pii]
10.15252/embj.201387605.

180.   Xu C, Hu Y, Hou L, Ju J, Li X, Du N, Guan X, Liu Z, Zhang T, Qin W, et al. (2014) beta-Blocker carvedilol protects cardiomyocytes against oxidative stress-induced apoptosis by up-regulating miR-133 expression. *J Mol Cell Cardiol* **75**, 111-121, doi: S0022-2828(14)00234-X [pii]
10.1016/j.yjmcc.2014.07.009.

181.   Horie T, Ono K, Nishi H, Iwanaga Y, Nagao K, Kinoshita M, Kuwabara Y, Takanabe R, Hasegawa K, Kita T, et al. (2009) MicroRNA-133 regulates the expression of GLUT4 by targeting KLF15 and is involved in metabolic control in cardiac myocytes. *Biochem Biophys Res Commun* **389**, 315-320, doi: S0006-291X(09)01738-0 [pii]
10.1016/j.bbrc.2009.08.136.

182.   Duisters RF, Tijsen AJ, Schroen B, Leenders JJ, Lentink V, van der Made I, Herias V, van Leeuwen RE, Schellings MW, Barenbrug P, et al. (2009) miR-133 and miR-30 regulate connective tissue growth factor: implications for a role of microRNAs in myocardial matrix remodeling. *Circ Res* **104**, 170-178, 176p following 178, doi: CIRCRESAHA.108.182535 [pii]
10.1161/CIRCRESAHA.108.182535.

183.   Izarra A, Moscoso I, Levent E, Canon S, Cerrada I, Diez-Juan A, Blanca V, Nunez-Gil IJ, Valiente I, Ruiz-Sauri A, et al. (2014) miR-133a enhances the protective capacity of cardiac progenitors cells after myocardial infarction. *Stem Cell Reports* **3**, 1029-1042, doi: S2213-6711(14)00332-4 [pii]
10.1016/j.stemcr.2014.10.010.

184.   Kim HK, Lee YS, Sivaprasad U, Malhotra A & Dutta A (2006) Muscle-specific microRNA miR-206 promotes muscle differentiation. *J Cell Biol* **174**, 677-687, doi: jcb.200603008 [pii]
10.1083/jcb.200603008.

185.   Miura P, Amirouche A, Clow C, Belanger G & Jasmin BJ (2012) Brain-derived neurotrophic factor expression is repressed during myogenic differentiation by miR-206. *J Neurochem* **120**, 230-238, doi: 10.1111/j.1471-4159.2011.07583.x.

186.   Rosenberg MI, Georges SA, Asawachaicharn A, Analau E & Tapscott SJ (2006) MyoD inhibits Fstl1 and Utrn expression by inducing transcription of miR-206. *J Cell Biol* **175**, 77-85, doi: jcb.200603039 [pii]
10.1083/jcb.200603039.

187.   van Rooij E, Sutherland LB, Qi X, Richardson JA, Hill J & Olson EN (2007) Control of stress-dependent cardiac growth and gene expression by a microRNA. *Science* **316**, 575-579, doi: 10.1126/science.1139089.

188.   Callis TE, Pandya K, Seok HY, Tang RH, Tatsuguchi M, Huang ZP, Chen JF, Deng Z, Gunn B, Shumate J, et al. (2009) MicroRNA-208a is a regulator of cardiac hypertrophy and conduction in mice. *J Clin Invest* **119**, 2772-2786, doi: 10.1172/jci36154.

189.   Sluijter JP, van Mil A, van Vliet P, Metz CH, Liu J, Doevendans PA & Goumans MJ (2010) MicroRNA-1 and -499 regulate differentiation and proliferation in human-derived cardiomyocyte progenitor cells. *Arterioscler Thromb Vasc Biol* **30**, 859-868, doi: 10.1161/atvbaha.109.197434.

190.   Crist CG, Montarras D, Pallafacchina G, Rocancourt D, Cumano A, Conway SJ, Buckingham M & Olson EN (2009) Muscle Stem Cell Behavior Is Modified by MicroRNA-27 Regulation of Pax3 Expression. *Proceedings of the National Academy of Sciences of the United States of America*, 13383, doi: 10.2307/40485375.

191.   Dey BK, Gagan J & Dutta A (2011) miR-206 and -486 induce myoblast differentiation by downregulating Pax7. *Molecular and cellular biology* **31**, 203-214, doi: 10.1128/MCB.01009-10.

192.   Chen JF, Tao Y, Li J, Deng Z, Yan Z, Xiao X & Wang DZ (2010) microRNA-1 and microRNA-206 regulate skeletal muscle satellite cell proliferation and differentiation by repressing Pax7. *J Cell Biol* **190**, 867-879, doi: 10.1083/jcb.200911036.

193.   Liu N, Williams AH, Maxeiner JM, Bezprozvannaya S, Shelton JM, Richardson JA, Bassel-Duby R & Olson EN (2012) microRNA-206 promotes skeletal muscle regeneration and delays progression of Duchenne muscular dystrophy in mice. *J Clin Invest* **122**, 2054-2065, doi: 10.1172/jci62656.

194.   Zhang J, Ying ZZ, Tang ZL, Long LQ & Li K (2012) MicroRNA-148a Promotes Myogenic Differentiation by Targeting the ROCK1 Gene. *Journal of Biological Chemistry* **287**, 21093-21101.

195.   Wang XH, Hu Z, Klein JD, Zhang L, Fang F & Mitch WE (2011) Decreased miR-29 Suppresses Myogenesis in CKD. *Journal of the American Society of Nephrology* **22**, 2068-2076, doi: 10.1681/asn.2010121278.

196.   Winbanks CE, Wang B, Beyer C, Koh P, White L, Kantharidis P & Gregorevic P (2011) TGF-beta Regulates miR-206 and miR-29 to Control Myogenic Differentiation through Regulation of HDAC4. *Journal of Biological Chemistry* **286**, 13805-13814.

197.   Zhou L, Wang LJ, Lu LN, Jiang PY, Sun H & Wang HT (2012) A Novel Target of MicroRNA-29, Ring1 and YY1-binding Protein (Rybp), Negatively Regulates Skeletal Myogenesis. *Journal of Biological Chemistry* **287**, 25255-25265.

198.   Koning M, Werker PMN, van Luyn MJA, Krenning G & Harmsen MC (2012) A global downregulation of microRNAs occurs in human quiescent satellite cells during myogenesis. *Differentiation* **84**, 314-321, doi: http://dx.doi.org/10.1016/j.diff.2012.08.002.

199.   Crist Colin G, Montarras D & Buckingham M (2012) Muscle Satellite Cells Are Primed for Myogenesis but Maintain Quiescence with Sequestration of Myf5 mRNA Targeted by microRNA-31 in mRNP Granules. *Cell stem cell* **11**, 118-126.

200.   Dey BK, Gagan J, Yan Z & Dutta A (2012) miR-26a is required for skeletal muscle differentiation and regeneration in mice. *Genes Dev* **26**, 2180-2191, doi: 10.1101/gad.198085.112.

201.   Wong CF & Tellam RL (2008) MicroRNA-26a targets the histone methyltransferase Enhancer of Zeste homolog 2 during myogenesis. *J Biol Chem* **283**, 9836-9843, doi: 10.1074/jbc.M709614200.

202.   Chen Y, Melton DW, Gelfond JA, McManus LM & Shireman PK (2012) MiR-351 transiently increases during muscle regeneration and promotes progenitor cell proliferation and survival upon differentiation. *Physiol Genomics* **44**, 1042-1051, doi: 10.1152/physiolgenomics.00052.2012.

203.   Clop A, Marcq F, Takeda H, Pirottin D, Tordoir X, Bibe B, Bouix J, Caiment F, Elsen JM, Eychenne F, et al. (2006) A mutation creating a potential illegitimate microRNA target site in the myostatin gene affects muscularity in sheep. *Nat Genet* **38**, 813-818, doi: 10.1038/ng1810.

204.   Callis TE, Pandya K, Seok HY, Tang R-H, Tatsuguchi M, Huang Z-P, Chen J-F, Deng Z, Gunn B, Shumate J, et al. (2009) MicroRNA-208a is a regulator of cardiac hypertrophy and conduction in mice. *The Journal of Clinical Investigation* **119**, 2772-2786, doi: 10.1172/JCI36154.

205.   Huang Z, Chen X, Yu B, He J & Chen D (2012) MicroRNA-27a promotes myoblast proliferation by targeting myostatin. *Biochem Biophys Res Commun* **423**, 265-269, doi: 10.1016/j.bbrc.2012.05.106.

206.   Davis BN, Hilyard AC, Lagna G & Hata A (2008) SMAD proteins control DROSHA-mediated microRNA maturation. *Nature* **454**, 56-61, doi: nature07086 [pii] 10.1038/nature07086.

207.   Sato MM, Nashimoto M, Katagiri T, Yawaka Y & Tamura M (2009) Bone morphogenetic protein-2 down-regulates miR-206 expression by blocking its maturation process. *Biochem Biophys Res Commun* **383**, 125-129, doi: S0006-291X(09)00628-7 [pii]
10.1016/j.bbrc.2009.03.142.

208.   Martin EC, Bratton MR, Zhu Y, Rhodes LV, Tilghman SL, Collins-Burow BM & Burow ME (2012) Insulin-like growth factor-1 signaling regulates miRNA expression in MCF-7 breast cancer cell line. *PLoS One* **7**, e49067, doi: 10.1371/journal.pone.0049067.

209.   Kong W, Yang H, He L, Zhao JJ, Coppola D, Dalton WS & Cheng JQ (2008) MicroRNA-155 is regulated by the transforming growth factor beta/Smad pathway and contributes to epithelial cell plasticity by targeting RhoA. *Molecular and cellular biology* **28**, 6773-6784, doi: 10.1128/mcb.00941-08.

210.   Rachagani S, Cheng Y & Reecy JM (2010) Myostatin genotype regulates muscle-specific miRNA expression in mouse pectoralis muscle. *BMC Res Notes* **3**, 297, doi: 1756-0500-3-297 [pii]
10.1186/1756-0500-3-297.

211.   Hitachi K, Nakatani M & Tsuchida K (2014) Myostatin signaling regulates Akt activity via the regulation of miR-486 expression. *Int J Biochem Cell Biol* **47**, 93-103, doi: S1357-2725(13)00369-5 [pii]
10.1016/j.biocel.2013.12.003.

212.   Sharma M, Kambadur R, Matthews KG, Somers WG, Devlin GP, Conaglen JV, Fowke PJ & Bass JJ (1999) Myostatin, a transforming growth factor-beta superfamily member, is expressed in heart muscle and is upregulated in cardiomyocytes after infarct. *J Cell Physiol* **180**, 1-9, doi: 10.1002/(SICI)1097-4652(199907)180:1<1::AID-JCP1>3.0.CO;2-V [pii]
10.1002/(SICI)1097-4652(199907)180:1<1::AID-JCP1>3.0.CO;2-V.

213.   Khandelia P, Yap K & Makeyev EV (2011) Streamlined platform for short hairpin RNA interference and transgenesis in cultured mammalian cells. *Proc Natl Acad Sci U S A* **108**, 12799-12804, doi: 10.1073/pnas.1103532108.

214.   Kitzmann M, Carnac G, Vandromme M, Primig M, Lamb NJ & Fernandez A (1998) The muscle regulatory factors MyoD and myf-5 undergo distinct cell cycle-specific expression in muscle cells. *J Cell Biol* **142**, 1447-1459.

215.   Langley B, Thomas M, McFarlane C, Gilmour S, Sharma M & Kambadur R (2004) Myostatin inhibits rhabdomyosarcoma cell proliferation through an Rb-independent pathway. *Oncogene* **23**, 524-534, doi: 10.1038/sj.onc.1207144.

216.   Li R, Shi X, Ling F, Wang C, Liu J, Wang W & Li M (2015) MiR-34a suppresses ovarian cancer proliferation and motility by targeting AXL. *Tumour biology : the journal of the International Society for Oncodevelopmental Biology and Medicine*, doi: 10.1007/s13277-015-3445-8.

217.   Sun H, Tian J, Xian W, Xie T & Yang X (2015) miR-34a inhibits proliferation and invasion of bladder cancer cells by targeting orphan nuclear receptor HNF4G. *Disease markers* **2015**, 879254, doi: 10.1155/2015/879254.

218.   Li J, Wang K, Chen X, Meng H, Song M, Wang Y, Xu X & Bai Y (2012) Transcriptional activation of microRNA-34a by NF-kappa B in human esophageal cancer cells. *BMC Mol Biol* **13**, 4, doi: 10.1186/1471-2199-13-4.

219.   Sriram S, Subramanian S, Sathiakumar D, Venkatesh R, Salerno MS, McFarlane CD, Kambadur R & Sharma M (2011) Modulation of reactive oxygen species in skeletal muscle by myostatin is mediated through NF-kappaB. *Aging cell* **10**, 931-948, doi: 10.1111/j.1474-9726.2011.00734.x.

220.   Hu JS, Olson EN & Kingston RE (1992) HEB, a helix-loop-helix protein related to E2A and ITF2 that can modulate the DNA-binding ability of myogenic regulatory factors. *Molecular and cellular biology* **12**, 1031-1042.

221.   McCroskery S, Thomas M, Maxwell L, Sharma M & Kambadur R (2003) Myostatin negatively regulates satellite cell activation and self-renewal. *J Cell Biol* **162**, 1135-1147, doi: 10.1083/jcb.200207056.

222.   Shi X & Garry DJ (2006) Muscle stem cells in development, regeneration, and disease. *Genes Dev* **20**, 1692-1708, doi: 10.1101/gad.1419406.

223.   Meyer SU, Thirion C, Polesskaya A, Bauersachs S, Kaiser S, Krause S & Pfaffl MW (2015) TNF-alpha and IGF1 modify the microRNA signature in skeletal muscle cell differentiation. *Cell Commun Signal* **13**, 4, doi: 10.1186/s12964-015-0083-0 s12964-015-0083-0 [pii].

224.   Winbanks CE, Wang B, Beyer C, Koh P, White L, Kantharidis P & Gregorevic P (2011) TGF-beta regulates miR-206 and miR-29 to control myogenic differentiation through regulation of HDAC4. *The Journal of biological chemistry* **286**, 13805-13814, doi: M110.192625 [pii]
10.1074/jbc.M110.192625.

225.   Javed R, Jing L, Yang J, Li X, Cao J & Zhao S (2014) miRNA transcriptome of hypertrophic skeletal muscle with overexpressed myostatin propeptide. *Biomed Res Int* **2014**, 328935, doi: 10.1155/2014/328935.

226.   Juan AH, Kumar RM, Marx JG, Young RA & Sartorelli V (2009) Mir-214-dependent regulation of the polycomb protein Ezh2 in skeletal muscle and embryonic stem cells. *Mol Cell* **36**, 61-74, doi: S1097-2765(09)00583-8 [pii]
10.1016/j.molcel.2009.08.008.

227.   Jia L, Li YF, Wu GF, Song ZY, Lu HZ, Song CC, Zhang QL, Zhu JY, Yang GS & Shi XE (2013) MiRNA-199a-3p regulates C2C12 myoblast differentiation through IGF-1/AKT/mTOR signal pathway. *Int J Mol Sci* **15**, 296-308.

228.   Mollinari C, Racaniello M, Berry A, Pieri M, de Stefano MC, Cardinale A, Zona C, Cirulli F, Garaci E & Merlo D (2015) miR-34a regulates cell proliferation, morphology and function of newborn neurons resulting in improved behavioural outcomes. *Cell Death Dis* **6**, e1622, doi: cddis2014589 [pii]
10.1038/cddis.2014.589.

229.   Boon RA, Iekushi K, Lechner S, Seeger T, Fischer A, Heydt S, Kaluza D, Treguer K, Carmona G, Bonauer A, et al. (2013) MicroRNA-34a regulates cardiac ageing and function. *Nature* **495**, 107-110, doi: nature11919 [pii]
10.1038/nature11919.

230.   Fu T, Seok S, Choi S, Huang Z, Suino-Powell K, Xu HE, Kemper B & Kemper JK (2014) MicroRNA 34a inhibits beige and brown fat formation in obesity in part by suppressing adipocyte fibroblast growth factor 21 signaling and SIRT1 function. *Molecular and cellular biology* **34**, 4130-4142, doi: 10.1128/mcb.00596-14.

231.   He L, He X, Lim LP, de Stanchina E, Xuan Z, Liang Y, Xue W, Zender L, Magnus J, Ridzon D, et al. (2007) A microRNA component of the p53 tumour suppressor network. *Nature* **447**, 1130-1134, doi: 10.1038/nature05939.

232.   Sun F, Fu H, Liu Q, Tie Y, Zhu J, Xing R, Sun Z & Zheng X (2008) Downregulation of CCND1 and CDK6 by miR-34a induces cell cycle arrest. *FEBS Lett* **582**, 1564-1568, doi: 10.1016/j.febslet.2008.03.057.

233.   Yang W, Zhang Y, Li Y, Wu Z & Zhu D (2007) Myostatin induces cyclin D1 degradation to cause cell cycle arrest through a phosphatidylinositol 3-kinase/AKT/GSK-3 beta pathway and is antagonized by insulin-like growth factor 1. *J Biol Chem* **282**, 3799-3808, doi: M610185200 [pii] 10.1074/jbc.M610185200.

234.   Zhao J, Lammers P, Torrance CJ & Bader AG (2013) TP53-independent function of miR-34a via HDAC1 and p21(CIP1/WAF1.). *Molecular therapy : the journal of the American Society of Gene Therapy* **21**, 1678-1686, doi: 10.1038/mt.2013.148.

235.   McKay BR, Ogborn DI, Bellamy LM, Tarnopolsky MA & Parise G (2012) Myostatin is associated with age-related human muscle stem cell dysfunction. *FASEB J* **26**, 2509-2521, doi: fj.11-198663 [pii] 10.1096/fj.11-198663.

236.   Kim JY, Park YK, Lee KP, Lee SM, Kang TW, Kim HJ, Dho SH, Kim SY & Kwon KS (2014) Genome-wide profiling of the microRNA-mRNA regulatory network in skeletal muscle with aging. *Aging (Albany NY)* **6**, 524-544, doi: 100677 [pii].

237.   Weeraratne SD, Amani V, Neiss A, Teider N, Scott DK, Pomeroy SL & Cho YJ (2011) miR-34a confers chemosensitivity through modulation of MAGE-A and p53 in medulloblastoma. *Neuro Oncol* **13**, 165-175, doi: 10.1093/neuonc/noq179.

238.   Rodgers JT, King KY, Brett JO, Cromie MJ, Charville GW, Maguire KK, Brunson C, Mastey N, Liu L, Tsai CR, et al. (2014) mTORC1 controls the adaptive transition of quiescent stem cells from G0 to G(Alert). *Nature* **510**, 393-396, doi: nature13255 [pii] 10.1038/nature13255.

239.   Conboy IM, Conboy MJ, Smythe GM & Rando TA (2003) Notch-mediated restoration of regenerative potential to aged muscle. *Science* **302**, 1575-1577, doi: 10.1126/science.1087573.

240.   Park EY, Chang E, Lee EJ, Lee HW, Kang HG, Chun KH, Woo YM, Kong HK, Ko JY, Suzuki H, et al. (2014) Targeting of miR34a-NOTCH1 axis reduced breast cancer stemness and chemoresistance. *Cancer Res* **74**, 7573-7582, doi: 0008-5472.CAN-14-1140 [pii] 10.1158/0008-5472.CAN-14-1140.

241.   Kashat M, Azzouz L, Sarkar SH, Kong D, Li Y & Sarkar FH (2012) Inactivation of AR and Notch-1 signaling by miR-34a attenuates prostate cancer aggressiveness. *Am J Transl Res* **4**, 432-442.

242.   Gallot YS, Durieux AC, Castells J, Desgeorges MM, Vernus B, Plantureux L, Remond D, Jahnke VE, Lefai E, Dardevet D, et al. (2014) Myostatin gene inactivation prevents skeletal muscle wasting in cancer. *Cancer Res* **74**, 7344-7356, doi: 0008-5472.CAN-14-0057 [pii] 10.1158/0008-5472.CAN-14-0057.

243.   Shao C, Liu M, Wu X & Ding F (2007) Time-dependent expression of myostatin RNA transcript and protein in gastrocnemius muscle of mice after sciatic nerve resection. *Microsurgery* **27**, 487-493, doi: 10.1002/micr.20392.

244.   Allen DL, Bandstra ER, Harrison BC, Thorng S, Stodieck LS, Kostenuik PJ, Morony S, Lacey DL, Hammond TG, Leinwand LL, et al. (2009) Effects of spaceflight on murine skeletal muscle gene expression. *Journal of applied physiology (Bethesda, Md : 1985)* **106**, 582-595, doi: 10.1152/japplphysiol.90780.2008.

245.   Reardon KA, Davis J, Kapsa RM, Choong P & Byrne E (2001) Myostatin, insulin-like growth factor-1, and leukemia inhibitory factor mRNAs are upregulated in chronic human disuse muscle atrophy. *Muscle & nerve* **24**, 893-899.

246.   Lokireddy S, Mouly V, Butler-Browne G, Gluckman PD, Sharma M, Kambadur R & McFarlane C (2011) Myostatin promotes the wasting of human myoblast cultures through promoting ubiquitin-proteasome pathway-mediated loss of sarcomeric proteins. *American journal of physiology Cell physiology* **301**, C1316-1324, doi: 10.1152/ajpcell.00114.2011.

247.   Eisenberg I, Eran A, Nishino I, Moggio M, Lamperti C, Amato AA, Lidov HG, Kang PB, North KN, Mitrani-Rosenbaum S, et al. (2007) Distinctive patterns of microRNA expression in primary muscular disorders. *Proc Natl Acad Sci U S A* **104**, 17016-17021, doi: 0708115104 [pii]
10.1073/pnas.0708115104.

248.   Siriett V, Platt L, Salerno MS, Ling N, Kambadur R & Sharma M (2006) Prolonged absence of myostatin reduces sarcopenia. *J Cell Physiol* **209**, 866-873, doi: 10.1002/jcp.20778.

249.   Leger B, Derave W, De Bock K, Hespel P & Russell AP (2008) Human sarcopenia reveals an increase in SOCS-3 and myostatin and a reduced efficiency of Akt phosphorylation. *Rejuvenation Res* **11**, 163-175B, doi: 10.1089/rej.2007.0588.

250.   Li X, Khanna A, Li N & Wang E (2011) Circulatory miR34a as an RNAbased, noninvasive biomarker for brain aging. *Aging (Albany NY)* **3**, 985-1002, doi: 100371 [pii].

251.   Hittel DS, Axelson M, Sarna N, Shearer J, Huffman KM & Kraus WE (2010) Myostatin decreases with aerobic exercise and associates with insulin resistance. *Med Sci Sports Exerc* **42**, 2023-2029, doi: 10.1249/MSS.0b013e3181e0b9a8.

252.   Dong J, Dong Y, Dong Y, Chen F, Mitch WE & Zhang L (2015) Inhibition of myostatin in mice improves insulin sensitivity via irisin-mediated cross talk between muscle and adipose tissues. *International journal of obesity (2005)*, doi: 10.1038/ijo.2015.200.

253.   Xu X, Chen W, Miao R, Zhou Y, Wang Z, Zhang L, Wan Y, Dong Y, Qu K & Liu C (2015) miR-34a induces cellular senescence via modulation of telomerase activity in human hepatocellular carcinoma by targeting FoxM1/c-Myc pathway. *Oncotarget* **6**, 3988-4004, doi: 2905 [pii].